Introductory Lectures on the Structure of the Hadrons from the Lattice

A. Schiller*
QCDSF collaboration†
Institut für Theoretische Physik and NTZ,
Universität Leipzig, D-04109 Leipzig, Germany

June 20, 1998 (Preliminary version)

Notes for Lectures Presented at the
Summer School on Lattice QCD for Beginners
ECT, Trento
June 21 – July 4, 1998

Abstract

In these lectures an overview is given about the activities of the QCDSF collaboration concerning various aspects of the hadron structure from lattice QCD in the quenched approximation, such as hadron and quark masse, decay constants, first moments of deep inelastic nucleon and meson structure functions. Aspects of perturbative and nonperturbative renormalisation of composite operators are discussed. The results present evidence that $O(a)$ Symanzik improvement brings us closer to the goal of calculating continuum masses and matrix elements in QCD.

*schiller@tph204.physik.uni-leipzig.de
†QCDSF collaboration: M. Göckeler, R. Horsley, H. Perlt, P. Rakow, G. Schierholz, A. Schiller, P. Stephenson

Contents

1 Introduction

In this lectures we give an overview over a nonpertubative calculation of the hadron structure using lattice QCD. We mainly review results obtained by the QCDSF collaboration, therefore the list of references is far from complete. To make these lectures selfcontained for the audience, in a first part we review the deep inelastic scattering and some well-known ideas of the operator product expansion closely following ref. [1] (see also ref [2]). Then the concept of two- and three-point correlation functions is discussed which represents the basis to determine several intersting properties of the hadron structure. We present techniques and results of our collaboration within the quenched approximation of lattice QCD for hadron and quark masses, decay constants for light hadrons and first moments of the deep inelastic structure functions. Of special importance is the comparison of results obtained in the standard Wilson formulation of lattice QCD with improved actions and operators allowing to remove unwanted discretisation errors of order $O(a)$. We also discuss the chiral limit and the approach to the continuum for several quantities measured. Some aspects of perturbative and nonperturbative renormalisation are reviewed, first results on measured renormalisation factors are given.

2 Deep inelastic scattering

2.1 Kinematics

In a deep inelastic scattering (DIS) experiment, an incoming beam of leptons with energy E scatters off a fixed hadronic target. The energy and direction of the scattered lepton are measured in the detector, but the final hadronic state (usually denoted by X) is not measured experimentally. The lepton interacts with the hadron target through the exchange of a virtual photon; the target hadron absorbs the virtual photon, to produce the final state X. The deep inelastic region is where the target hadron is blown apart by the virtual photon, and fragments into many particles. If the target hadron remains intact, the process is called elastic scattering.

The basic diagram for DIS is shown schematically in fig. 1 In the following definitions the $\hat{z}$ axis is taken

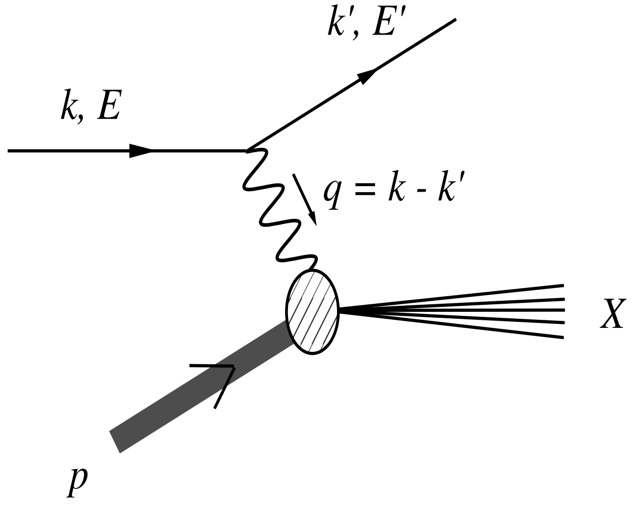

Figure 1: Basic diagram for deep inelastic lepton hadron scattering.

to be along the incident lepton beam direction. The kinematic variables used in DIS are:

M The mass of the target hadron. The most important case is for a proton or neutron target, in which case M is the nucleon mass.

E The energy of the incident lepton.

k The momentum of the initial lepton. $k = (E, 0, 0, E)$, if the lepton mass is neglected.

k' The momentum of the scattered lepton, $k' = (E', E' \sin\theta \cos\phi, E' \sin\theta \sin\phi, E' \cos\theta)$.

Ω The solid angle into which the outgoing lepton is scattered.

E' The energy of the scattered lepton.

p The momentum of the target, $p = (M, 0, 0, 0)$, for a fixed target experiment.

q $= k - k'$, the momentum transfer in the scattering process, *i.e.* the momentum of the virtual photon.

ν $= E - E' = p \cdot q/M$, the energy loss of the lepton.

y $= \nu/E = p \cdot q/p \cdot k$, the fractional energy loss of the lepton.

Q^2 $= -q^2 = 2EE'(1 - \cos\theta) = 4EE' \sin^2 \theta/2$.

x $= Q^2/2M\nu = Q^2/2p \cdot q = Q^2/2MEy$.

ω $= 1/x$.

The variable x was first introduced by Bjorken, and is crucial to understanding deep inelastic scattering because we will see that QCD predicts that structure functions are functions of x and independent of Q^2 to leading order, a property known as scaling. Higher order corrections in QCD produce a small logarithmic Q^2 dependence of the structure functions which is calculable for large Q^2 since QCD is asymptotically free. Therefore it is useful to define use the deep inelastic scattering as the following limit:

$$x \text{ fixed}, \; Q^2 \to \infty.$$

The invariant mass of the final hadronic system X is

$$M_X^2 = (p+q)^2 = M^2 + 2p \cdot q + q^2. \tag{2.1}$$

The invariant mass of X must be at least that of a nucleon, since the baryon number is conserved in the scattering process. This gives the inequality

$$M_X^2 \geq M^2 \quad \Rightarrow \quad M^2 + 2p \cdot q - Q^2 \geq M^2 \quad \Rightarrow \quad x \leq 1. \tag{2.2}$$

Since Q^2 and ν are both positive, x must also be positive. The lepton energy loss $E - E'$ must be between zero and E, so the physically allowed kinematic region is

$$0 \leq x \leq 1, \qquad 0 \leq y \leq 1. \tag{2.3}$$

Eq. (2.2) can be written in the form

$$x = \frac{Q^2}{2p \cdot q} = 1 - \frac{M_X^2 - M^2}{2p \cdot q}. \tag{2.4}$$

The value $x = 1$ implies that $M_X^2 = M^2$, and so $x = 1$ corresponds to elastic scattering. Any fixed hadron state X with invariant mass M_X^2 contributes to the cross-section at the value of x obtained from eq. (2.4),

$$x = \frac{1}{1 + (M_X^2 - M^2)/Q^2}. \tag{2.5}$$

In the deep inelastic limit $Q^2 \to \infty$, so that any state X with fixed mass M_X gets driven to $x = 1$. In particular, all nucleon resonances such as the N^* get pushed to $x = 1$. The invariant mass of the hadronic state that contributes to the cross-section at a given value of Q^2 increases as $x \to 0$. For a fixed value of Q^2, there is a small region around $x = 1$ of width $\Lambda_{\text{QCD}}^2/Q^2$ which probes hadronic resonances with masses around that of the nucleon. This resonance region is present in any real experiment since Q^2 is finite, but

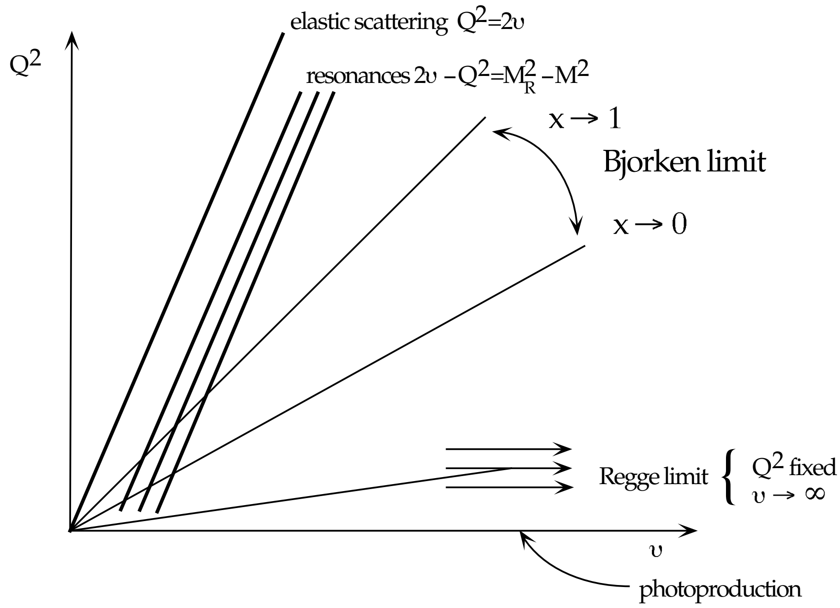

Figure 2: Kinematic domains in lepton nucleon scattering.

is not present in the formal deep inelastic limit. Outside the resonance region, the invariant mass M_X^2 is of order Q^2. The different kinematic domains of interest in inelastic electron scattering are shown in fig. (2).

The experimental measurements give the cross-section as a function of the final lepton energy and scattering angle, $d^2\sigma/dE'd\Omega$. The results are often presented instead by giving the differential cross-section as a function of $(x,\, Q^2,\, \phi)$ or $(x,\, y,\, \phi)$. The cross-sections are related by

$$\frac{d^2\sigma}{dx\,dy\,d\phi} = \left(\frac{M\nu}{E'}\right)\frac{d^2\sigma}{dE'd\Omega} = \left(\frac{Q^2}{y}\right)\frac{d^2\sigma}{dx\,dQ^2d\phi}. \tag{2.6}$$

Since the variables x and y are Lorentz invariant the formula for the differential cross-section as a function of x, y, and ϕ is also valid for the kinematics at HERA.

Note that the scattering angle θ is of order M/Q,

$$\theta \;\propto\; \frac{M}{Q}, \tag{2.7}$$

and goes to zero as $Q^2 \to \infty$.

and it is elementary to find It is also useful to have formulæ for the different components of q as a function of x and y:

$$\begin{aligned} q^0 &= \frac{Q^2}{2Mxy}, \qquad q^3 = \frac{Q^2}{2Mxy} + Mxy, \\ q^\perp &= Q\sqrt{1-y}\sqrt{1-\frac{M^2x^2y^2}{Q^2(1-y)}} \approx Q\sqrt{1-y}. \end{aligned} \tag{2.8}$$

Note that $q^\perp$ is of order Q, whereas q^0 and q^3 are both of order Q^2/M. Also, q^0 and q^3 are nearly equal, with $q^0 - q^3$ being of order M. These properties of Q will be useful when we compute cross-sections in the deep inelastic limit.

2.2 Deep inelastic cross section

The scattering amplitude $\mathcal{M}$ according to fig. 1 is given by

$$i\mathcal{M} = (-ie)^2\left(\frac{-ig_{\mu\nu}}{q^2}\right)\langle k'|\, j_\ell^\mu(0)\, |k, s_\ell\rangle\, \langle X|\, j_h^\nu(0)\, |p, \lambda\rangle\,, \tag{2.9}$$

where s_ℓ is the polarisation of the initial lepton, λ is the polarisation of the initial hadron, and j_ℓ^μ, j_h^μ are the leptonic and hadronic electromagnetic currents respectively. The coupling constant e has been included explicitly in $\mathcal{M}$. The quantity λ which describes the hadron polarisation can be chosen to be the value of the spin along an arbitrary quantisation axis (usually chosen to be the beam direction). For a spin 1/2 target, $\lambda = \pm 1/2$.

The differential scattering cross-section is obtained from $\mathcal{M}$ by squaring, and multiplying by the phase space factors. The polarisation of the final lepton and hadron states are not measured, and have to be summed over. This gives the differential cross-section

$$\begin{aligned} d\sigma &= \sum_X \int \frac{d^3k'}{(2\pi)^3 2E'} \, (2\pi)^4 \delta^4(k+p-k'-p_X) \, \frac{|\mathcal{M}|^2}{(2E)(2M)(v_{\rm rel}=1)}, \\ &= \sum_X \int \frac{d^3k'}{(2\pi)^3 2E'} \, \frac{(2\pi)^4 \delta^4(k+p-k'-p_X)}{(2E)(2M)} \, \frac{e^4}{Q^4} \\ &\times \langle p,\lambda| \, j_h^\mu(0) \, |X\rangle \, \langle X| \, j_h^\nu(0) \, |p,\lambda\rangle \, \langle k,s_\ell| \, j_{\ell\mu}(0) \, |k'\rangle \, \langle k'| \, j_{\ell\nu}(0) \, |k,s_\ell\rangle \, , \end{aligned} \tag{2.10}$$

where the hermicity of currents $j_\mu^\dagger = j_\mu$ has been used

$$\langle\alpha| \, j^\mu \, |\beta\rangle^* = \langle\beta| \, j^\mu \, |\alpha\rangle \, . \tag{2.11}$$

It is conventional to define the leptonic tensor $\ell_{\mu\nu}$ by

$$\ell^{\mu\nu} = \sum_{\text{final spin}} \langle k'| \, j_\ell^\nu(0) \, |k,s_\ell\rangle \, \langle k,s_\ell| \, j_\ell^\mu(0) \, |k'\rangle \, . \tag{2.12}$$

The definition of the hadronic tensor is slightly more complicated. The tensor $W_{\mu\nu}$ is defined by

$$W_{\mu\nu}(p,q,\lambda',\lambda) = \frac{1}{4\pi} \int d^4x \, e^{iq\cdot x} \langle p,\lambda'|[j_\mu(x), j_\nu(0)]|p,\lambda\rangle \, , \tag{2.13}$$

where λ and λ' are the polarisations of the initial and final hadron. Inserting a complete set of states gives

$$\begin{aligned} W_{\mu\nu}(p,q,\lambda',\lambda) &= \frac{1}{4\pi} \sum_X \int d^4x \, e^{iq\cdot x} \Big[\langle p,\lambda'| \, j_\mu(x) \, |X\rangle \, \langle X| \, j_\nu(0) \, |p,\lambda\rangle \\ &- \langle p,\lambda'| \, j_\nu(0) \, |X\rangle \, \langle X| \, j_\mu(x) \, |p,\lambda\rangle \Big], \end{aligned} \tag{2.14}$$

where the sum on X is a sum over the allowed phase space for the final state X. Translation invariance implies that

$$\begin{aligned} \langle p,\lambda'| \, j_\mu(x) \, |X\rangle &= \langle p,\lambda'| \, j_\mu(0) \, |X\rangle \, e^{i(p-p_X)\cdot x}, \\ \langle X| \, j_\mu(x) \, |p,\lambda\rangle &= \langle X| \, j_\mu(0) \, |p,\lambda\rangle \, e^{i(p_X-p)\cdot x}. \end{aligned} \tag{2.15}$$

Inserting eq. (2.15) into eq. (2.14) gives

$$\begin{aligned} W_{\mu\nu}(p,q,\lambda',\lambda) &= \frac{1}{4\pi} \sum_X \Big[(2\pi)^4 \delta^4(q+p-p_X) \, \langle p,\lambda'| \, j_\mu(0) \, |X\rangle \, \langle X| \, j_\nu(0) \, |p,\lambda\rangle \\ &\quad - (2\pi)^4 \delta^4(q+p_X-p) \, \langle p,\lambda'| \, j_\nu(0) \, |X\rangle \, \langle X| \, j_\mu(0) \, |p,\lambda\rangle \Big]. \end{aligned} \tag{2.16}$$

The only allowed final states are those with $p_X^0 \geq p^0$, since $M_X^2 \geq M^2$. Since $q^0 > 0$, only the first delta function in eq. (2.16) can be satisfied, and the sum in $W_{\mu\nu}$ reduces to the expression in eq. (2.10) involving the hadronic currents, and the energy-momentum conserving delta function (up to a factor of $1/4\pi$). The reason for using the commutator is that then $W_{\mu\nu}$ has a nicer analytic structure when continued away from the physical region which we will use extensively in Sect. 3.3. Substituting for $\ell^{\mu\nu}$ and $W_{\mu\nu}$ in eq. (2.10) gives

$$d\sigma = \frac{e^4}{Q^4} \int \frac{d^3k'}{(2\pi)^3 2E'} \, \frac{4\pi \, \ell_{\mu\nu} \, W_{\mu\nu}(p,k-k',\lambda,\lambda)}{(2E)(2M)} \, , \tag{2.17}$$

so that

$$\begin{aligned}\frac{d^2\sigma}{dE'd\Omega} &= \frac{e^4}{16\pi^2 Q^4}\left(\frac{E'}{ME}\right)\ell^{\mu\nu}\; W_{\mu\nu}(p,q,\lambda,\lambda)\,,\\ \frac{d^2\sigma}{dx\,dy\,d\phi} &= \frac{e^4}{16\pi^2 Q^4}\,y\;\ell^{\mu\nu}\; W_{\mu\nu}(p,q,\lambda,\lambda)\,.\end{aligned} \tag{2.18}$$

All the information about the deep inelastic scattering cross-section is contained in the leptonic and hadronic tensors $\ell_{\mu\nu}$ and $W_{\mu\nu}$ (see also fig. 3). Note that the initial and final spin states of the target are equal: $\lambda' = \lambda$.

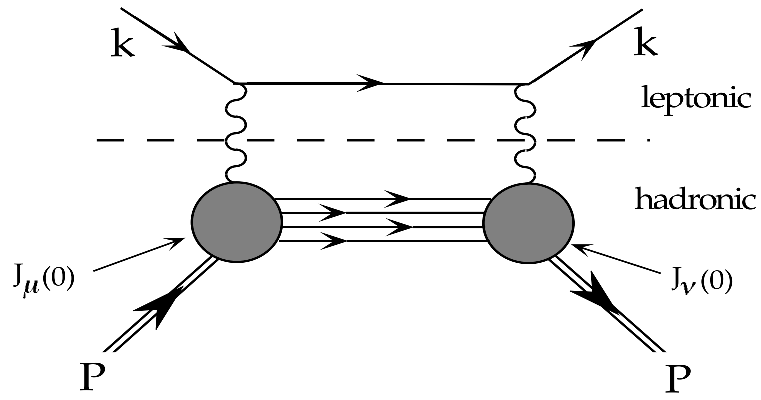

Figure 3: The squared amplitude $\mathcal{M}$ separated into leptonic $\ell_{\mu\nu}$ and hadronic $W_{\mu\nu}$ tensors.

2.3 Leptonic tensor

The leptonic tensor is trivial to compute since the leptons are pointlike fermions,

$$\ell^{\mu\nu} = \sum_{\text{final spin}} \overline{u}(k')\,\gamma^\nu\,u(k,s_\ell)\;\overline{u}(k,s_\ell)\,\gamma^\mu\,u(k'). \tag{2.19}$$

The sum over final state spinors uses the identity

$$\sum_{\text{final spin}} u(k')\,\overline{u}(k') = \not{k}' + m, \tag{2.20}$$

where the spinors are normalised to $2E$.

The polarisation of a spin 1/2 particle can be described by a spin vector s_ℓ, defined in the rest frame of the particle by

$$2\vec{s}_\ell = \overline{u}(k,s_\ell)\,\vec{\sigma}\,u(k,s_\ell) = \overline{u}(k,s_\ell)\,\vec{\gamma}\,\gamma_5\,u(k,s_\ell), \tag{2.21}$$

where the states have the conventional relativistic norm of $2m$ in the rest frame. The vector s_ℓ^μ is defined in an arbitrary Lorentz frame by boosting $s_\ell = (0,\vec{s}_\ell)$ from the rest frame, or equivalently, by

$$2s_\ell^\mu = \overline{u}(k,s_\ell)\,\gamma^\mu\gamma_5\,u(k,s_\ell). \tag{2.22}$$

For a spin-1/2 particle at rest with spin up along the $\hat{z}$ axis, the spin vector is $\vec{s}_\ell = m\hat{z}$. This differs from the conventional normalisation of s_ℓ by a factor of the fermion mass m. It is extremely useful to use this normalisation for the spin to avoid unnecessary factors of m appearing in the spin dependent cross-section. In the extreme relativistic limit, all mass effects can be neglected in the calculation, and all formulæ should be written in terms of relativistic spinors normalised to $2E$, without any additional factors of m. With this normalisation for s_ℓ, longitudinally polarised fermions in the extreme relativistic limit have $s_\ell = \mathcal{H}_\ell k$, where k is the lepton momentum and $\mathcal{H}_\ell = \pm$ is the lepton helicity.

The initial state spinor product can be written in terms of the standard spin projection operator,

$$u(k,s_\ell)\,\overline{u}(k,s_\ell) = (\not{k}+m)\;\frac{1+\gamma_5\not{s}_\ell/m_\ell}{2}. \tag{2.23}$$

Substituting eq. (2.20) and (2.23) into eq. (2.19) gives

$$\begin{aligned}
\ell^{\mu\nu} &= \mathrm{Tr}\;(\not{k}'+m_\ell)\,\gamma^\nu\,(\not{k}+m_\ell)\;\frac{1+\gamma_5\not{s}_\ell/m_\ell}{2}\;\gamma^\mu, \\
&= 2\left(k^\mu k'^\nu + k^\nu k'^\mu - g^{\mu\nu}(k\cdot k' - m_\ell^2) - i\epsilon^{\mu\nu\alpha\beta}q_\alpha s_{\ell\beta}\right), && (2.24)\\
&\approx 2\left(k^\mu k'^\nu + k^\nu k'^\mu - g^{\mu\nu}k\cdot k' - i\epsilon^{\mu\nu\alpha\beta}q_\alpha s_{\ell\beta}\right), && (2.25)
\end{aligned}$$

neglecting the lepton mass. There are no factors of m_ℓ in the spin term with our normalisation convention eq. (2.22). Note that the spin-independent part of the leptonic tensor is symmetric in $\mu\nu$, and the spin-dependent part is antisymmetric in $\mu\nu$. Thus an unpolarised lepton beam probes only the symmetric part of $W_{\mu\nu}$, and the polarisation asymmetry in the cross-sections probes only the antisymmetric part of $W_{\mu\nu}$.

2.4 Hadronic tensor for spin $J = 1/2$ target

The structure of the hadron relevant for deep inelastic scattering can be completely characterised by the hadronic tensor $W_{\mu\nu}$. Unlike the leptonic tensor which is known, $W_{\mu\nu}$ cannot be computed directly from QCD perturbation theory because of nonperturbative effects in the strong interactions. The strong interactions are invariant under parity and time reversal, and these symmetries place restrictions on the form of $W_{\mu\nu}$. The tensor $W_{\mu\nu}$ depends on the polarisations λ, λ'. We will need to discuss the case where $\lambda \neq \lambda'$ to describe an arbitrary target polarisation, even though it appears that only $\lambda = \lambda'$ occurs in eq. (2.18).

The most general polarisation state of a spin J target in its rest frame can be written as a density matrix

$$\rho = \sum_{\lambda=-J}^{J}\;\sum_{\lambda'=-J}^{J} \left|\lambda\right\rangle \rho_{\lambda\lambda'} \left\langle\lambda'\right|. \tag{2.26}$$

The states $|\lambda\rangle$ and $|\lambda'\rangle$ transform as the spin-J representation under the rotation group. Thus the density matrix ρ transforms under the representation $J\otimes J = 0\oplus 1\oplus\ldots\oplus 2J$. The density matrix of a spin-J target can thus be described by $2J+1$ irreducible tensors.

The polarisation density matrix fo spin $J = 1/2$ can be decomposed into irreducible tensors of spin 0 and 1, *i.e.* by a scalar and a vector. It is easy to see that one can define a scalar and a vector from ρ by

$$\rho_{\text{scalar}} \equiv \mathrm{Tr}\,\rho = 1, \qquad \vec{\rho}_{\text{vector}} \equiv \mathrm{Tr}\,\rho\,\vec{\sigma} = \vec{s}_h/M, \tag{2.27}$$

which defines $\vec{s}_h$. ρ can be expressed in terms of these irreducible tensors,

$$\rho = \frac{1}{2}\left(1+\vec{\sigma}\cdot\frac{\vec{s}_h}{M}\right). \tag{2.28}$$

A spin-1/2 polarised target can be described by an axial vector s_h, which has been defined with an additional factor of the target mass M for the same reasons that we absorbed a factor of the leptonic mass into the lepton polarisation vector s_ℓ. The magnitude of $\vec{s}_h$ depends on the degree of polarisation of the target; for an unpolarised target, $\vec{s}_h = 0$, for a 100% polarised target, $|\vec{s}_h| = M$, and for a target with fractional polarisation f, $|\vec{s}_h| = fM$. The four vector s_h^μ is defined to be $(0, \vec{s}_h)$ in the rest frame of the target, and is defined in other reference frames by a Lorentz boost.

The tensor $W_{\mu\nu}(p,q,s_h)$ for a spin-1/2 target is defined by

$$W_{\mu\nu}(p,q,s_h) = \sum_{\lambda,\lambda'} \rho_{\lambda\lambda'}\,W_{\mu\nu}(p,q,\lambda'\lambda) = \mathrm{Tr}\,\rho\,W_{\mu\nu} \tag{2.29}$$

treating $W_{\mu\nu}$ as a matrix in spin space with labels λ, λ'. Thus the most general tensor $W_{\mu\nu}$ for a spin-1/2 target can be written as a function of the vectors p, q and s_h. Note that s_h contains the spin information of both the initial and final state spinors through the decomposition of the density matrix eq. (2.28). Thus s_h can only occur *linearly* in $W_{\mu\nu}$; there are no terms with two factors of s_h. This is specific for $J = 1/2$ targets.

The deep inelastic structure functions are obtained by writing down the most general tensor decomposition of $W_{\mu\nu}$ using parity P, time reversal T invariance, hermicity of currents and the density matrix as well as antisymmetry of commutator and translational invariance. The invariance under parity implies:

$$W^{\mu\nu}(p,q,s_h) = W^{\mu_P \nu_P}(p_P, q_P, (s_h)_P) \tag{2.30}$$

where $q_P = (q^0, -\vec{q})$, $(s_h)_P = (-s_h^0, \vec{s}_h)$ (with $q_P \cdot x_P = q \cdot x$) and $\mu_P = \mu$ for $\mu = 0$, and $\mu_P = -\mu$ for $\mu = 1,2,3$. Time reversal invariance can be written as

$$W^{\mu\nu}(p,q,s_h) = W^{\mu_T \nu_T}(p_T, q_T, (s_h)_T)^* \tag{2.31}$$

with $p_T = (p^0, -\vec{p})$, $x_T = (-t, \vec{x})$ and $(s_h)_T = (s_h^0, -\vec{s}_h)$. The hermicity condition leads to

$$W^{\mu\nu}(p,q,s_h)^* = W^{\nu\mu}(p,q,s_h). \tag{2.32}$$

Note that all three identities, Eqs. (2.30-2.32) relate $W^{\mu\nu}$ for q^0 to a transformed $W^{\mu\nu}$ at the same value of q^0. There is a final identity that relates $W_{\mu\nu}$ for $q^0 > 0$ to $W_{\mu\nu}$ for $q^0 < 0$ which follows from the antisymmetry of the commutator and translation invariance:

$$W^{\mu\nu}(p,q,s_h) = -W^{\nu\mu}(p,-q,s_h). \tag{2.33}$$

This identity is the photon crossing symmetry identity for $W_{\mu\nu}$, since exchanging $\mu\nu$ and letting $q \to -q$ is equivalent to exchanging the outgoing and incoming photons. Finally current conservation, $\partial_\mu j^\mu(x) = 0$, implies that

$$q_\mu W^{\mu\nu}(p,q,s_h) = q_\nu W^{\mu\nu}(p,q,s_h) = 0, \tag{2.34}$$

which greatly restricts the possible tensor structures allowed for $W_{\mu\nu}$.

The most general hadronic tensor for polarised deep inelastic scattering from spin-1/2 targets can be written in terms of p, q, s_h and the invariant tensors $g_{\alpha\beta}$ and $\epsilon_{\alpha\beta\lambda\sigma}$ with the constraints Eqs. (2.30–2.34). The algebra is straightforward but tedious. It is conventional to write $W_{\mu\nu}$ in the form

$$\begin{aligned} W_{\mu\nu} &= F_1 \left(-g_{\mu\nu} + \frac{q_\mu q_\nu}{q^2}\right) + \frac{F_2}{p\cdot q}\left(p_\mu - \frac{p\cdot q\; q_\mu}{q^2}\right)\left(p_\nu - \frac{p\cdot q\; q_\nu}{q^2}\right) \\ &+ \frac{i g_1}{p\cdot q}\, \epsilon_{\mu\nu\lambda\sigma} q^\lambda s^\sigma + \frac{i g_2}{(p\cdot q)^2}\, \epsilon_{\mu\nu\lambda\sigma} q^\lambda \left(p\cdot q\, s^\sigma - s\cdot q\, p^\sigma\right) \ , \end{aligned} \tag{2.35}$$

where the coefficients of the different tensor structures are called structure functions. The leptonic current is also conserved, so that $q^\mu \ell_{\mu\nu} = q^\nu \ell_{\mu\nu} = 0$. Thus it is convenient to simplify the expression for $W_{\mu\nu}$ by omitting all q_μ and q_ν terms before contracting with $\ell_{\mu\nu}$,

$$W_{\mu\nu} = -F_1\, g_{\mu\nu} + \frac{F_2}{p\cdot q}\, p_\mu p_\nu + \frac{i g_1}{\nu}\, \epsilon_{\mu\nu\lambda\sigma} q^\lambda s_h^\sigma + \frac{i g_2}{\nu^2}\, \epsilon_{\mu\nu\lambda\sigma} q^\lambda \left(p\cdot q\, s_h^\sigma - s_h\cdot q\, p^\sigma\right) \ . \tag{2.36}$$

For a spin-1/2 target, the symmetric part of $W_{\mu\nu}$ is independent of the hadron spin, and the spin dependent part of $W_{\mu\nu}$ is antisymmetric in $\mu\nu$. Thus the combination $W^{\mu\nu}\ell_{\mu\nu}$ has no terms which have only the hadron spin, or only the lepton spin; all terms contain either both or none. Thus the structure functions F_1 and F_2 can be measured using an unpolarised beam and target, but to measure the structure functions g_1 and g_2 requires both a polarised beam and a polarised target. There is no advantage to doing an experiment with only a polarised beam or only a polarised target. This is not true for target spins greater than 1/2 (see Sect. 2.7).

The cross-section can now be obtained by combining the expressions eq. (2.36) for $W_{\mu\nu}$, eq. (2.12) for $\ell_{\mu\nu}$, eq. (2.18) for the cross-section, and using the identity

$$\epsilon^{\mu\nu\alpha\beta}\epsilon_{\mu\nu\lambda\sigma} = -2\left(g^\alpha_\lambda g^\beta_\sigma - g^\alpha_\sigma g^\beta_\lambda\right), \tag{2.37}$$

$$\begin{aligned} \frac{d^2\sigma}{dx\,dy\,d\phi} &= \frac{e^4 ME}{4\pi^2 Q^4}\Big[\, xy^2 F_1 + (1-y)F_2 + y^2 g_1\left(2x\,\frac{s_\ell\cdot s_h}{p\cdot q} + \frac{q\cdot s_\ell}{p\cdot q}\frac{q\cdot s_h}{p\cdot q}\right) \\ &+ 2xy^2 g_2\left(\frac{s_h\cdot s_\ell}{p\cdot q} - \frac{p\cdot s_\ell}{p\cdot q}\frac{q\cdot s_h}{p\cdot q}\right)\Big] \ . \end{aligned} \tag{2.38}$$

As mentioned earlier, the spin dependent terms involve both s_ℓ and s_h. Let us look at the cross-section for the two cases which are most interesting for current experiments, a longitudinally polarised lepton beam incident on a target which is either longitudinally or transversely polarised. For a longitudinally polarised lepton beam, the polarisation is $s_\ell = \mathcal{H}_\ell k$, where $\mathcal{H}_\ell = \pm$ is the lepton helicity. The lepton polarisation terms in eq. (2.38) can be written as

$$\frac{q \cdot s_\ell}{p \cdot q} = -\mathcal{H}_\ell\, x, \qquad \frac{p \cdot s_\ell}{p \cdot q} = \frac{\mathcal{H}_\ell}{y}, \qquad \frac{s_h \cdot s_\ell}{p \cdot q} = \mathcal{H}_\ell\, \frac{s_h \cdot k}{p \cdot q}. \tag{2.39}$$

A target polarised along the incident beam direction has $\vec{s}_h = M\mathcal{H}_h \hat{z}$, where $\mathcal{H}_h = \pm$ for a target polarised parallel or antiparallel to the beam. s_h is dotted into either q or k both of which have 0 and 3 components which are almost equal. Thus s_h can be replaced by $-\mathcal{H}_h\, p$ and we obtain the cross section for the longitudinally polarised target

$$\frac{d^2\sigma}{dx\, dy} = \frac{e^4 ME}{2\pi Q^4}\left[xy^2 F_1 + (1-y)F_2 - \mathcal{H}_\ell \mathcal{H}_h y(2-y)x g_1 + \mathcal{O}\left(M^2/Q^2\right)\right] . \tag{2.40}$$

The polarisation vector of a transversely polarised target can be chosen to point along the $\hat{x}$ axis. In this case

$$\frac{d^2\sigma}{dx\, dy\, d\phi} = \frac{e^4 ME}{4\pi^2 Q^4}\left[xy^2 F_1 + (1-y)F_2 + 2x^2\, \mathcal{H}_\ell \mathcal{H}_h\, \frac{M}{Q}\sqrt{1-y}\, \cos\phi\, \left(g_1 y + 2 g_2\right)\right], \tag{2.41}$$

where eq. (2.8) is used for the magnitude of the transverse component of q. The structure functions g_1 and g_2 are equally important for a transversely polarised target, and so an experiment with a transversely polarised target can be used to determine g_2 (by studying the $\cos\phi$ dependence of the polarisation asymmetry), once g_1 has been measured using a longitudinally polarised target. Note that the spin-dependent piece of the cross-section for a transversely polarised target is smaller than the spin-averaged piece by a factor of M/Q, unlike in eq. (2.40) where both terms are comparable in magnitude.

2.5 Structure functions and optical theorem

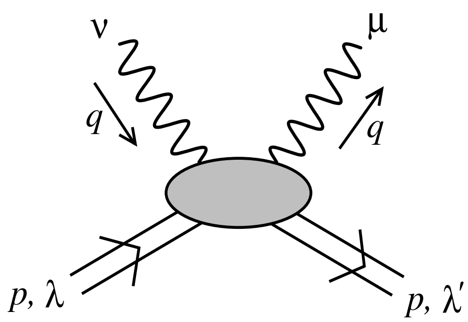

Figure 4: Forward Compton scattering amplitude

To interpret the structure function, it is useful to look at the amplitude for forward Compton scattering off a hadron target (see fig. 4)

$$(T_{\mu\nu}(p,q,\lambda'\lambda) = i\int d^4x\, e^{iq\cdot x}\, \langle p,\lambda'|\, T\left(j_\mu(x) j_\nu(x)\right) |p,\lambda\rangle\ . \tag{2.42}$$

The tensor $T_{\mu\nu}(p,q,s_h)$ can be written in terms $(T_{\mu\nu})(p,q,\lambda',\lambda)$ by analogy with eq. (2.29),

$$T_{\mu\nu}(p,q,s_h) = \sum_{\lambda,\lambda'} \rho_{\lambda\lambda'}\, T_{\mu\nu}(p,q,\lambda',\lambda) = \mathrm{Tr}\, \rho\, T_{\mu\nu}\ . \tag{2.43}$$

The tensor $T_{\mu\nu}(p,q,s_h)$ has the same symmetry properties as $W_{\mu\nu}(p,q,s_h)$, Eqs. (2.30), (2.31), (2.32), and the current conservation constraint eq. (2.34). Thus $T_{\mu\nu}(p,q,s_h)$ can be expanded in the same tensors as $W_{\mu\nu}$. The structure functions for $T_{\mu\nu}(p,q,s_h)$ will be denoted by a tilde to distinguish them for the corresponding structure functions for $W_{\mu\nu}$:

$$\begin{aligned} T_{\mu\nu} &= \widetilde{F}_1\left(-g_{\mu\nu}+\frac{q_\mu q_\nu}{q^2}\right)+\frac{\widetilde{F}_2}{p\cdot q}\left(p_\mu-\frac{p\cdot q\; q_\mu}{q^2}\right)\left(p_\nu-\frac{p\cdot q\; q_\nu}{q^2}\right) \\ &\quad +\frac{i\,\widetilde{g}_1}{p\cdot q}\,\epsilon_{\mu\nu\lambda\sigma}q^\lambda s^\sigma+\frac{i\,\widetilde{g}_2}{(p\cdot q)^2}\,\epsilon_{\mu\nu\lambda\sigma}q^\lambda\left(p\cdot q\, s^\sigma-s\cdot q\, p^\sigma\right). \end{aligned} \tag{2.44}$$

The photon crossing symmetry relation

$$T_{\mu\nu}(p,q,s_h)=T_{\nu\mu}(p,-q,s_h) \tag{2.45}$$

implies that $\widetilde{F}_1$ is an even function of ω, and $\widetilde{F}_2$, $\widetilde{g}_1$, and $\widetilde{g}_2$ are odd functions of ω,

$$\widetilde{F}_1(-\omega)=\widetilde{F}_1(\omega)\quad \widetilde{F}_2(-\omega)=-\widetilde{F}_2(\omega)\quad \widetilde{g}_1(-\omega)=-\widetilde{g}_1(\omega)\quad \widetilde{g}_2(-\omega)=-\widetilde{g}_2(\omega)\,. \tag{2.46}$$

Now the optical theorem tells us that twice the imaginary part of the forward scattering amplitude is the total cross-section. Using our conventions for $W_{\mu\nu}$ and $T_{\mu\nu}$ this theorem leads to

$$\mathrm{Im}\, T_{\mu\nu}=2\pi W_{\mu\nu}\,. \tag{2.47}$$

A graphical representation is shown in fig. 5 and the analytic structure is presented in fig. 6. The discontinuity

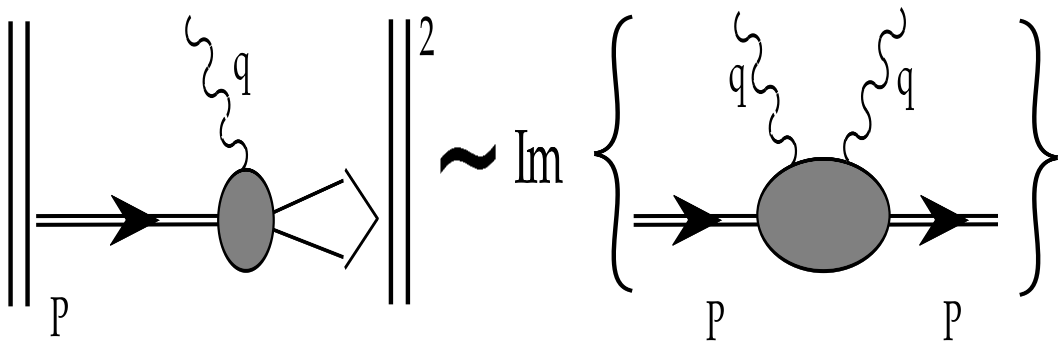

Figure 5: Optical theorem relating the hadronic tensor $W_{\mu\nu}$ to the imaginary part of forward virtual Compton scattering.

across the cuts $1\le|\omega|\le\infty$ is related to $W_{\mu\nu}$, the same is true for the structure functions. The discontinuity across the right/left hand cut gives the hadronic tensor $W_{\mu\nu}$ for nucleon/antinucleon targets.

2.6 Naive parton model

In the parton model the hadron target is considered to be made up of a number of free on-shell partons (quarks and gluons) in the deep inelastic limit. The scattering cross-section can then be computed in terms of the incoherent scattering of free quarks and gluons. The hadronic tensor $W_{\mu\nu}$ can be computed in terms of parton distribution functions. For example, the distribution function $u_\uparrow(\xi)$ is the probability to find an up quark in the hadron with polarisation parallel to that of the hadron, and momentum ξp. It is conventional to go to an infinite momentum frame to neglect target mass effects. Instead of using the infinite momentum frame, one can work in the rest frame of the target neglecting all target mass effects.

To lowest order in the strong interactions, only quarks scatter off the virtual photon, since gluons do not have electric charge. The contribution to $W_{\mu\nu}$ from a single polarised quark can be computed from the Feynman graph of fig. 7.

The computation of the scattering amplitude can be obtained from $\ell_{\mu\nu}$, eq. (2.12), by the replacements $k\to\xi p$, $k'\to p'$, $s_\ell\to s$ and $q\to -q$ assuming a quark charge one. Comparing eq. (2.12) and eq. (2.16), we

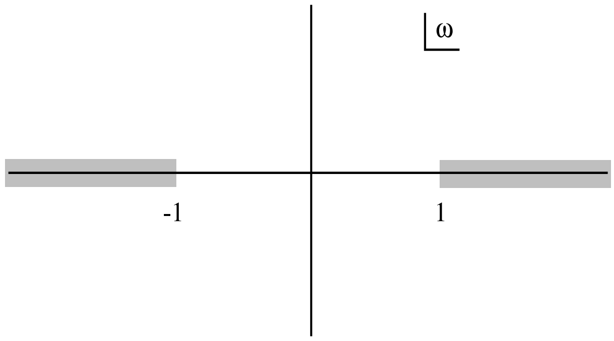

Figure 6: Analytic structure of $T_{\mu\nu}$ in the complex ω plane.

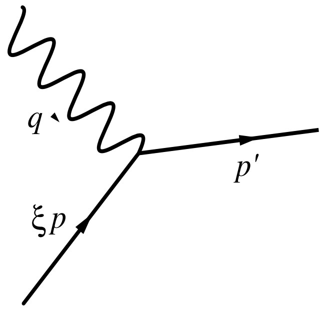

Figure 7: Contribution to $W_{\mu\nu}$ from a single quark with momentum fraction ξ.

see that $W_{\mu\nu}$ has an additional factor of integration over the final particle phase space. Thus we find

$$\begin{aligned} W_{\mu\nu} &= \frac{1}{4\pi}\mathcal{Q}^2 \int \frac{d^3p'}{(2\pi)^3 2E_{p'}} \, \frac{1}{\xi} \, (2\pi)^4 \delta^4(\xi p + q - p') \\ &\quad \times 2\left[\xi p^\mu p'^\nu + \xi p^\nu p'^\mu - g^{\mu\nu}\xi p\cdot p' + i\epsilon^{\mu\nu\alpha\beta} q_\alpha s_\beta\right] \,. \end{aligned} \tag{2.48}$$

The origin of the factor $1/\xi$ is that the proton states in $W_{\mu\nu}$ are normalised to $2p^0$, whereas the parton states in eq. (2.48) are normalised to $2p^0\xi$ what effects the particle flux. The integral in eq. (2.48) is easily done using the identity

$$\int \frac{d^3p'}{(2\pi)^3 2E_{p'}} = \int \frac{d^4p'}{(2\pi)^4} \, (2\pi)\, \delta\left((\xi p + q - p')^2\right) = \int \frac{d^4p'}{(2\pi)^4} \, \frac{(2\pi)}{2p\cdot q} \, \delta\left(\xi + \frac{q^2}{2p\cdot q}\right) \,. \tag{2.49}$$

Since the partons are massless, $s_\beta = h\xi p_\beta$, where h is the helicity of the parton, so that

$$\begin{aligned} W_{\mu\nu} &= \frac{1}{2\xi \; p\cdot q}\left[\xi p^\mu p'^\nu + \xi p^\nu p'^\mu - g^{\mu\nu}\xi p\cdot p' + ih\xi\,\epsilon^{\mu\nu\alpha\beta} q_\alpha p_\beta\right]\delta(\xi - x)\,, \\ &= \frac{1}{2\xi \; p\cdot q}\left[2\xi^2 p^\mu p^\nu - g^{\mu\nu}\xi p\cdot q + ih\xi\,\epsilon^{\mu\nu\alpha\beta} q_\alpha p_\beta\right]\delta(\xi - x)\,, \end{aligned} \tag{2.50}$$

where p' has been replaced by $\xi p + q$, and the q^μ and q^ν terms have been dropped. To compare with $W_{\mu\nu}$, we need eq. (2.36) neglecting target mass effects. Thus the target spin s_h in eq. (2.36) can be replaced by

$\mathcal{H}p$, where $\mathcal{H}$ is the helicity of the target, and p is the target momentum. We find that the contribution of quarks to the structure functions is (for quark charge squared one)

$$F_1 = \frac{1}{2}\delta(\xi - x), \quad F_2 = \xi\,\delta(\xi - x), \quad g_1 = \frac{1}{2}h\mathcal{H}\,\delta(\xi - x), \quad g_2 = 0\,. \tag{2.51}$$

The antiquark contribution can be computed similarly, and is identical to the quark contribution.

The total structure function is obtained by integrating with the quark distribution functions, $q_+(\xi)$ (the probability to find a quark in the nucleon with momentum fraction ξ and helicity equal to that of the nucleon ($h\mathcal{H} = +$)) and $q_-(\xi)$ (the probability to find a quark in the nucleon with momentum fraction ξ, and helicity opposite to that of the nucleon ($h\mathcal{H} = -$)) and the antiquark distribution functions $\overline{q}_\pm(\xi)$ and weighting by the square of the quak charge Q_q^2 of flavour q:

$$\begin{aligned} F_1(x,Q^2) &= \sum_q \frac{Q_q^2}{2}\left(q_+(x) + q_-(x) + \overline{q}_+(x) + \overline{q}_-(x)\right)\,, \\ F_2(x,Q^2) &= \sum_q Q_q^2\, x\,\left(q_+(x) + q_-(x) + \overline{q}_+(x) + \overline{q}_-(x)\right)\,, \end{aligned} \tag{2.52}$$

$$\begin{aligned} g_1(x,Q^2) &= \sum_q \frac{Q_q^2}{2}\left(q_+(x) - q_-(x) + \overline{q}_+(x) - \overline{q}_-(x)\right)\,, \\ g_2(x,Q^2) &= 0\,, \end{aligned} \tag{2.53}$$

where the sum is over all quark flavours which can be considered light compared with Q^2. The most important feature of this result is that the structure functions depend only on x, and are independent of Q^2. We also see that the structure functions satisfy the Callan-Gross relation,

$$F_2(x) = 2xF_1(x) \quad \Rightarrow \quad F_L(x) = 0\,. \tag{2.54}$$

F_1 is the probability to find a quark in the hadron with momentum fraction x, and g_1 is the difference in probabilities to find a quark in the hadron with momentum fraction x with spin parallel and antiparallel to the hadron. Both quantities weight each quark flavour by the square of the electric charge. The combination $F_1(x) - g_1(x)$ depends only on $q_-(x)$, $F_1(x) + g_1(x)$ only on $q_+(x)$ There is no simple interpretation for g_2 in the parton model.

2.7 Hadronic tensor for spin $J = 1$ target

For a spin-0 target like the pion, the kinematical framework is simpler than in the familiar nucleon case. The details for the case of a polarised spin-1 particle have been worked out by Hoodbhoy et al. [3]. The hadronic tensor (imaginary part of the forward current-hadron scattering amplitude) defined in eq. (2.13) decomposes now into eight structure functions:

$$\begin{aligned} W_{\mu\nu} &= -F_1 g_{\mu\nu} + F_2\frac{p_\mu p_\nu}{p\cdot q} - b_1 r_{\mu\nu} + \frac{1}{6}b_2(s_{\mu\nu} + t_{\mu\nu} + u_{\mu\nu}) + \frac{1}{2}b_3(s_{\mu\nu} - u_{\mu\nu}) \\ &\quad + \frac{1}{2}b_4(s_{\mu\nu} - t_{\mu\nu}) + \mathrm{i}\frac{g_1}{\nu}\epsilon_{\mu\nu\lambda\sigma}q^\lambda s^\sigma + \mathrm{i}\frac{g_2}{\nu^2}\epsilon_{\mu\nu\lambda\sigma}q^\lambda(p\cdot q s^\sigma - s\cdot q p^\sigma)\,, \end{aligned} \tag{2.55}$$

where $r_{\mu\nu}$, $s_{\mu\nu}$, $t_{\mu\nu}$, $u_{\mu\nu}$ are kinematical tensors [3] constructed from the momentum transfer q and the polarisation vector ϵ. The latter satisfies $\epsilon\cdot p = 0$, $\epsilon^2 = -M^2$ (some relation for them are collected in App. A, and

$$s^\sigma = \frac{-\mathrm{i}}{M^2}\epsilon^{\sigma\alpha\beta\tau}\epsilon^*_\alpha\epsilon_\beta p_\tau \quad , \tag{2.56}$$

with M being the hadron mass. Here $\epsilon^{\mu\nu\lambda\sigma}$ is the completely antisymmetric tensor with $\epsilon^{0123} = -1$. Differently to spin-1/2 target, there is a target polarisation dependence in the symmetric part of $W_{\mu\nu}$, which can be measured using a polarised target and an unpolarised beam.

The structure functions F_1, F_2, g_1, and g_2 play the same role as for a spin-1/2 target. In the parton model, the structure of the hadron can be described by the probability $q_\uparrow^m(x)$ ($q_\downarrow^m(x)$) of finding a quark with momentum fraction x and spin up (down) along the direction of motion when the hadron is moving with infinite momentum and has spin projection $m = 0, \pm 1$. Symmetry implies

$$q_\uparrow^1(x) = q_\downarrow^{-1}(x), \qquad q_\downarrow^1(x) = q_\uparrow^{-1}(x) \quad ,$$

$$q_\uparrow^0(x) = q_\downarrow^0(x) \quad , \tag{2.57}$$

so there remain only three independent parton distribution functions $q_\uparrow^1(x)$, $q_\downarrow^1(x)$, and $q_\uparrow^0(x)$. In leading order, the single-flavour structure function $F_1^{(q)}(x)$ is one half of the probability to find a quark q with momentum fraction x, and $F_2^{(q)}(x)$ obeys the Callan-Gross relation:

$$\begin{aligned} F_1^{(q)}(x) &= \frac{1}{3}\left(q_\uparrow^1(x) + q_\downarrow^1(x) + q_\uparrow^0(x)\right) \quad , \\ F_2^{(q)}(x) &= 2xF_1^{(q)}(x) \quad . \end{aligned} \tag{2.58}$$

In the complete structure function, $F_1^{(q)}(x)$ is weighted by the electric charge Q_q of the quarks:

$$F_1(x) = \sum_q Q_q^2 F_1^{(q)}(x) \quad . \tag{2.59}$$

In the following, we will only specify single-flavour structure functions and omit the superscript (q). For the mesons under consideration, the structure functions are identical for both flavours. The polarised structure function $g_1(x)$ gives the fraction of spin carried by quarks:

$$g_1(x) = \frac{1}{2}\left[q_\uparrow^1(x) - q_\downarrow^1(x)\right] \quad . \tag{2.60}$$

The structure function $g_2(x)$ does not have a parton model interpretation.

The structure functions $b_1(x)$, $b_2(x)$, $b_3(x)$, and $b_4(x)$ are particular to spin-1 targets as the kinematical factors in eq. (2.55) involve the target polarisation vector to second order, a feature that does not occur for spin-1/2 targets. In parton model language $b_1(x)$ and $b_2(x)$ depend on the quark-spin averaged distributions $q^m = \frac{1}{2}(q_\uparrow^m + q_\downarrow^m)$ only:

$$b_1(x) = q^0(x) - q^1(x) \quad , \tag{2.61}$$

$$b_2(x) = 2xb_1(x) \quad . \tag{2.62}$$

Thus $b_1(x)$ and $b_2(x)$ measure the difference in parton distributions of an $m = 1$ and $m = 0$ target. This difference is due to the fact that in quantum field theory any Lorentz boost changes the particle content of a state. These changes differ for different spin orientations relative to the boost direction.

3 Operator product expansion

3.1 OPE and twist

The parton model provides an interpretation for the deep inelastic structure functions. In the following we will derive sum rules for the moments of structure functions directly from QCD using the operator product expansion (OPE).

The starting point in the derivation is the time-ordered product of two currents

$$t_{\mu\nu} \equiv i \int d^4x\, e^{iq\cdot x} T\left(j_\mu(x) j_\nu(0)\right) . \tag{3.1}$$

The nucleon matrix element of $t_{\mu\nu}$ gives the familiar Compton amplitude $T_{\mu\nu}$ (eq. (2.42). OPE allows to calculate $T_{\mu\nu}$. Consider the product of two local operators,

$$\mathcal{O}_a(x)\ \mathcal{O}_b(0) . \tag{3.2}$$

In the limit that $x \to 0$, where the operators are at practically the same point, the operator product can be written as an expansion in local operators,

$$\lim_{x\to 0} \mathcal{O}_a(x)\ \mathcal{O}_b(0) = \sum_k c_{abk}(x)\ \mathcal{O}_k(0) . \tag{3.3}$$

The coefficient functions depend on the separation x. The left hand side is completely equivalent to the right hand side as long as one does not probe the operator product on distance scales which are small compared with the separation x.

Thus one can replace the product $\mathcal{O}_a(x)\mathcal{O}_b(0)$ in the computation of matrix elements by the expansion eq. (3.3) where the coefficients $c_{abk}(x)$ are independent of the matrix elements, provided that the external states have momentum components which are small compared with the separation x. In QCD, the coupling constant is small at short distances because of asymptotic freedom. Therefore, the coefficient functions can be computed in perturbation theory, since all nonperturbative effects occur at scales which are much larger than x.

The momentum space version of OPE is for the product

$$\int d^4x\, e^{iq\cdot x}\ \mathcal{O}_a(x)\ \mathcal{O}_b(0)\,. \tag{3.4}$$

In the limit that $q \to \infty$, the Fourier transform in eq. (3.1) forces $x \to 0$, and again the operator product can be expanded in terms of local operators with coefficient functions that depend on q,

$$\lim_{q\to\infty} \int d^4x\, e^{iq\cdot x}\ \mathcal{O}_a(x)\ \mathcal{O}_b(0) = \sum_k c_{abk}(q)\ \mathcal{O}_k(0)\,. \tag{3.5}$$

This expansion is valid for all matrix elements, provided q is much larger than the characteristic momentum in any of the external states ($\Lambda_{\rm QCD}$).

The local operators in the operator product expansion for QCD are quark and gluon operators with arbitrary dimension d and spin n. An operator with spin n and dimension d can be written as

$$\mathcal{O}_{d,n}^{\mu_1\ldots\mu_n}\,, \tag{3.6}$$

where $\mathcal{O}_{d,n}$ is symmetric and traceless in $\mu_1 \ldots \mu_n$. The matrix element of $\mathcal{O}_{d,n}$ in the hadron target is proportional to

$$M^{d-n-2}\ \mathcal{S}\left[p^{\mu_1}\ldots p^{\mu_n}\right], \tag{3.7}$$

for a vector operator, and to

$$M^{d-n-2}\ \mathcal{S}\left[s^{\mu_1}p^{\mu_2}\ldots p^{\mu_n}\right]\,, \tag{3.8}$$

for an axial operator. $\mathcal{S}$ acts on a tensor to project out the completely symmetric traceless component. The power of M follows from dimensional analysis, since a hadron state with the conventional relativistic normalisation has dimension minus one.

The coefficient functions in the operator product expansion are functions only of q. Thus the free indices on the operator $\mathcal{O}$ must be either μ,ν, or be contracted with q^α. Every index on $\mathcal{O}$ contracted with q^α produces a factor of $p\cdot q$ (or $s\cdot q$) which is of order Q^2/M in the deep inelastic limit. An index μ or ν is contracted with $\ell_{\mu\nu}$, and produces a factor of $p\cdot k$ or $p\cdot k'$ (or $s\cdot k$ or $s\cdot k'$), both of which are also of order Q^2/M in the deep inelastic limit. In addition, since $t_{\mu\nu}$ has dimension two, the coefficient of $\mathcal{O}$ must have dimension Q^{2-d} in the operator product expansion. Thus the contribution of any operator $\mathcal{O}$ to $W_{\mu\nu}\ell^{\mu\nu}$ is of order

$$\begin{aligned}
c_{\mu_1\ldots\mu_n}\mathcal{O}_{d,n}^{\mu_1\ldots\mu_n} &\to \frac{q_{\mu_1}}{Q}\cdots\frac{q_{\mu_n}}{Q}\ Q^{2-d}\,\langle\mathcal{O}_d^{\mu_1\ldots\mu_n}\rangle\,,\\
&\to \frac{q_{\mu_1}}{Q}\cdots\frac{q_{\mu_n}}{Q}\ Q^{2-d}M^{d-n-2}\ p^{\mu_1}\ldots p^{\mu_n}\,,\\
&\to \frac{(p\cdot q)^n}{Q^n}\ Q^{2-d}\ M^{d-n-2}\,,\\
&\to \omega^n\left(\frac{Q}{M}\right)^{2+n-d} = \omega^n\left(\frac{Q}{M}\right)^{2-t}\,,
\end{aligned} \tag{3.9}$$

where the twist t is defined as

$$\text{twist} = t = d-n = \text{dimension} - \text{spin}. \tag{3.10}$$

The most important operators in OPE are those with the lowest possible twist. Twist two operators contribute a finite amount to the structure functions in the deep inelastic limit, twist three contributions are suppressed by M/Q, *etc.*

3.2 QCD operators of twist 2

The fundamental fields in QCD are quark and gluon fields, so the operators in the operator product expansion can be written in terms of quark fields ψ, the gluon field strength $F_{\mu\nu}$ and the covariant derivative D^μ. We can make a table listing the basic objects, with their dimension and twist:

	ψ	$F_{\mu\nu}$	D^μ
d	3/2	2	1
n	1/2	1	1
t	1	1	0

Any gauge invariant operator must contain at least two quark fields, or two gluon field strength tensors. Thus the lowest possible twist is two. A twist two operator has either two ψ's or two $F_{\mu\nu}$'s and an arbitrary number of covariant derivatives. The indices of the covariant derivatives are not contracted, because an operator such as D^2 has twist two, whereas $D^\alpha D^\beta$ has twist zero.

In order to perform OPE, all linearly independent operators that can occur have to be found. The Lorentz structure of the quark operators must be either $\overline{\psi}\gamma^\mu\psi$ or $\overline{\psi}\gamma^\mu\gamma_5\psi$ in the limit that light quark masses can be neglected, because the operator $j^\mu j^\nu$ does not change chirality.

For unpolarised DIS we use as conventional basis for twist two quark and gluon operators

$$\mathcal{O}^{(f,V)}_{\mu_1\ldots\mu_n} = G_{ff'}\left(\frac{i}{2}\right)^{n-1}\overline{\psi}^{(f)}\gamma_{\mu_1}\overleftrightarrow{D}_{\mu_2}\ldots\overleftrightarrow{D}_{\mu_n}\psi^{(f)} - \text{traces}\,, \tag{3.11}$$

$$\mathcal{O}^{(g,V)}_{\mu_1\ldots\mu_n} = i^{n-2}\,\mathrm{Tr}\,F^{\alpha}_{\;\;\mu_1}D_{\mu_2}\ldots D_{\mu_{n-1}}F_{\alpha\mu_n} - \text{traces} \tag{3.12}$$

where $\psi^{(f)}$ denote the quark fields of given flavour, $F_{\alpha\beta}$ is the gluon field strength tensor and the covariant derivatives D_μ and $\overleftrightarrow{D}_\mu=\overrightarrow{D}_\mu - \overleftarrow{D}_\mu$, $G_{ff'}$ is a suitably chosen diagonal flavour matrix. Taking into account polarisation, the following towers of operators have to be added

$$\mathcal{O}^{(f,5)}_{\sigma\mu_1\ldots\mu_n} = G_{ff'}\left(\frac{i}{2}\right)^{n}\overline{\psi}^{(f)}\gamma_\sigma\gamma_5\overleftrightarrow{D}_{\mu_1}\ldots\overleftrightarrow{D}_{\mu_n}\psi^{(f)} - \text{traces}\,, \tag{3.13}$$

$$\mathcal{O}^{(g,5)}_{\sigma\mu_1\ldots\mu_n} = i^{n-1}\,\mathrm{Tr}\,\widetilde{F}^{\alpha}_{\;\;\sigma}D_{\mu_1}\ldots D_{\mu_{n-1}}F_{\alpha\mu_n} - \text{traces} \tag{3.14}$$

with the dual field strength tensor $\widetilde{F}_{\alpha\beta} = \frac{1}{2}\epsilon_{\alpha\beta\gamma\delta}F^{\gamma\delta}$. All operators are given in Minkowski space.

3.3 Example for determination of a coefficient function

The next step in doing an OPE is to determine the coefficient functions of the operators. The best way to do this to to evaluate enough on-shell matrix elements to determine all the coefficients. Since we have argued that the coefficients can be computed reliably in QCD perturbation theory, we will evaluate the coefficients by taking matrix elements in on-shell quark and gluon states. We will illustrate here the computation of the coefficients to lowest non-trivial order (*i.e.* $(\alpha_s)^0$). The generic term in the operator product expansion can be written as

$$jj \sim c_q\mathcal{O}_q + c_g\mathcal{O}_g\,, \tag{3.15}$$

where q and g refer to quark and gluon operators. Taking the matrix element of both sides in a free quark state, gives

$$\langle q|\,jj\,|q\rangle \sim c_q\,\langle q|\,\mathcal{O}_q\,|q\rangle + c_g\,\langle q|\,\mathcal{O}_g\,|q\rangle\;. \tag{3.16}$$

The electromagnetic current is a quark operator. Thus the left hand side is of order $(\alpha_s)^0$. The matrix element $\langle q|\,\mathcal{O}_q\,|q\rangle$ is also of order $(\alpha_s)^0$, whereas the matrix element $\langle q|\,\mathcal{O}_g\,|q\rangle$ is of order $(\alpha_s)^1$ since there are at least two gluons in $\mathcal{O}_g$, each of which contributes a factor of the QCD coupling constant g to the matrix element. Thus one can determine c_q to leading order by taking the quark matrix element of both sides of the operator product expansion, neglecting the gluon operators. For simplicity we use a theory with a single quark flavour with charge one.

The quark matrix element of the left hand side of the operator product expansion, eq. (3.15), is given by the Feynman graphs in fig. 8,

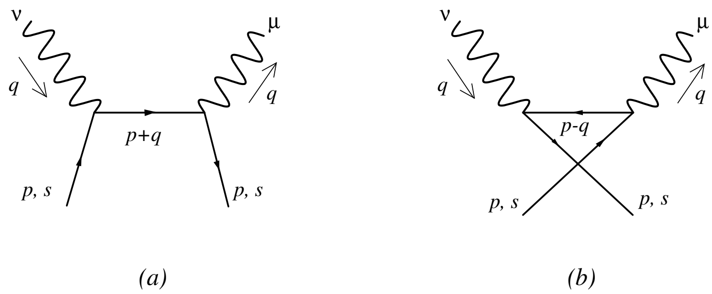

Figure 8: Lowest order diagrams contributing to the quark matrix element of the product of two electromagnetic currents.

$$\mathcal{M}^{\mu\nu} = i\,\overline{u}(p,s)\,\gamma^\mu\, i\frac{\not{p}+\not{q}}{(p+q)^2}\,\gamma^\nu\, u(p,s) + (\mu \leftrightarrow \nu, q \to -q)\,. \tag{3.17}$$

The denominator is transformed to ($p^2 = 0$ for on-shell massless quarks)

$$(p+q)^2 = q^2\,(1-\omega)\ . \tag{3.18}$$

The numerator can be simplified using the γ matrix identity

$$\gamma^\mu\gamma^\alpha\gamma^\nu = g^{\mu\alpha}\gamma^\nu + g^{\nu\alpha}\gamma^\mu - g^{\mu\nu}\gamma^\alpha + i\epsilon^{\mu\nu\alpha\lambda}\gamma_\lambda\gamma_5, \tag{3.19}$$

$$\begin{aligned}\overline{u}(p,s)\gamma^\mu(\not{p}+\not{q})\gamma^\nu u(p,s) \quad &= \quad \overline{u}(p,s)\Big[(p+q)^\mu\gamma^\nu + (p+q)^\nu\gamma^\mu - g^{\mu\nu}\,(\not{p}+\not{q}) \\ &\qquad + i\epsilon^{\mu\nu\alpha\lambda}(p+q)_\alpha\gamma_\lambda\gamma_5\Big]u(p,s)\,.\end{aligned} \tag{3.20}$$

For an on-shell massless quark,

$$\not{p}\; u(p,s) = 0\,, \quad \overline{u}(p,s)\,\gamma_\lambda\, u(p,s) = 2p_\lambda\,, \quad \overline{u}(p,s)\,\gamma_\lambda\gamma_5\, u(p,s) = 2h\, p_\lambda\,, \tag{3.21}$$

where h is the quark helicity. Thus the $\not{p}$ and $\epsilon^{\mu\nu\alpha\lambda}p_\alpha\gamma_\lambda\gamma_5$ terms both give zero.

Combining the various terms, and using

$$(1-\omega)^{-1} = \sum_{n=0}^{\infty}\omega^n, \tag{3.22}$$

gives

$$\mathcal{M}^{\mu\nu}_{\text{direct}} = -\frac{2}{q^2}\sum_{n=0}^{\infty}\omega^n\,\left[(p+q)^\mu p^\nu + (p+q)^\nu q^\mu - g^{\mu\nu}p\cdot q + ih\,\epsilon^{\mu\nu\alpha\lambda}\,q_\alpha p_\lambda\right]\,. \tag{3.23}$$

To complete the operator product expansion, we need the free quark matrix element of the right hand side of the operator product. The matrix element of the quark operators of eq. (3.11) and (3.13) in a free quark state is

$$\langle p,s|\,\mathcal{O}^{(V)}_{\mu_1\cdots\mu_n}\,|p,s\rangle = p_{\mu_1}\ldots p_{\mu_n}\ , \tag{3.24}$$

$$\langle p,s|\,\mathcal{O}^{(5)}_{\mu_1\cdots\mu_n}\,|p,s\rangle = h\;p_{\mu_1}\ldots p_{\mu_n}\ . \tag{3.25}$$

As an example we determine the coefficient functions for the spin dependent term on the left hand side of the operator product

$$\mathcal{M}^{[\mu\nu]} = -\frac{2}{q^2}\sum_{n=0}^{\infty}\omega^n\ ih\,\epsilon^{\mu\nu\alpha\lambda}\,q_\alpha p_\lambda + \ (\mu\leftrightarrow\nu,\ q\to -q,\ \omega\to-\omega)\,, \tag{3.26}$$

since ω is odd in q. The crossed diagram causes half the terms to cancel, so that the matrix element is

$$
\begin{aligned}
\mathcal{M}^{[\mu\nu]} &= -\frac{4}{q^2}\sum_{n=0,2,4}^{\infty} \omega^n \, ih\,\epsilon^{\mu\nu\alpha\lambda}\, q_\alpha p_\lambda = -\frac{4}{q^2}\sum_{n=0,2,4}^{\infty}\left(\frac{-2p\cdot q}{q^2}\right)^n ih\,\epsilon^{\mu\nu\alpha\lambda}\, q_\alpha p_\lambda \,, \\
&= \sum_{n=0,2,4}^{\infty} -\frac{4}{q^2}\,\frac{2^n q^{\mu_1}\ldots q^{\mu_n}}{(-q^2)^n}\, ih\,\epsilon^{\mu\nu\alpha\lambda}\, q_\alpha p_\lambda \, p_{\mu_1}\ldots p_{\mu_n}\,, \qquad (3.27)\\
&= \sum_{n=0,2,4}^{\infty} 2\,\frac{2^{n+1} q^{\mu_1}\ldots q^{\mu_n}}{(-q^2)^{n+1}}\, ih\,\epsilon^{\mu\nu\alpha\mu_{n+1}}\, q_\alpha \, p_{\mu_1}\ldots p_{\mu_{n+1}}\,,
\end{aligned}
$$

where the dummy index λ has been replaced by μ_{n+1} in the last line. Replacing $n \to n+1$, and permuting the dummy indices $\mu_1 \ldots \mu_n$ gives

$$
\mathcal{M}^{[\mu\nu]} = \sum_{n=1,3,5}^{\infty} 2\,\frac{2^n q^{\mu_2}\ldots q^{\mu_n}}{(-q^2)^n}\, ih\,\epsilon^{\mu\nu\alpha\mu_1}\, q_\alpha \, p_{\mu_1}\ldots p_{\mu_n}\,. \qquad (3.28)
$$

The coefficient functions in the operator product depend only on q, and the matrix elements depend only on p. We have separated the operator product into pieces which depend only on q and only on p. By comparing with eq. (3.25), we can write eq. (3.28) as

$$
\mathcal{M}^{[\mu\nu]} = \sum_{n=1,3,5}^{\infty} 2\,\frac{2^n q^{\mu_2}\ldots q^{\mu_n}}{(-q^2)^n}\, i\epsilon^{\mu\nu\alpha\mu_1}\, q_\alpha \left\langle \mathcal{O}^{(5)}_{\mu_1\ldots\mu_n}\right\rangle\,, \qquad (3.29)
$$

so that

$$
t^{[\mu\nu]} = \sum_{n=1,3,5}^{\infty} 2\,\frac{2^n q^{\mu_2}\ldots q^{\mu_n}}{(-q^2)^n}\, i\epsilon^{\mu\nu\alpha\mu_1}\, q_\alpha \, \mathcal{O}^{(5)}_{\mu_1\ldots\mu_n}\,. \qquad (3.30)
$$

This is the OPE for the spin dependent part of $t_{\mu\nu}$. To include quark flavours and charges in our analysis, $\mathcal{O}^{(5)}$ has to be replaced by $\sum Q_f^2 \mathcal{O}^{(f,5)}$, where Q_f is the charge of flavour f in units of e. Odd spin axial vector operators are charge conjugation even, and even spin axial vector operators are charge conjugation odd. Since electroproduction is a charge conjugation even process, only the odd spin axial vector operators appear in eq. (3.30). The contribution of the symmetric part can be written in terms of only even spin vector operators.

The most general operator product expansion at twist two and spin-1/2 target can be written in the form

$$
\begin{aligned}
t^{\mu\nu} &= \sum_{n=2,4,\cdots}^{\infty}\left(-g^{\mu\nu}+\frac{q^\mu q^\nu}{q^2}\right)\frac{2^n q^{\mu_1}\ldots q^{\mu_n}}{(-q^2)^n}\sum_j 2\, C^{(1)}_{j,n}\, \mathcal{O}^{(j,V)}_{\mu_1\ldots\mu_n} \\
&+ \sum_{n=2,4,\ldots}^{\infty}\left(g^{\mu\mu_1}-\frac{q^\mu q^{\mu_1}}{q^2}\right)\left(g^{\nu\mu_2}-\frac{q^\nu q^{\mu_2}}{q^2}\right)\frac{2^n q^{\mu_3}\ldots q^{\mu_n}}{(-q^2)^{n-1}}\sum_j 2\, C^{(2)}_{j,n}\, \mathcal{O}^{(j,V)}_{\mu_1\ldots\mu_n} \\
&+ \sum_{n=1,3,\ldots}^{\infty} i\epsilon^{\mu\nu\lambda\mu_1} q_\lambda \frac{2^n q^{\mu_2}\ldots q^{\mu_n}}{(-q^2)^n}\sum_j 2\, C^{(3)}_{j,n}\, \mathcal{O}^{(j,5)}_{\mu_1\ldots\mu_n} \qquad (3.31)\\
&+ \sum_{n=2,4,\cdots}^{\infty}\frac{2^n q^{\mu_1}\ldots q^{\mu_n}}{(-q^2)^n}\sum_j 2\, C^{(4)}_{j,n}\, \mathcal{O}^{(j,\Delta)\,\mu\nu}_{\mu_1\ldots\mu_n}\,.
\end{aligned}
$$

The sum in the various terms is over twist two quark and gluon operators. What we have just shown is that $C^{(3)}_{j,n}$ at leading order is zero for the gluon operators, and is Q_q^2 for the quark axial operator of flavour type q, as can be seen by comparing eq. (3.31) with eq. (3.30). A similar calculation for the spin-independent pieces shows that at leading order $C^{(1)}_n$ and $C^{(2)}_n$ are both equal to Q_q^2 and all gluon operator coefficients are zero. (The terms of type $C^{(4)}_n$ have only gluon contributions, and so vanish to this order. They contribute to a structure function $\Delta(x)$ not explicitly discussed here.)

3.4 Moments of the structure functions for nucleon target

Now we are prepared to find the moments of structure functions of the nucleon. The $n^{\rm th}$ moment of a function f is defined by

$$M_n(f) \equiv \int_0^1 dx\; x^{n-1} f(x)\,. \tag{3.32}$$

To compute $T_{\mu\nu}$, we need the hadronic matrix element of the operator product expansion, so we have to evaluate the hadronic matrix elements of the operators eqs.. (3.11) and (3.13). The matrix elements of these operators in the target have to be determined *nonperturbatively*. One promising possibility using lattice gauge theory is described below.

We parameterise the matrix elements in terms of a known tensor structure times a normalisation coefficient.

For the spin-1/2 target (the nucleon) we have the following matrix elements:

$$\frac{1}{2}\sum_{\vec{s}}\langle\vec{p},\vec{s}|\mathcal{O}^{(V,f)}_{\{\mu_1\cdots\mu_n\}}|\vec{p},\vec{s}\rangle \;=\; 2v_n^{(f)}(p_{\mu_1}\ldots p_{\mu_n} - \text{traces})\,, \tag{3.33}$$

$$\langle\vec{p},\vec{s}|\mathcal{O}^{(5,f)}_{\{\sigma\mu_1\cdots\mu_n\}}|\vec{p},\vec{s}\rangle \;=\; \frac{1}{n+1}a_n^{(f)}(s_\sigma p_{\mu_1}\ldots p_{\mu_n} + \ldots - \text{traces})\,, \tag{3.34}$$

$$\langle\vec{p},\vec{s}|\mathcal{O}^{(5,f)}_{[\sigma\{\mu_1]\cdots\mu_n\}}|\vec{p},\vec{s}\rangle \;=\; \frac{1}{n+1}d_n^{(f)}\;(s_{[\sigma}p_{\mu_1]}p_{\mu_2}\ldots p_{\mu_n} + \ldots - \text{traces})\,. \tag{3.35}$$

To calculate $T^{\mu\nu}$ let us concentrate again on the term antisymmetric in $\mu\nu$ and spin 1/2 target. Substituting the simplified version

$$\langle\vec{p},\vec{s}|\mathcal{O}^{(5,f)}_{\{\mu_1\cdots\mu_n\}}|\vec{p},\vec{s}\rangle = A_N\mathcal{S}[s_1^{\mu}\ldots p^{\mu_n}] \tag{3.36}$$

of eq. (3.34) into eq. (3.31), one finds

$$T^{[\mu\nu]} = \sum_{n=1,3,5}^{\infty} 2\;C_n^{(3)}\; i\epsilon^{\mu\nu\alpha\mu_1}q_\alpha\;\frac{2^n q^{\mu_2}\ldots q^{\mu_n}}{(-q^2)^n}A_n\;\mathcal{S}\left[s^{\mu_1}\ldots p^{\mu_n}\right]\,. \tag{3.37}$$

Let us write

$$\mathcal{S}\left[s^{\mu_1}\ldots p^{\mu_n}\right] = s^{\mu_1}\ldots p^{\mu_n} + \mathcal{R}^{\mu_1\cdots\mu_n}\,, \tag{3.38}$$

where the tensor $\mathcal{R}^{\mu_1\cdots\mu_n}$ has no completely symmetric part, and so has spin $n-1$ rather than spin n. Thus the contribution of $\mathcal{R}$ to DIS is twist three, rather than twist two and can be omitted. Then we find

$$T^{[\mu\nu]} = \sum_{n=1,3,5}^{\infty} -\frac{4}{q^2}\;C_n^{(3)} i\epsilon^{\mu\nu\alpha\mu_1}q_\alpha s_{\mu_1}A_n\omega^{n-1} = i\epsilon^{\mu\nu\alpha\lambda}q_\alpha s_\lambda\;\frac{\widetilde{g}_1}{p\cdot q}\,, \tag{3.39}$$

using the definition of $\widetilde{g}_1$ from eq. (2.44). This gives us the power series expansion

$$\widetilde{g}_1 = \sum_{n=1,3,5}^{\infty} -\frac{4p\cdot q}{q^2}\;C_n^{(3)}\;A_n\,\omega^{n-1} = \sum_{n=1,3,5}^{\infty} 2\,C_n^{(3)}\;A_n\omega^n\,. \tag{3.40}$$

The operator product expansion has allowed us to compute $\widetilde{g}_1$ as a power series in ω about $\omega=0$ in QCD. The $n^{\rm th}$ term in the power series is due to an operator of twist two and spin n. The radius of convergence of the power series is $|\omega|=1$, since that is the location of the first singularity in the complex ω plane. This is precisely where the physical region begins.

We can relate $\widetilde{g}_1$ in the unphysical region to its value in the physical region using contour integration. The coefficient $2C_n^{(3)}\;A_n$ can be extracted by the contour integral over a circle in the complex ω plane around the origin, as shown in fig. 9. The contour of integration can then be deformed to the contour C. This gives

$$2C_n^{(3)}\;A_n = \frac{1}{2\pi i}\oint_{|\omega|=r<1}\widetilde{g}_1(\omega)\;\frac{d\omega}{\omega^{n+1}} = \frac{1}{2\pi i}\oint_C\;\widetilde{g}_1(\omega)\;\frac{d\omega}{\omega^{n+1}}\,. \tag{3.41}$$

Assuming that the contour at infinity does not contribute to the integral, only the discontinuities across the cuts contribute to the integral over contour C. Using the optical theorem, we obtain

$$\widetilde{g}_1(\omega+i\epsilon) - \widetilde{g}_1(\omega-i\epsilon) = 4\pi i\,g_1(\omega)\,, \tag{3.42}$$

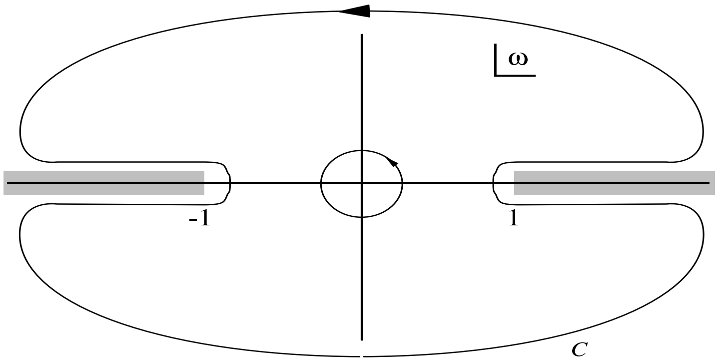

Figure 9: Contours used to derive the moment sum rules.

here is $g_1(\omega)$ the experimentally measurable structure function. Taking into account eq. (2.46)

$$g_1(-\omega) = -g_1(\omega)\,, \tag{3.43}$$

we get

$$2C_n^{(3)}\, a_n^{(f)} = 2\left[1-(-1)^n\right]\int_1^\infty g_1(\omega)\,\frac{d\omega}{\omega^{n+1}}\,, \tag{3.44}$$

where the 1 term is from the right hand cut, and the $(-1)^n$ term is from the left hand cut. Substituting $\omega = 1/x$, and using the definition of a moment (eq. (3.32)) gives

$$2M_n(g_1) = 2\int_0^1 dx\; x^{n-1} g_1(x) = C_n^{(3)} A_n, \quad n \text{ odd} \tag{3.45}$$

There is no sum rule for n even, because eq. (3.44) reduces to the identity $0 = 0$. The sum rules for F_1 and F_2 are obtained in direct analogy to the derivation of the g_1 sum rule. The result is that

$$\begin{aligned} 2M_n(F_1) &= C_n^{(1)} v_n^{(f)}, \quad n \text{ even}\,, \\ 2M_n\left(\frac{F_2}{2x}\right) &= C_n^{(2)} v_n^{(f)}, \quad n \text{ even}\,. \end{aligned} \tag{3.46}$$

The moment sum rules relate a quantity defined at high energy such as F_1 to a low energy quantity, the zero momentum transfer matrix element of a local operator. One can derive sum rules in QCD only for the even moments of F_1, and the odd moments of g_1. There are no sum rules for the other moments.

In the quenched approximation used in our calculation the above mentioned equations hold for odd n as well. The moments of F_1 and F_2 have the parton model interpretation

$$v_n^{(f)} = \langle x^{n-1}\rangle^{(f)}\,. \tag{3.47}$$

In that language,

$$A_1^{(u)} = 2\Delta u\,, \quad A_1^{(d)} = 2\Delta d\,, \tag{3.48}$$

and a similar interpretation holds for higher spin operators. In our conventional notation used in the lattice papers, the moments of the structure functions including also g_2 are given in eqs. (8.2).

3.5 Moments of the structure functions for pion and rho targets

For a spin-0 target, the momentum vector p is the only quantity the matrix element can depend on, and the reduced matrix element v_n is defined by

$$\langle\vec{p}|\mathcal{O}^{(V)}_{\{\mu_1\cdots\mu_n\}} - \text{traces}|\vec{p}\rangle = 2v_n\,\left[p_{\mu_1}\cdots p_{\mu_n} - \text{traces}\right]\,. \tag{3.49}$$

The notation $\{\mu_1 \cdots \mu_n\}$ denotes symmetrisation in the indices $\mu_1, \ldots, \mu_n$. Expectation values of operators involving the γ_5 matrix vanish from symmetry considerations as the pion is a pseudoscalar particle.

For a spin-1 target, the structure of the matrix elements is more complicated due to the polarisation degrees of freedom. Now both types of quark operators contribute:

$$\begin{aligned}
\langle p,\lambda|\mathcal{O}^{(V)}_{\{\mu_1\cdots\mu_n\}} - \text{traces}|p,\lambda\rangle &= 2\mathcal{S}\Big[a_n\, p_{\mu_1}\cdots p_{\mu_n} \\
&\quad + d_n\,(\epsilon_{*\mu_1}(\vec{p},\lambda)\epsilon_{\mu_2}(\vec{p},\lambda) - \frac{1}{3}p_{\mu_1}p_{\mu_2})\, p_{\mu_3}\cdots p_{\mu_n}\Big]\,, \qquad (3.50) \\
\langle p,\lambda|\mathcal{O}^{(5,f)}_{\{\mu_1\cdots\mu_n\}} - \text{traces}|p,\lambda\rangle & \\
&= \frac{2\mathrm{i}}{m^2}\,\mathcal{S}\left[r_n\,\epsilon_{\rho\sigma\tau\mu_1}\epsilon^{*\rho}(\vec{p},\lambda)\epsilon^{\sigma}(\vec{p},\lambda)p_\tau p_{\mu_2}\cdots p_{\mu_n}\right]\,. \qquad (3.51)
\end{aligned}$$

$\mathcal{S}$ denotes symmetrisation in the indices $\mu_1, \ldots, \mu_n$ and removal of traces. In the spin-1 case, the reduced matrix elements are a_n for the polarisation-averaged contribution, d_n for the polarised contributions, and r_n for the operators involving γ_5.

One then finds to leading order, which is twist two, the following representation of the moments of the pion structure functions:

$$2M_n(F_1) = C_n^{(1)}\, v_n\,, \quad M_{n-1}(F_2) = C_n^{(2)}\, v_n\,. \qquad (3.52)$$

For the rho structure functions one obtains [3]:

$$\begin{aligned}
2M_n(F_1) &= C_n^{(1)}\, a_n\,, \\
M_{n-1}(F_2) &= C_n^{(2)}\, a_n\,, \\
2M_n(b_1) &= C_n^{(1)}\, d_n\,, \qquad (3.53) \\
M_{n-1}(b_2) &= C_n^{(2)}\, d_n\,, \\
2M_n(g_1) &= C_n^{(3)}\, r_n\,,
\end{aligned}$$

where $C_n^{(k)} = 1 + O(\alpha_s)$ are the Wilson coefficients of the operator product expansion. These relations hold for even n, except for the last one, which is valid for odd n. However, since we are calculating in the quenched approximation, we are allowed to make use of all moment formulas for all n keeping in mind that our results can be meaningfully compared only with the non-singlet valence quark distribution.

In the case of the pion, the moments of the quark distribution are given by

$$\langle x^{n-1}\rangle = v_n\,, \qquad (3.54)$$

while for the rho they are related to the matrix elements a_n:

$$\langle x^{n-1}\rangle = a_n\,. \qquad (3.55)$$

4 Two-point and three-point functions

4.1 Expectation values in lattice QCD and quenched approximation

In the following subsections we closely follow the book [4]. Let us shortly repeat how to derive expectation values. In lattice QCD the expectation value of physical quantities are given in terms of path integrals over gauge and quark field variables

$$\langle F \rangle = \frac{\int [dU\, d\overline{\psi}\, d\psi] \mathrm{e}^{-S_g - S_q} F[U,\psi,\overline{\psi}]}{\int [dU\, d\overline{\psi}\, d\psi] \mathrm{e}^{-S_g - S_q}} \tag{4.1}$$

where S_g and S_q are the gauge and fermion parts of the action. The form of F, in which we are interested in, is a function of n pairs of quark fields times link variables (schematically shown by the function $A[U]$) connecting the fermion fields in a gauge invariant way:

$$F[U,\psi,\overline{\psi}] = \psi_{y_1}\overline{\psi}_{x_1} \ldots \psi_{y_n}\overline{\psi}_{x_n} A[U]\,. \tag{4.2}$$

The integral over the fermionic Grassmann variables can be performed, in particular

$$\int [d\overline{\psi}\, d\psi] \mathrm{e}^{-S_q} = \det Q[U]\,, \tag{4.3}$$

where $Q[U]$ is the quark matrix in the quark part of the action

$$S_q[U,\psi,\overline{\psi}] = \sum_{x,y} \overline{\psi}_y Q[U]_{yx} \psi_x\,. \tag{4.4}$$

For Wilson fermions with a single quark and $r=1$ the matrix Q is given by

$$Q[U]_{yx} = \delta_{yx} - \kappa \sum_{\mu=\pm 1}^{\pm 4} \delta_{y,x+\hat{\mu}} (1+\gamma_\mu) U_{x\mu}\,, \quad \kappa = \frac{1}{2am+8} \tag{4.5}$$

and satisfies

$$Q_{yx} = \gamma_5 Q^\dagger_{xy} \gamma_5\,. \tag{4.6}$$

$Q^\dagger_{xy}$ denotes the adjoint with respect to the Dirac spinor and colour indices. Therefore, the quark determinant is real

$$\det Q = \det Q^+ = (\det Q)^*\,, \tag{4.7}$$

now Q^+ means a complete adjoint including point indices.

If we introduce the effective gauge action

$$S_{\mathrm{eff}} \equiv S_g[U] - \log\det Q[U] = S_g - \mathrm{Tr}\log Q[U] \tag{4.8}$$

we obtain for eqs. (4.1,4.2) after the Grassmann integration

$$\langle F \rangle = \frac{1}{Z} \int [dU] \mathrm{e}^{-S_{\mathrm{eff}}} A[U] \sum_{z_1 \ldots z_n} \epsilon^{z_1 \ldots z_n}_{y_1 \ldots y_n} Q^{-1}[U]_{z_1 x_1} \ldots Q^{-1}[U]_{z_n x_n} \tag{4.9}$$

with the partition function

$$Z \equiv \int [dU] \mathrm{e}^{-S_{\mathrm{eff}}} = \int [dU] \mathrm{e}^{-S_g} \det Q[U]\,. \tag{4.10}$$

Here $Q^{-1}[U]$ are the quark propagators. In other words, all possible contractions between the fermion pairs have to be considered.

The replacement

$$\det Q[U] \Longrightarrow \mathrm{const} \tag{4.11}$$

is the basis of the so-called *quenched approximation*. In this approximation internal quarks loops are neglected (κ is set to zero in the quark determinant). Its enormous advantage is that the gauge field updating can be done by the pure *local* gauge action $S_g[U]$. The only numerical task left is to evaluate the full quark propagator $Q[U]^{-1}$ by inverting the fermion matrix $Q[U]$.

4.2 Hadronic two-point functions

Hadronic masses are obtained by studying the behaviour of Euclidean hadronic two-point functions. Let us start with the vacuum expectation value of the time-ordered product of two hadronic operators after Wick rotation to Euclidean times x_4 and y_4

$$\begin{aligned} &\langle 0|T\{B(y_4)A(x_4)\}|0\rangle = \langle B(y_4)A(x_4)\rangle \\ &= \begin{cases} \langle 0|B(y_4)A(x_4)|0\rangle\,, & y_4 \geq x_4 \\ \langle 0|A(x_4)B(y_4)|0\rangle\,, & x_4 > y_4 \end{cases} \quad . \end{aligned} \tag{4.12}$$

This can be written as

$$\langle B(y_4)A(x_4)\rangle = \lim_{T\to\infty} \left(\mathrm{Tr}\,\mathrm{e}^{-TH}\right)^{-1} \begin{cases} \mathrm{Tr}[B(0)\mathrm{e}^{-(y_4-x_4)H}A(0)\mathrm{e}^{-(T-y_4+x_4)H}] \\ \pm\,\mathrm{Tr}[A(0)\mathrm{e}^{-(x_4-y_4)H}B(0)\mathrm{e}^{-(T-x_4+y_4)H}] \end{cases} . \tag{4.13}$$

Here H is the Hamiltonian and the sign $\pm$ stands for bosonic/fermionic operators. The lattice extension is T with periodic/antiperiodic boundary conditions.

Inserting in the traces complete sets of orthonormal intermediate states, for large T and large $|y_4 - x_4|$ only the states with lowest energy contribute, and we have (considering explicitly the bosonic case)

$$\begin{aligned} &\langle B(y_4)A(x_4)\rangle \overset{T\to\infty}{\underset{|y_4-x_4|\to\infty}{\longrightarrow}} \\ &\begin{cases} C_{BA}\mathrm{e}^{-(y_4-x_4)E_{BA}} + C_{AB}\mathrm{e}^{-(T-y_4+x_4)E_{AB}} \\ C_{AB}\mathrm{e}^{-(x_4-y_4)E_{AB}} + C_{BA}\mathrm{e}^{-(T-x_4+y_4)E_{BA}} \end{cases} . \end{aligned} \tag{4.14}$$

Here E_{BA}/E_{AB} denote the energies of the lowest contributing states $|n_{BA}\rangle/|n_{AB}\rangle$ in lattice units, if the vacuum energy is set equal to zero. The constant factors C_{BA}/C_{AB} are given by the matrix elements between the vacuum and the lowest states

$$\begin{aligned} C_{BA} &= \langle 0|\,B(0)\,|n_{BA}\rangle\,\langle n_{BA}|\,A(0)\,|0\rangle\ , \\ C_{AB} &= \langle 0|\,A(0)\,|n_{AB}\rangle\,\langle n_{AB}|\,B(0)\,|0\rangle\ . \end{aligned} \tag{4.15}$$

In the special case of $B(y_4) = A(y_4)^\dagger$ these factors are real and equal to each other, we denote them by C, the corresponding energies are also equal: E. Therefore we obtain from eq. (4.14)

$$\langle A(y_4)^\dagger A(x_4)\rangle \overset{T\to\infty}{\underset{|y_4-x_4|\to\infty}{\longrightarrow}} C\left[\mathrm{e}^{-(y_4-x_4)E} + \mathrm{e}^{-(T-y_4+x_4)E}\right] . \tag{4.16}$$

Besides this dominant contribution with the lowest energy there are excited states with the next lowest energies in the sector specified by the quantum numbers of the operator $A(x_4)$. On a finite lattice the energy spectrum is discrete, therefore in the discussed limit the excited states are exponentially suppressed.

In most applications the local operators are summed over the space-like coordinate (coordinates transverse to the Euclidean time direction). These timeslices $S_t, t = 1, 2, \ldots, T$ are projecting out the intermediate states with zero spatial momentum. Therefore, if there is a single-particle state in the given channel, the lowest energy is equal to its mass m_A, and the asymptotic behaviour for large time separations is

$$\begin{aligned} \langle S^\dagger_{t_2} S_{t_1}\rangle &\overset{T\to\infty}{\underset{|t_2-t_1|\to\infty}{\longrightarrow}} C_0\left[\mathrm{e}^{-(t_2-t_1)m_a} + \mathrm{e}^{-(T-t_2+t_1)m_a}\right] \\ &= 2C_0\mathrm{e}^{-Tm_a/2}\cosh\left[m_a\left(\frac{T}{2} - |t_2-t_1|\right)\right] . \end{aligned} \tag{4.17}$$

In the case of fermionic timeslice operators for baryons B_{t_2}, $\overline{B}_{t_1}$ the asymptotics at large T and $|t_2 - t_1|$ is again dominated by the contribution from the lowest mass state in the given channel.

It has been shown (see [4]) that in the continuum limit one can take the limit $am \to 0$ of the timeslices of free Wilson fermions and one finds for $T \to \infty$

$$\langle B_{t_2}\overline{B}_{t_1}\rangle \propto \frac{1}{2}[1 + \mathrm{sign}(t_2 - t_1)\gamma_4]\mathrm{e}^{-|t_2-t_1|m_B} . \tag{4.18}$$

The factor $(1 \pm \gamma_4)/2$ is the Dirac projection matrix arising from the spin sum at zero spatial momentum, m_B is the lowest mass in lattice units.

In general, the simplest operators B_t used for the prescription of the baryons are coupled to both parities, therefore the asymptotic form contains the lowest masses m_{B^+} and m_{B^-} of both parities. Taking into account the finite time extension T with $0 \leq t_2 - t_1 \leq T$ and that the sign of γ_4 is reversed for negative parity states we get

$$\begin{aligned} \langle B_{t_2} \overline{B}_{t_1} \rangle \quad \xrightarrow[|t_2-t_1|\to\infty]{T\to\infty} \quad & (1+\gamma_4)\left[C_{B^+}\mathrm{e}^{-(t_2-t_1)m_{B^+}} + C_{B^-}\mathrm{e}^{-(T-t_2+t_1)m_{B^-}}\right] \\ + \quad & (1-\gamma_4)\left[C_{B^+}\mathrm{e}^{-(T-t_2+t_1)m_{B^+}} + C_{B^-}\mathrm{e}^{-(t_2-t_1)m_{B^-}}\right] . \end{aligned} \tag{4.19}$$

4.3 Simplest hadronic sources and two-point functions

In order to project out the channels with different quantum numbers the appropriate hadronic operators have to be constructed from the quark and gluon fields. The choice of the composite operators is to a large extent arbitrary. In fact, for given values of the coupling constants (β and the hopping parameter κ of the Wilson action) one has to find the optimal operator, which has a strong enough coupling to hadron in question and, at the same time, can be evaluated without too much difficulties.

We restrict ourselves to Wilson quarks and to the ground state mesons and baryons using $SU(6)$ flavour symmetry containing u, d and s quarks. The spin dependence of the operators is dictated by the relativistic generalisation of $SU(6)$ symmetry. The $J^{PC} = 0^{-+}$ pseudoscalar mesons are described by bilinear quark-antiquark composite operators like, for instance,

$$\mathcal{M}^{\pi^+}(x) \equiv \overline{d}_{c\alpha}(x)(\gamma_5)_{\alpha\beta}u^c_\beta(x)\,, \quad \mathcal{M}^{K^+}(x) \equiv \overline{s}_{c\alpha}(x)(\gamma_5)_{\alpha\beta}u^c_\beta(x)\,, \tag{4.20}$$

where $\alpha, \beta, \ldots$ denote Dirac indices and $c, d, \ldots$ $SU(3)$ colour indices. The corresponding 1^{--} vector meson states are $(k = 1, 2, 3)$:

$$\mathcal{M}^{\rho^+}_k(x) \equiv \overline{d}_{c\alpha}(x)(\gamma_k)_{\alpha\beta}u^c_\beta(x)\,, \quad \mathcal{M}^{K^{*+}}_k(x) \equiv \overline{s}_{c\alpha}(x)(\gamma_k)_{\alpha\beta}u^c_\beta(x)\,. \tag{4.21}$$

For baryons the three-quark composite operators can be chosen in different ways. Non-relativistic operators can be constructed in the non-relativistic representation of the Dirac matrices. Relativistic baryon operators involve the charge conjugation matrix C, which satisfies

$$C\gamma_\mu C^{-1} = -\gamma_\mu^T \qquad -C = C^T = C^{-1} = C^\dagger\,. \tag{4.22}$$

In the non-relativistic Dirac matrix representation a possible choice is

$$C \equiv \gamma_4\gamma_2 = -\gamma_1\gamma_3\gamma_5 = \begin{pmatrix} 0 & -\mathrm{i}\sigma_2 \\ -\mathrm{i}\sigma_2 & 0 \end{pmatrix}\,. \tag{4.23}$$

As an example, we obtain for the proton

$$\mathcal{B}^p_\alpha(x) \equiv \epsilon^{cde}(C\gamma_5)_{\beta\gamma}u_{c\alpha}(x)\left(u_{d\beta}(x)d_{e\gamma}(x) - d_{d\beta}(x)u_{e\gamma}(x)\right) \tag{4.24}$$

with the totally antisymmetric $SU(3)$ unit tensor ϵ^{cde}. The overlined operator is given by

$$\overline{\mathcal{B}}^p_\delta(y) \equiv \epsilon^{fgh}(C\gamma_5)_{\epsilon\varphi}\overline{u}_{f\delta}(y)\left(\overline{d}_{g\epsilon}(y)\overline{u}_{h\varphi}(y) - \overline{u}_{g\epsilon}(y)\overline{d}_{h\varphi}(y)\right)\,. \tag{4.25}$$

Now the expectation value of two-point functions of composite operators can be determined on the basis of eq. (4.9). This leads to products of quark propagators $Q^{-1}[U;\kappa_f]$ evaluated in some gauge configuration $[U]$ at some hopping parameter κ_f depending on flavour (in general).

Introducing U, D and S propagators

$$\begin{aligned} U_{x\alpha c,y\beta d} &\equiv Q^{-1}[U,\kappa_u]_{x\alpha c,y\beta d}\,, \\ D_{x\alpha c,y\beta d} &\equiv Q^{-1}[U,\kappa_d]_{x\alpha c,y\beta d}\,, \\ S_{x\alpha c,y\beta d} &\equiv Q^{-1}[U,\kappa_s]_{x\alpha c,y\beta d} \end{aligned} \tag{4.26}$$

one has to calculate for the charged pion and rho two-point functions $\langle \mathcal{M}_x^{\pi^+} \mathcal{M}_y^{\pi^-} \rangle$ and $\langle \mathcal{M}_{xk}^{\rho^+} \mathcal{M}_{yl}^{\rho^-} \rangle$ the following expressions:

$$\langle -\mathrm{Tr}_{sc}\{\gamma_5 D_{yx} \gamma_5 U_{xy}\}\rangle_{S_{\mathrm{eff}}} \ , \quad \langle -\mathrm{Tr}_{sc}\{\gamma_l D_{yx} \gamma_k U_{xy}\}\rangle_{S_{\mathrm{eff}}} \tag{4.27}$$

where Tr_{sc} stands for a trace of spin and colour indices, and $\langle \ldots \rangle_{S_{\mathrm{eff}}}$ denotes an expectation value with respect to the effective gauge action.

The calculation of combinations of quark propagator matrix elements is facilitated by the relation

$$Q^{-1}_{yx} = \gamma_5 {Q^{-1}_{xy}}^{\dagger} \gamma_5 \ , \tag{4.28}$$

which, for instance, implies that the charged pion two-point function (4.27) can be written as (being simple to compute)

$$\langle -\mathrm{Tr}_{sc}\{D^{\dagger}_{yx} \ U_{xy}\}\rangle_{S_{\mathrm{eff}}} \ . \tag{4.29}$$

Finally let us give an expression for the proton two-point function $\langle \mathcal{B}^p_{x\alpha} \overline{\mathcal{B}}^p_{y\delta} \rangle$:

$$\epsilon_{cde}\epsilon_{fgh} (C\gamma_5)_{\beta\gamma} (C\gamma_5)_{\varepsilon\varphi} (U_{x\alpha c,y\delta f} U_{x\beta d,y\varepsilon g} + U_{x\alpha c,y\varepsilon f} U_{x\beta d,y\delta g}) D_{x\gamma e,y\varphi h}) \, . \tag{4.30}$$

4.4 Three-point functions and matrix elements for pion and rho

In order to calculate the reduced matrix elements on the lattice, we must calculate the expectation values of local operators of the form (3.11) and (3.13). To this end, we first need the connection between the Minkowski operators and those in Euclidean space. Defining Euclidean operators by

$$\hat{O}^{(E)}_{\mu_1 \cdots \mu_n} \ = \ G_{ff'} \, \frac{1}{2^{n-1}} \, \overline{\psi}_f \gamma^{(E)}_{\mu_1} \, \overleftrightarrow{D}^{(E)}_{\mu_2} \ldots \overleftrightarrow{D}^{(E)}_{\mu_n} \psi_{f'} \quad , \tag{4.31}$$

$$\hat{O}^{(E)5}_{\mu_1 \cdots \mu_n} \ = \ G_{ff'} \, \frac{1}{2^{n-1}} \, \overline{\psi}_f \gamma^{(E)}_{\mu_1} \gamma_5 \, \overleftrightarrow{D}^{(E)}_{\mu_2} \ldots \overleftrightarrow{D}^{(E)}_{\mu_n} \psi_{f'} \quad , \tag{4.32}$$

we obtain the following relation to the operators in Minkowski space:

$$\hat{O}^{(M)\mu_1 \cdots \mu_n} = (-)\,(-)^{n_4+n_5}\,(-\mathrm{i})^{n_{123}}\,\hat{O}^{(E)}_{\mu_1 \cdots \mu_n} \quad , \tag{4.33}$$

where n_4 is the number of time-like indices, n_{123} the number of spatial indices, and $n_5 = 1$ if the operator carries a γ_5 matrix. For our Euclidean conventions, see Appendix A.

Lattice operators with the appropriate continuum behaviour can be constructed from the Wilson fermion fields by considering their symmetry properties under the hypercubic group $H(4)$ [5]. The operators we have chosen and their relation to the reduced matrix elements are listed in Appendix B of [6].

The required expectation values of our operators are extracted from ratios of two- and three-point functions. The three-point functions we consider are of the general form

$$\langle \eta(t,\vec{p})\, \mathcal{O}(\tau)\, \eta^{\dagger}(0,\vec{p}) \rangle \tag{4.34}$$

where $\eta(t,\vec{p})$ is the sink operator for a particle moving with momentum $\vec{p}$ in time slice t, and $\eta^{\dagger}(0,\vec{p})$ is the corresponding source at time slice $t = 0$. These operators are required to have the correct symmetry properties for the particles in question and their corresponding Hilbert space operators $\hat{\eta}(\vec{p})$ should create the desired particles from the vacuum with nonzero amplitude. $\mathcal{O}(\tau)$ represents the operator $\hat{O}$ whose expectation value is to be calculated.

For the pion we write

$$\langle 0|\hat{\eta}(\pi;\vec{p})|\pi;\vec{p}\rangle = \sqrt{Z_\pi} \quad , \tag{4.35}$$

while for the rho there are three different particle states and correspondingly three different operators arranged in a vector $\eta_i(\rho;t,\vec{p})$ that satisfy

$$\langle 0|\hat{\eta}_j(\rho;\vec{p})|\rho;\vec{p},\lambda\rangle = \sqrt{Z_\rho}\,\epsilon_j(\vec{p},\lambda) \tag{4.36}$$

up to lattice artifacts (see Appendix A for the definition of the polarisation vectors ϵ_i). The correlation function for the rho depends on the polarisation vectors:

$$C_{jk} = \langle \eta_j(\rho;t,\vec{p})\, \mathcal{O}(\tau)\, \eta^{\dagger}_k(\rho;0,\vec{p}) \rangle \quad . \tag{4.37}$$

In order to relate (4.37) to the matrix elements we are interested in, we express this correlation function in terms of traces involving the transfer matrix $\hat{S}$:

$$\begin{aligned} &\langle \eta_j(\rho;t,\vec{p})\,\mathcal{O}(\tau)\,\eta_k^\dagger(\rho;0,\vec{p})\rangle = \\ &\qquad = \left\{ \begin{array}{ll} \mathrm{Tr}\left[\hat{S}^{T-t}\hat{\eta}_j(\rho;\vec{p})\hat{S}^{t-\tau}\hat{O}\hat{S}^{\tau}\hat{\eta}_k^\dagger(\rho;\vec{p})\right] & T \geq t \geq \tau \geq 0 \quad , \\ \mathrm{Tr}\left[\hat{S}^{T-\tau}\hat{O}\hat{S}^{\tau-t}\hat{\eta}_j(\rho;\vec{p})\hat{S}^{t}\hat{\eta}_k^\dagger(\rho;\vec{p})\right] & T \geq \tau \geq t \geq 0 \quad . \end{array} \right. \end{aligned} \tag{4.38}$$

Here T denotes the time extent of our lattice whose spacing is put equal to 1. Then we insert a complete set of orthonormal eigenstates of the transfer matrix. If the time differences are chosen sufficiently large, we can restrict ourselves to the lowest contributing states $|\vec{p},\lambda\rangle$, λ labelling the three degenerate polarisation states of the rho. For the first case in (4.38) one obtains

$$\begin{aligned} C_{jk}^{(1)} &= \sum_{\lambda\lambda'} \langle 0|\hat{\eta}_j(\rho;\vec{p})|\rho;\vec{p},\lambda\rangle\,\langle\rho;\vec{p},\lambda|\hat{O}|\rho;\vec{p},\lambda'\rangle\,\langle\rho;\vec{p},\lambda'|\hat{\eta}_k(\rho;\vec{p})|0\rangle\,e^{-Et} \\ &= Z_\rho \sum_{\lambda\lambda'} \epsilon_j(\vec{p},\lambda)\,\epsilon_k^*(\vec{p},\lambda')\,\langle\rho;\vec{p},\lambda|\hat{O}|\rho;\vec{p},\lambda'\rangle\,e^{-Et} \\ &= Z_\rho\,m^2\,T_{jk}\,e^{-Et} \quad , \end{aligned} \tag{4.39}$$

where T_{jk} is the matrix element between Cartesian states,

$$T_{jk} = \frac{1}{m^2}\sum_{\lambda\lambda'} \epsilon_j(\vec{p},\lambda)\epsilon_k^*(\vec{p},\lambda')\langle\rho;\vec{p},\lambda|\hat{O}|\rho;\vec{p},\lambda'\rangle \quad . \tag{4.40}$$

In the second case, one finds an additional sign factor:

$$C_{jk}^{(2)} = (-1)^{n_4+n_5}\,Z_\rho\,m^2\,T_{jk}\,e^{-E(T-t)} \quad . \tag{4.41}$$

To calculate all C_{jk} components for a given momentum would be expensive in computer time. Choosing the momentum in 1-direction, we have restricted ourselves to the components C_{33} and C_{32}. If $\langle\rho;\vec{p},+|\hat{O}|\rho;\vec{p},-\rangle = 0$ and $\langle\rho;\vec{p},+|\hat{O}|\rho;\vec{p},+\rangle = \langle\rho;\vec{p},-|\hat{O}|\rho;\vec{p},-\rangle$, then

$$\langle\rho;\vec{p},+|\hat{O}|\rho;\vec{p},+\rangle = T_{33} \quad , \qquad T_{32} = 0 \quad , \tag{4.42}$$

whereas for $\langle\rho;\vec{p},+|\hat{O}|\rho;\vec{p},+\rangle = -\langle\rho;\vec{p},-|\hat{O}|\rho;\vec{p},-\rangle$,

$$\langle\rho;\vec{p},+|\hat{O}|\rho;\vec{p},+\rangle = -\mathrm{i}T_{32} \quad , \qquad T_{33} = 0 \quad . \tag{4.43}$$

The latter case is relevant to spin-dependent operators. To satisfy

$$\langle\rho;\vec{p},+|\hat{O}|\rho;\vec{p},-\rangle = 0 \quad ,$$

it is sufficient that the operators commute with rotations in the plane transverse to $\vec{p}$. This has also motivated our choice of operators.

The factors that do not depend on the operator $\hat{O}$ can be eliminated by taking the ratio of (4.37) to another correlator, e.g. the two-point correlator

$$\begin{aligned} C(t) &= \sum_j \langle \eta_j(\rho;t,\vec{p})\,\eta_j^\dagger(\rho;0,\vec{p})\rangle \\ &= \sum_\lambda \Big[\langle 0|\hat{\eta}_j(\rho;\vec{p})|\rho;\vec{p},\lambda\rangle\,\langle\rho;\vec{p},\lambda|\hat{\eta}_k^\dagger(\rho;\vec{p})|0\rangle\,e^{-Et} \\ &\qquad + \langle\rho;\vec{p},\lambda|\hat{\eta}_j(\rho;\vec{p})|0\rangle\,\langle 0|\hat{\eta}_k^\dagger(\rho;\vec{p})|\rho;\vec{p},\lambda\rangle\,e^{-E(T-t)}\Big] \quad . \end{aligned} \tag{4.44}$$

Using the relations (4.36) and (A.10), this reduces to

$$C(t) = Z_\rho\,(2m^2 + E^2)\,\left(e^{-Et} + e^{-E(T-t)}\right) \quad . \tag{4.45}$$

We therefore arrive at the following relation between the ratio of a three- to a two-point correlation function and the expectation value of the corresponding operator, valid for $t \gg \tau \gg 0$:

$$\begin{aligned} R_{jk} &= \frac{\langle \eta_j(\rho;t,\vec{p})\, \mathcal{O}(\tau)\, \eta_k^\dagger(\rho;0,\vec{p})\rangle}{\sum_l \langle \eta_l(\rho;t,\vec{p}) \eta_l^\dagger(\rho;0,\vec{p})\rangle} \\ &= \frac{1}{2+E^2/m^2}\, \frac{e^{-Et}}{e^{-Et}+e^{-E(T-t)}} T_{jk} \quad . \end{aligned} \tag{4.46}$$

For $T \gg \tau \gg t \gg 0$, we get an analogous equation with the additional sign factor from (4.41) and with t replaced by $T-t$. For $t = T/2$, which is the choice in our numerical work, (4.46) gives

$$R_{jk} = \frac{1}{2+E^2/m^2}\, \frac{1}{2} T_{jk} \quad . \tag{4.47}$$

The ratio may still depend on τ due to contributions from the higher states neglected in (4.39). By searching for plateaus in the τ-dependence, one can extract the value of the ratio with the smallest contamination from higher states.

In the case of the pion, there is no polarisation, and the relation (4.47) reduces to

$$R = \frac{\langle \pi;\vec{p}|\hat{O}|\pi;\vec{p}\rangle}{2} \quad . \tag{4.48}$$

4.5 Evaluation of three-point functions on the lattice

The actual form of the three-point correlator is given by

$$\langle \eta_\Gamma^F(t,\vec{p})\, \mathcal{O}^G(\tau)\, \eta_{\Gamma'}^{F'}(0,-\vec{p})\rangle \quad . \tag{4.49}$$

Here we explicitly indicate the flavour matrices F, F', and G. $\eta_\Gamma^F(t,\vec{p})$ is a meson operator with momentum $\vec{p}$ at time t:

$$\eta_\Gamma^F(t,\vec{p}) = \sum_{x:x_4=t} e^{-\mathrm{i}\vec{p}\cdot\vec{x}}\, F_{ff'}\, \overline{\psi}^a_{f\alpha}(x) \Gamma_{\alpha\beta} \psi^a_{f'\beta}(x) \tag{4.50}$$

(a colour, f flavour, α Dirac index) with a suitably chosen Dirac matrix Γ. In the case of the rho, $\Gamma = \gamma_j$, while for the pion $\Gamma = \gamma_5$. A second meson operator is set at time slice 0 with momentum $-\vec{p}$, and $F' = F^\dagger$. The operator $\mathcal{O}^G(\tau)$ has the general form

$$\mathcal{O}^G(\tau) = \sum_{x,z,z':x_4=\tau} G_{ff'}\, \overline{\psi}^a_{f\alpha}(z) J^{ab}_{\alpha\beta}(z,z';x) \psi^b_{f'\beta}(z') \tag{4.51}$$

where $J^{ab}_{\alpha\beta}(z,z';x)$ is a matrix that represents the flavour, Dirac, and derivative structure of the corresponding local operator. x can be imagined as the "center of mass" of the operator while the sum over z and z' represents the derivative structure.

Inserting these definitions, the correlation function is

$$\begin{aligned} &\langle \eta_\Gamma^F(t,\vec{p})\, \mathcal{O}^G(\tau)\, \eta_{\Gamma'}^{F'}(0,-\vec{p})\rangle \\ = \; & V_3 \sum_{x:x_4=\tau} \sum_{y:y_4=t} \sum_{z,z'} e^{-\mathrm{i}(\vec{p}\cdot\vec{y})}\, F_{fg}\, F'_{f'g'}\, G_{hh'}\, \Gamma_{\alpha\beta}\, \Gamma'_{\alpha'\beta'} \\ & \times \langle J^{bc}_{\gamma\delta}(z,z';x)\, \overline{\psi}^a_{f\alpha}(y) \psi^a_{g\beta}(y)\, \overline{\psi}^b_{h\gamma}(z) \psi^c_{h'\delta}(z')\, \overline{\psi}^{a'}_{f'\alpha'}(0) \psi^{a'}_{g'\beta'}(0)\rangle \end{aligned} \tag{4.52}$$

where V_3 is the volume of a time slice.

We integrate out the fermion fields in the quenched approximation and define

$$\langle \psi^a_{f\alpha}(x) \overline{\psi}^b_{f'\beta}(y)\rangle_{\text{fermions}} = \delta_{ff'} G^{ab}_{\alpha\beta}(U|x,y) \tag{4.53}$$

where $G(U|x,y)$ is the fermion propagator in the gauge field configuration U (the U dependence will be indicated explicitly only when needed), and the average is over fermion fields. There are six different contraction terms. In four of them, two operators at the same location are contracted. These fermion line disconnected contributions are proportional to $\mathrm{Tr}\, F$, $\mathrm{Tr}\, F'$, and $\mathrm{Tr}\, G$ and vanish if these matrices are chosen traceless. However, this is in general impossible for $\mathrm{Tr}\, G$, as we shall see below, and the omission of the corresponding contraction must be regarded an approximation, which is however consistent with quenching. We use this approximation for the same reason we use quenching: it is very hard to go beyond it. The remaining two terms are the fermion line connected contributions

$$\begin{aligned}
&-V_3 \sum_{x:x_4=\tau} \sum_{y:y_4=t} \sum_{z,z'} e^{-\mathrm{i}\vec{p}\cdot\vec{y}} \\
&\Big\langle (\mathrm{Tr}\, FGF')\ \mathrm{Tr}_{\,DC}\, (\Gamma G(y,z) J(z,z';x) G(z',0)\Gamma' G(0,y)) \\
&+(\mathrm{Tr}\, F'GF)\ \mathrm{Tr}_{\,DC}\, (\Gamma G(y,0)\Gamma' G(0,z) J(z,z';x) G(z',y)) \Big\rangle_g
\end{aligned} \tag{4.54}$$

where the traces are over Dirac and colour indices, and the average is over the gauge field alone.

The two terms can be related to each other by means of the following relations

$$G(x,y)^\dagger = \gamma_5 G(y,x)\gamma_5 \tag{4.55}$$
$$\gamma_5\Gamma = s\Gamma^\dagger\gamma_5 \tag{4.56}$$
$$\gamma_5\Gamma' = s'\Gamma'^\dagger\gamma_5 \tag{4.57}$$
$$\gamma_5 J(z,z';x)^\dagger\gamma_5 = s_J J(z',z;x) \tag{4.58}$$

where $s, s', s_J = \pm 1$, and eq. (4.58) is valid only if the corresponding operator is suitably symmetrised in its space-time indices. For the pion, $\Gamma = \Gamma' = \gamma_5$ and thus $s = s' = 1$, while for the rho, $\Gamma, \Gamma' \in \{\gamma_1, \gamma_2, \gamma_3\}$ and $s = s' = -1$. Then the correlation function reduces to

$$-V_3 \sum_{x:x_4=\tau} \sum_{y:y_4=t} e^{-\mathrm{i}\vec{p}\cdot\vec{y}}\ [(\mathrm{Tr}\, FGF')M(x,y) + ss's_J\, (\mathrm{Tr}\, F'GF)\, M(x,y)^*] \tag{4.59}$$

with the basic single-flavour correlation function

$$M(x,y) = \sum_{z,z'} \langle \mathrm{Tr}_{\,DC}\, \Gamma G(y,z) J(z,z';x) G(z',0)\Gamma' G(0,y)\rangle_g \quad . \tag{4.60}$$

Note that the calculation of this quantity on the lattice requires only two inversions of the fermion matrix, one at 0 and one at y or z.

Using the charge conjugation matrix, defined by eq. (4.22) and the relations

$$G(U|x,y) = C\, G(U^*|y,x)^T\, C^{-1} \tag{4.61}$$
$$C\Gamma^T C^{-1} = \sigma\Gamma \tag{4.62}$$
$$C\Gamma'^T C^{-1} = \sigma'\Gamma' \tag{4.63}$$
$$CJ(U^*|z',z;x)^T C^{-1} = \sigma_J J(U|z,z';x) \tag{4.64}$$

(where we explicitly denoted the dependence of J on the gauge field) with $\sigma, \sigma', \sigma_J = \pm 1$ one can further show that

$$M(x,y)^* = \sigma\sigma'\sigma_J\, ss's_J\, M(x,y) \quad . \tag{4.65}$$

We choose traceless matrices for F and F',

$$F = \begin{pmatrix} 0 & 1 \\ 0 & 0 \end{pmatrix} \quad , \qquad F' = \begin{pmatrix} 0 & 0 \\ 1 & 0 \end{pmatrix} \quad , \tag{4.66}$$

and therefore

$$\mathrm{Tr}\, F'GF = G_{11} \quad , \qquad \mathrm{Tr}\, FGF' = G_{22} \quad . \tag{4.67}$$

We finally arrive at the following expression relating the propagators $M(x,y)$ to the three-point correlation function:

$$\begin{aligned}
&\langle \eta_\Gamma^F(t,\vec{p})\, \mathcal{O}^G(\tau)\, \eta_{\Gamma'}^{F'}(0,-\vec{p})\rangle = \\
&\qquad = \ -V_3\ (G_{11} + \sigma_J\, G_{22}\,) \times \sum_{x:x_4=\tau} \sum_{y:y_4=t} e^{-\mathrm{i}\vec{p}\cdot\vec{y}}\, M(x,y)
\end{aligned} \tag{4.68}$$

For an operator with n derivatives, σ_J is $(-1)^{n+n_5+1}$, where $n_5 = 1$ if the operator contains a γ_5 matrix, $n_5 = 0$ otherwise. Thus, for odd $n + n_5$, G must not be traceless.

The analogous expression for the two-point correlation function reads

$$\begin{aligned} \langle \eta^F_\Gamma(t,\vec{p})\, \eta^{F'}_{\Gamma'}(0,-\vec{p})\rangle = & \\ = & -V_3 \sum_{x:x_4=t} e^{-\mathrm{i}\vec{p}\cdot\vec{x}} \langle \mathrm{Tr}_{DC}\, G(x,0)\Gamma' G(0,x)\Gamma\rangle_g \quad . \end{aligned} \tag{4.69}$$

4.6 Smearing

The method we use for smearing is to smear the quark in a plane $x_4 = t$ [18]:

$$^S\psi^a_{f\alpha}(\vec{x},t) = \sum_{\vec{y}} {}^S H^{ab}(\vec{x},\vec{y};U,t)\psi^b_{f\alpha}(\vec{y},t)\,, \tag{4.70}$$

where the kernel H is chosen to have the correct gauge transformation properties and is diagonal in spin space. S is the smearing label. So for example for no smearing $S = L =$ local, then ${}^L H^{ab}(\vec{x},\vec{y};U,t) = \delta^{ab}\delta_{\vec{x}\vec{y}}$. ${}^S H$ is also taken as Hermitian:

$$^S H^{ba}(\vec{y},\vec{x};U,t)^* = {}^S H^{ab}(\vec{x},\vec{y};U,t)\,. \tag{4.71}$$

Also the smeared anti-quark is defined as

$$^S\overline{\psi}^a_{f\alpha}(\vec{x},t) = \sum_{\vec{y}} \overline{\psi}^b_{f\alpha}(\vec{y},t) H^{ba}_S(\vec{y},\vec{x};U,t)\,. \tag{4.72}$$

Note that we can choose different smearing for the quark and anti-quark. Thus for a smeared meson operator we have

$$^{S'S}\eta(t,\vec{p}) = \sum_{\vec{x}} F_{ff'} e^{-\mathrm{i}\vec{p}\cdot\vec{x}}\, {}^{S'}\overline{\psi}^a_{f\alpha}(\vec{x},t)\Gamma_{\alpha\beta}\, {}^S\psi^a_{f'\beta}(\vec{x},t) \tag{4.73}$$

with the appropriate correlation function

$$C^{S'S}(t,\vec{p};t_0) = \langle {}^{S'S'}\eta(t,\vec{p})\, {}^{SS}\eta(t_0,-\vec{p})\rangle \tag{4.74}$$

so that S and S' is smearing at the source, sink respectively.

The smeared quark propagator is defined by

$$^{S'S}G^{fab}_{\alpha\beta}(x,y;U)\delta_{ff'} = \langle {}^{S'}\psi^a_{f\alpha}(x)\, {}^S\overline{\psi}^b_{f'\beta}(y)\rangle_{\mathrm{fermions}} \tag{4.75}$$

(${}^{LL}G \equiv G$). So in meson correlation functions we can simply replace G with ${}^{S'S}G$ to allow for smearing.

The smeared quark propagators are found sequentially:

- Generate the smeared source ${}^S S$ from a point source at $(\vec{x}_0, t_0)$ and so with $S^a_{0\alpha}(\vec{x}t) = \delta_{\vec{x}\vec{x}_0}\delta_{tt_0}\delta^{aa_0}\delta_{\alpha\alpha_0}$,

$$^S S^{faa_0}_{\alpha\alpha_0}(\vec{x},t;\vec{x}_0,t_0) = {}^S H^{aa_0}(\vec{x},\vec{x}_0;U,t)\delta_{tt_0}\delta_{\alpha\alpha_0}\,. \tag{4.76}$$

- Find ${}^{LS}G$, by solving $M\,{}^{LS}G = {}^S S$. We thus have

$$^{LS}G^{fab}_{\alpha\beta}(\vec{x},t;\vec{x}_0,t_0) \equiv \sum_{\vec{y}} G^{fab'}_{\alpha\beta}(\vec{x},t;\vec{y},t_0)\, {}^S H^{b'b}(\vec{y},\vec{x}_0;U,t_0)\,. \tag{4.77}$$

- From ${}^{LS}G$ we generate ${}^{S'S}G$ by applying ${}^{S'}H$:

$$^{S'S}G^{fab}_{\alpha\beta}(\vec{x},t;\vec{x}_0,t_0) = \sum_{\vec{y}} {}^{S'}H^{aa'}(\vec{x},\vec{y};U,t)\, {}^{LS}G^{fa'b}_{\alpha\beta}(\vec{y},t;\vec{x}_0,t_0)\,. \tag{4.78}$$

  Note that this step can be expensive (in CPU time) in comparison to eq. (4.76) as we must smear on every $x_4 = t$ plane.

Practically we shall use Jacobi smearing (as advocated mainly by [19]). This is given by

$$\sum_{\vec{x}'} K(\vec{x},t;\vec{x}'t)\,{}^S S(\vec{x}',t) = S_0(\vec{x},t)\,, \tag{4.79}$$

where S_0 is the original point source. Here

$$K = 1 - \kappa_s D_s \tag{4.80}$$

and D_s is a covariant derivative in the $x_4 = t$ plane, viz.

$$D^{ab}_{s\alpha\beta}(\vec{x},t;\vec{y},t) = \delta_{\alpha\beta}\sum_{i=1}^{3}\left[U_i^{ab}(\vec{x},t)\delta_{\vec{x}+\vec{\imath},\vec{y}} + U_i^{\dagger ab}(\vec{x}-\vec{\imath},t)\delta_{\vec{x}-\vec{\imath},\vec{y}}\right]\,. \tag{4.81}$$

Hence we need $H = K^{-1}$. Rather than performing this inversion completely we Jacobi iterate N_s times, so

$${}^S S^{(n)}(\vec{x},t) = S_0(\vec{x},t) + \kappa_s D_s\,{}^S S^{(n-1)}(\vec{x},t) \qquad n = 1,2,\ldots \tag{4.82}$$

with ${}^S S^{(0)}(\vec{x},t) = S_0(\vec{x},t)$.

We thus have two parameters, κ_s, N_s at our disposal. κ_s controls the coarseness of the iteration, while increasing N_s increases the size of the smeared object roughly like a random walk. Physically we wish to smear until our source is about the size of the meson. A suitable measure of the (rms) radius is given by

$$r^2 = \frac{\sum_{\vec{x}}(\vec{x}-\vec{x}_0)^2\left|{}^S S(\vec{x},t_0;\vec{x}_0,t_0)\right|^2}{\left|{}^S S(\vec{x},t_0;\vec{x}_0,t_0)\right|^2}\,. \tag{4.83}$$

(Note that on a periodic lattice, $(\vec{x}-\vec{x}_0)^2$ is taken as the minimum distance from $\vec{x}$ to $\vec{x}_0$.) Explicitly for $\beta = 6.0$ we have chosen $\kappa_s = 0.21$, $N_s = 50$.This gives ra of about $3.5a \gtrsim 0.5$fm which corresponds roughly to the hadron radius.

5 Hadron Masses

5.1 Sheikholeslami-Wohlert action

The calculation of hadron masses in lattice gauge theory has a long history. Over the years there has been a steady improvement in computing power and methods allowing simulations on larger volumes and smaller quark masses with higher statistics. However, the progress to smaller lattice spacing a has been slower because of the high computer cost which increases by at least a factor of $(1/a)^5$. Since it is so expensive to reduce cut-off effects by reducing a, we should consider reducing them by improving the action.

A systematic improvement program reducing the cut-off errors order by order in a has been proposed by Symanzik [7] and developed for on-shell quantities in ref. [8]. The standard gluonic action has discretisation errors of $O(a^2)$, but those for Wilson fermions are of $O(a)$. Therefore it is the fermionic action which is most in need of improvement. Sheikholeslami and Wohlert [9] proposed an action where a higher dimensional operator is added to the Wilson action S_W which is restricted by the same symmetries as the original unimproved action. This action takes the form (we assume $r = 1$)

$$S_F = S_W - \frac{\mathrm{i}}{2}\,\kappa\, g\, c_{SW}(g)\, a\, a^4 \sum_x \overline{\psi}(x)\sigma_{\mu\nu}F_{\mu\nu}(x)\psi(x), \tag{5.1}$$

where S_W is the original Wilson action

$$S_W = \beta\sum_{\Box}\left(1-\frac{1}{3}\mathrm{Re\,Tr}\,U_{\Box}\right) + \sum_x \overline{\psi}(x)\psi(x) - \kappa\sum_{\mu=\pm1}^{\pm4}\overline{\psi}(x+\hat{\mu})(1+\gamma_\mu)U_{x,\mu}\psi(x) \tag{5.2}$$

with the plaquette variable

$$U_{\Box} \equiv U_{x,\mu\nu} = U^\dagger_{x,\nu}U^\dagger_{x+\hat{\nu},\mu}U_{x+\hat{\mu},\nu}Ux,\mu\,, \tag{5.3}$$

$\beta \equiv 6/g^2$ and

$$F_{\mu\nu}(x) = \frac{1}{8\mathrm{i}ga^2}\sum_{\mu,\nu=\pm}(U_{x,\mu\nu} - U^\dagger_{x,\mu\nu}). \tag{5.4}$$

is the clover leaf form of the lattice field strength, $\sigma_{\mu\nu} = (i/2)(\gamma_\mu\gamma_\nu - \gamma_\nu\gamma - |mu)$. In eq. (5.4) the sum extends over the four plaquettes in the $\mu\nu$-plane which have x as one corner, and the plaquette operators $U_{x,\mu\nu}$ are the products of the four link matrices comprising the plaquettes taken in a clockwise sense. If c_{SW} giving the strength of the higher dimensional operator in the action is appropriately chosen, this action removes all $O(a)$ errors from on-shell quantities such as the hadron masses. A nonperturbative evaluation of this function leads to [20]

$$c_{SW}(g) = \frac{1-0.656\,g^2-0.152\,g^4-0.054\,g^6}{1-0.922\,g^2}\ ,\ g^2 \le 1. \tag{5.5}$$

In a perturbative expansion c_{SW} operator is given as $c_{SW} = 1 + 0.2659g^2$ [76, 77]. When we talk about improved fermions in the following, we always understand that c_{SW} has been chosen according to eq. (5.5).

In the next Sections we present results for the light hadron mass spectrum, the light and strange quark masses and the light meson decay constants using the improved action. The calculation is done for two values of the coupling, $\beta = 6.0$ and 6.2, which allows us to test for scaling. To exhibit the effect of improvement, we have also done calculations with Wilson fermions on the same lattices. Most of our Wilson data come from our structure function calculations [10, 11], and we combine this with masses from the literature at other β values to see the dependence on a clearly.

From the meson correlation functions we also extract meson decay constants and quark masses. However, simply improving the action is not sufficient to remove all $O(a)$ errors from these quantities. Here we also have to improve the operators which is done by adding higher dimensional terms with the same quantum numbers in an appropriate fashion.

5.2 Computational Details

Our calculations have mainly been done at $\beta = 6.0$ and 6.2 on $16^3 32$, $24^3 32$ and $24^3 48$ lattices. We use Quadrics (formerly called *APE*) parallel computers. For the improved case the parameter c_{SW} is given from eq. (5.5) as $c_{SW} = 1.769$ at $\beta = 6.0$ and $c_{SW} = 1.614$ at $\beta = 6.2$. The simulations are done for at least five different κ values in each case. This helps with the extrapolation to the chiral limit.

For the gauge field update we use a combination of 16 overrelaxation sweeps followed by a three-hit Metropolis update. This procedure is repeated 50 times to generate a new configuration.

The improvement term in eq. (5.1) appears in the site-diagonal part of the action. The major overhead in our case is multiplication by this term during inversion of the fermion mass matrix. In our basis of hermitean gamma matrices we can rewrite this term as

$$\begin{aligned} 1 - \frac{\mathrm{i}}{2}\kappa g c_{SW}\sigma \cdot F &= \begin{pmatrix} A & B \\ B & A \end{pmatrix} \\ &= \frac{1}{2}\begin{pmatrix} 1 & -1 \\ 1 & 1 \end{pmatrix}\begin{pmatrix} A+B & 0 \\ 0 & A-B \end{pmatrix}\begin{pmatrix} 1 & 1 \\ -1 & 1 \end{pmatrix}, \end{aligned} \tag{5.6}$$

where A, B are 6×6 matrices (two-spinors with colour), so that instead of a 12×12 multiplication we have two 6×6 multiplications and two inexpensive coordinate transformations. This reduces the overhead for the improvement in the inverter from 45% to 30%. Also, the inverse of the matrix in eq. (5.6) is required on half the lattice due to the even-odd preconditioning. We now have to invert two 6×6 instead of a 12×12 matrix. However, this is only required once for each propagator inversion.

For the matrix inversion we mainly used the minimal residue algorithm, except for the lightest quark mass on the larger lattices where we used the BiCGstab algorithm [14, 15]. As convergence criterion we chose

$$|r| \leq 10^{-6} \tag{5.7}$$

for the residue, which is the best that can be achieved for our single precision machine.

For the mass calculations we used Jacobi smearing for source and sink. For a detailed description of our application of this procedure see Sect. 4.6 and [6]. We have two parameters we can use to set the size of our source, the number of smearing steps, N_s, and the smearing hopping parameter, κ_s. We chose $N_s = 50$ for $\beta = 6.0$ and 100 for $\beta = 6.2$ and $\kappa_s = 0.21$ at both β values. This gives roughly the same r.m.s. radius in physical units in both cases, namely 0.4 fm. To define the matrix elements for the decay constants and quark masses, we have also computed correlation functions with smeared source and local sink. This does not require any additional matrix inversions.

At $\beta = 6.0$ and $c_{SW} = 0$ we had generated $O(5000)$ configurations for our structure function project on which we have computed the hadron masses. To these we added $O(150)$ new configurations on which we computed the meson decay constants and the chiral Ward identity. For $c_{SW} = 1.769$ we have analyzed $O(1000)$ configurations. For the heavier quark masses, $\kappa = 0.1487$ and $\kappa = 0.1300, 0.1310, 0.1320$, respectively, the number of configurations was $O(200)$. On the 24^3 lattice we have generated $O(100)$ and $O(200)$ configurations at $c_{SW} = 0$ and 1.769, respectively. At $\beta = 6.2$ we only ran on 24^3 lattices. Here we have analyzed $O(100)$ configurations for $c_{SW} = 0$ and $O(300)$ configurations for $c_{SW} = 1.614$. We employed both relativistic and non-relativistic wave functions [10, 11], except for the high statistics runs where we only looked at the non-relativistic wave function in order to save computer time.

Besides our calculations at $\beta = 6.0$ and 6.2 we also made exploratory studies at $\beta = 5.7$ to see what effect varying c_{SW} has on coarser lattices. If one decreases β, increases c_{SW} or increases κ, one starts to get problems with exceptional configurations. This showed up in non-convergence of our fermion matrix inversions. It was, however, only a real problem at $\beta = 5.7$, $c_{SW} = 2.25$ and [12] $\beta = 6.0$, $c_{SW} = 3.0$.

5.3 Results for hadron masses

We consider hadrons where all the quarks have degenerate masses. We looked at π, ρ, nucleon (N), a_0, a_1 and b_1 masses, and we have used this nomenclature for all quark masses, not just in the chiral limit.

In our mass calculations we have made single exponential fits to meson and baryon correlators over appropriate fit ranges. The errors are determined using the bootstrap method with 50 data samples. We present hadron mass results for $\beta = 6.0$ and 6.2 in tables 1 and 2, results for a coarser lattice at $\beta = 5.7$ results can be found in ref. [13]. For the meson masses we found very little difference between using relativistic and non-relativistic wave functions, and we settled for relativistic wave functions (except for the high statistics runs). For the nucleon we have chosen non-relativistic wave functions [10] which performed slightly better because the effective mass plateaus extended to larger times. At $\beta = 6.0$ we repeated the lightest quark mass on $16^3 32$ on the $24^3 32$ lattice, for both improved and Wilson fermions. The values agree within less than 3%. This indicates that all our results on the $16^3 32$ lattice do not suffer from significant finite size effects.

$\beta = 6.0$							
$c_{SW} = 0$							
V	κ	am_π	am_ρ	am_N	am_{a_0}	am_{a_1}	am_{b_1}
$16^3 32$	0.1487	0.6384(18)	0.683(2)	1.071(7)	0.885(19)	0.933(13)	0.940(19)
	0.1515	0.5037(8)	0.5696(10)	0.9019(17)	0.817(7)	0.851(7)	0.849(13)
	0.1530	0.4237(8)	0.5080(11)	0.7977(20)	0.763(11)	0.797(6)	0.809(7)
	0.1550	0.3009(10)	0.4264(14)	0.6517(30)	0.735(15)	0.717(12)	0.736(9)
$24^3 32$	0.1550	0.292(2)	0.418(5)	0.638(8)	0.610(48)	0.657(33)	0.659(35)
	0.1558	0.229(2)	0.384(7)	0.555(12)	0.616(90)	0.613(41)	0.638(38)
	0.1563	0.179(3)	0.358(11)	0.488(22)	0.88(15)	0.584(52)	0.615(44)
c. l.	0.15713(3)	0	0.327(6)	0.412(16)	*0.658(19)*	*0.632(14)*	*0.650(13)*
$c_{SW} = 1.769$							
V	κ	am_π	am_ρ	am_N	am_{a_0}	am_{a_1}	am_{b_1}
$16^3 32$	0.1300	0.707(2)	0.783(6)	1.190(6)			
	0.1310	0.627(2)	0.714(3)	1.079(7)			
	0.1320	0.545(5)	0.644(8)	0.974(16)			
	0.1324	0.5039(7)	0.6157(16)	0.932(4)	0.779(14)	0.829(12)	0.853(7)
	0.1333	0.4122(8)	0.5502(23)	0.821(5)	0.738(15)	0.773(7)	0.799(10)
	0.1342	0.2988(17)	0.487(3)	0.705(9)	0.92(5)	0.68(2)	0.775(15)
$24^3 32$	0.1342	0.3020(11)	0.491(3)	0.686(7)	0.82(3)	0.715(19)	0.758(16)
	0.1346	0.2388(14)	0.467(6)	0.626(10)	1.00(8)	0.684(26)	0.745(20)
	0.1348	0.194(4)	0.448(13)	0.593(19)	1.52(20)	0.664(34)	0.736(29)
c. l.	0.13531(1)	0	0.417(7)	0.511(15)	*0.816(33)*	*0.625(19)*	*0.710(14)*

Table 1: Hadron masses at $\beta = 6.0$ for Wilson fermions ($c_{SW} = 0$) and improved fermions ($c_{SW} = 1.769$). The numbers in roman (*italic*) are from three-parameter (two-parameter) fits. The errors are bootstrap errors.

$\beta = 6.2$							
$c_{SW} = 0$							
V	κ	am_π	am_ρ	am_N	am_{a_0}	am_{a_1}	am_{b_1}
$24^3 48$	0.1468	0.5258(12)	0.5585(16)	0.872(5)	0.685(8)	0.700(21)	0.695(21)
	0.1489	0.4148(13)	0.4615(19)	0.720(6)	0.589(8)	0.624(9)	0.626(9)
	0.1509	0.2947(14)	0.3672(27)	0.560(10)	0.507(14)	0.536(13)	0.540(13)
	0.1518	0.2299(15)	0.326(4)	0.487(12)	0.474(20)	0.509(16)	0.519(17)
	0.1523	0.1867(17)	0.307(6)	0.448(14)	0.479(30)	0.492(17)	0.511(21)
c. l.	0.15336(4)	0	0.255(9)	0.342(28)	*0.407(17)*	*0.449(15)*	*0.464(16)*
$c_{SW} = 1.614$							
V	κ	am_π	am_ρ	am_N	am_{a_0}	am_{a_1}	am_{b_1}
$24^3 48$	0.1321	0.5179(7)	0.5738(11)	0.877(4)	0.691(5)	0.723(6)	0.727(6)
	0.1333	0.4143(8)	0.4850(15)	0.735(5)	0.603(10)	0.642(5)	0.638(8)
	0.1344	0.3046(9)	0.4005(26)	0.592(9)	0.532(21)	0.563(7)	0.566(9)
	0.1349	0.2444(9)	0.3626(43)	0.521(13)	0.543(22)	0.529(10)	0.539(12)
	0.1352	0.2016(11)	0.3430(53)	0.485(6)	0.646(53)	0.514(13)	0.523(25)
c. l.	0.13589(2)	0	0.287(9)	0.378(18)	*0.460(21)*	*0.460(9)*	*0.465(12)*

Table 2: Hadron masses at $\beta = 6.2$ for Wilson fermions ($c_{SW} = 0$) and improved fermions ($c_{SW} = 1.614$). Otherwise the notation is the same as in table 1.

5.3.1 Chiral behaviour

To obtain the critical value of κ, κ_c, and the hadron masses in the chiral limit, we extrapolate our data to zero π mass. We first tried

$$m_\pi^2 = b\left(\frac{1}{\kappa} - \frac{1}{\kappa_c}\right). \tag{5.8}$$

Using this relation gives a rather poor fit of the data, and we saw that there was a slight curvature in a plot of m_π^2 against $1/\kappa$. Quenched chiral perturbation theory predicts [16]

$$m_\pi^2 = b'\left(\frac{1}{\kappa} - \frac{1}{\kappa_c}\right)^{\frac{1}{1+\delta}}, \tag{5.9}$$

where δ is small and positive. We made fits using this formula but found that δ was always negative. As in our previous work [12] we conclude that our κ values are too far from κ_c for the formula to be applicable. This is in agreement with observations made by other authors [17]. As an alternative parameterisation of the curvature we used the phenomenological fit

$$\frac{1}{\kappa} = \frac{1}{\kappa_c} + b_2 m_\pi^2 + b_3 m_\pi^3. \tag{5.10}$$

The linear fits give χ^2/dof values of up to 40. The other two fits both give acceptable values of χ^2, but eq. (5.10) usually gives a lower χ^2 than eq. (5.9). In the following we shall take κ_c from the phenomenological fits.

In fig. 10 we plot κ_c for improved Wilson fermions. We compare our results with the results of ref. [20].

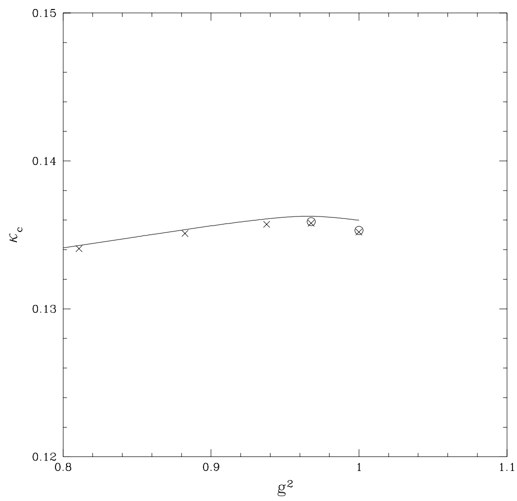

Figure 10: The critical values of κ for improved Wilson fermions as a function of g^2 from this work ($\bigcirc$) and ref. [20] ($\times$). The curve is the tadpole improved result given in eq. (5.12).

The agreement is excellent. In one-loop perturbation theory κ_c is given by [12]

$$\kappa_c = \frac{1}{8}[1 + g^2(0.108571 - 0.028989\, c_{SW} - 0.012064\, c_{SW}^2)]. \tag{5.11}$$

The tadpole improved value of κ_c that follows from this result is

$$\kappa_c = \frac{1}{8}[1 + g^{*\,2}(0.025238 - 0.028989\, c_{SW} u_0^3 - 0.012064\, (c_{SW} u_0^3)^2)] u_0^{-1}, \tag{5.12}$$

where c_{SW} is given by eq. (5.5),

$$u_0 = \langle \frac{1}{3} \mathrm{Tr} U_\Box \rangle^{\frac{1}{4}} \tag{5.13}$$

and $g^{*\,2}$ is the boosted coupling constant defined by

$$g^{*\,2} = g^2/u_0^4. \tag{5.14}$$

In fig. 10 we compare the tadpole improved perturbative formula (5.12) with the data where for the larger couplings we have taken u_0 from [27, 36]. The curve and the data points agree within less than 1%. In eq. (5.12) one has the choice of using the lowest order tadpole improved value of c_{SW}, namely u_0^{-3} [20], or the value from eq. (5.5) which is the value actually used in the simulations. Both procedures remove all the tadpole diagrams and differ only by small $O(g^4)$ terms, so they are both reasonable. We prefer the second choice.

We fit the other hadron masses by the formula

$$m_H^2 = b_0 + b_2 m_\pi^2 + b_3 m_\pi^3\ ,\ H = \rho, N, \cdots. \tag{5.15}$$

The result of the fit is shown in fig. 11 for both improved and Wilson fermion world data compiled by us in

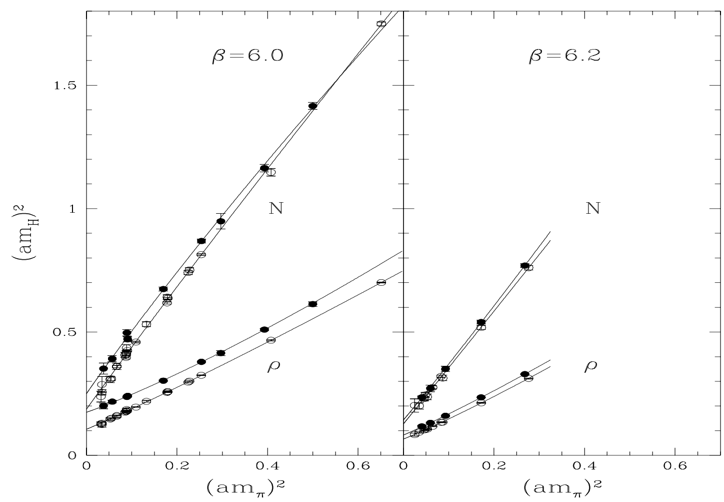

Figure 11: Fits and chiral extrapolations of ρ and nucleon masses for improved (●) and Wilson fermions (○).

ref. [13].

For the a_0, a_1 and b_1 masses only a two-parameter fit with b_3 set to zero was reasonable. The mass values in the chiral limit for our data are also given in tables 1 and 2.

We see that the effect of improvement is largest for the ρ mass. In the chiral limit the difference between improved and Wilson results is 25% at $\beta = 6.0$ and still 12% at $\beta = 6.2$. It is quite common to define the physical scale from the ρ mass. The relatively large change of this quantity from the Wilson to the improved case suggests that it contains large $O(a)$ corrections, and that this procedure is misleading. A better procedure is to use the string tension or r_0 [33], the force parameter, as the scale. For the nucleon mass the difference between the two actions is smaller.

5.3.2 *APE* plots

In figs. 12 and 13 we show the dimensionless ratio m_N/m_ρ as a function of $(m_\pi/m_\rho)^2$, a so-called *APE* plot, for $\beta = 6.0$ and 6.2, both for improved and Wilson fermions (collected world data). The solid lines are the results of the ratio of the fits in fig. 11. At $\beta = 6.0$ we find that the mass ratio data are rather different for the two actions. The improved results lie consistently lower than the Wilson results. At $\beta = 6.2$ we find the same pattern in the data.

At $\beta = 6.0$ we can say something about the chiral limit. Our fits give $m_N/m_\rho = 1.20(6)$ for improved fermions and $m_N/m_\rho = 1.33(2)$ for Wilson fermions. The improved results come closer to the physical value than the Wilson results. At $\beta = 6.2$ we are lacking data at small quark masses and on larger volumes. In the chiral limit our fits give $m_N/m_\rho = 1.32(11)$ for improved fermions and $m_N/m_\rho = 1.39(12)$ for Wilson fermions, so that we cannot say anything conclusive about the behaviour of the two actions in the chiral limit in this case.

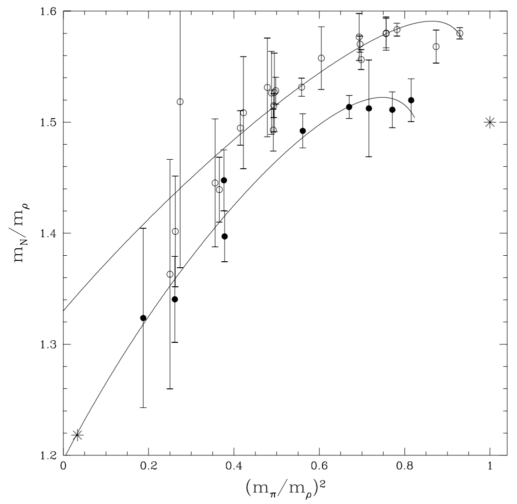

Figure 12: *APE* plot at $\beta = 6.0$ for improved (●) and Wilson fermions (○) compared with the physical mass ratio (✳) at the physical quark mass and in the heavy quark limit. The solid lines are from the mass fits described in the text.

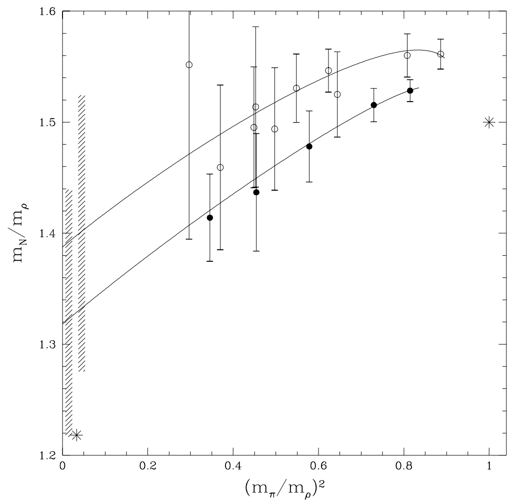

Figure 13: The same as fig. 12, but for $\beta = 6.2$. The hatched bars indicate the errors in the chiral limit.

5.3.3 Scaling behaviour

Let us now look at and compare the scaling behaviour of the two actions. We shall limit our discussion to the ρ mass because the errors of the nucleon are too large to make precise statements. In order to exhibit the cut-off effects most clearly, it has been suggested [34] that m_ρ should be plotted in units of the square-root of the string tension K which has cut-off errors of $O(a^2)$ only. In table 3 we have compiled the world string

β	$a\sqrt{K}$	Reference	r_0/a	Reference	$r_0\sqrt{K}$
6.8	0.0730(12)	[35]	16.7(4)	[36]	1.22(4)
6.5	0.1068(10)	[37]			
6.4	0.1215(11)	Combined [35],[38]	9.85(8)	Combined [36],[38]	1.197(15)
6.3	0.1394(11)	Interpolated			
6.2	0.1610(8)	Combined [39],[38],[40]	7.36(4)	Combined [36],[38]	1.185(9)
6.17	0.1677(8)	Interpolated			
6.0	0.2191(15)	Combined [39],[38]	5.30(4)	Combined [36],[38]	1.161(12)
5.93	0.2536(29)	Interpolated			
5.90	0.2702(37)	[42]	4.62(11)	[36]	1.25(3)
5.85	0.2986(27)	Interpolated			
5.8	0.3302(30)	[42]	3.63(5)	[36]	1.199(20)
5.7	0.4099(24)	[42]	2.86(5)	[36]	1.172(22)
5.6			2.29(6)	[36]	
5.5			2.01(3)	[36]	

Table 3: The lattice spacing expressed in terms of the world average string tension K and the force parameter r_0. When several groups have computed these quantities, we have taken the weighted average, while we interpolate logarithmically whenever the values are not known.

tension data. When there are several calculations, we performed the weighted average.

In fig. 14 we plot the ratio $m_\rho/\sqrt{K}$ as a function of $a\sqrt{K}$. This is done for fixed physical π masses with $m_\pi^2 = 0$, $2K$ and $4K$. Comparing hadron masses at larger quark masses has the advantage that this does not require large extrapolations of the lattice data but rather involves small interpolations only. The Wilson fermion data shown are a fit to the world data compiled in ref. [13]. As expected, the Wilson masses show practically a linear behaviour in the lattice spacing a. We have done a simultaneous linear plus quadratic fit to the Wilson data and a quadratic fit to the improved data. The fit is constrained to agree in the continuum limit. The result of the fit is shown by the solid lines in fig. 14. In the continuum limit we obtain

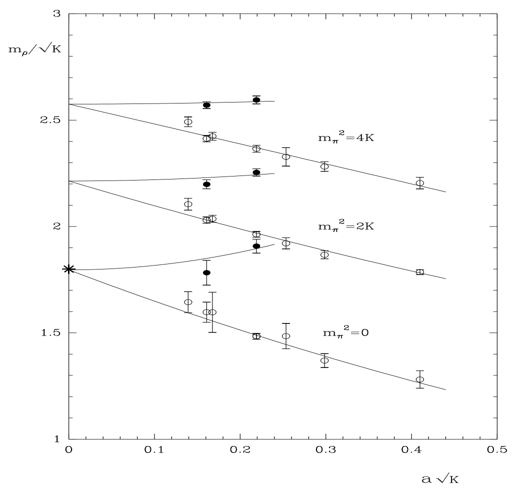

Figure 14: The ratio $m_\rho/\sqrt{K}$ as a function of the lattice spacing for improved (●) and Wilson fermions (○). The solid lines are from a simultaneous linear plus quadratic fit to the Wilson data and a quadratic fit to the improved data. This is compared with the experimental value ($\ast$) using $\sqrt{K} = 427\,\mathrm{MeV}$.

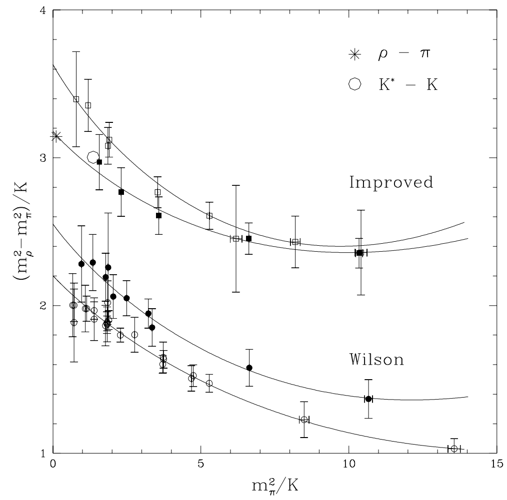

Figure 15: The vector-pseudoscalar mass splitting as a function of the quark mass. Open symbols correspond to $\beta = 6.0$, solid symbols to $\beta = 6.2$. This is compared with the physical ρ-π ($\ast$) and K^*-K (octogon) mass splitting. The curves are from the mass fits.

$m_\rho/\sqrt{K} = 1.80(10)$. We compare this result with the experimental ρ mass. For the string tension we take the value

$$\sqrt{K} = 427\,\mathrm{MeV} \tag{5.16}$$

which has been obtained from a potential fit to the charmonium mass spectrum [21]. Using this value the physical $m_\rho/\sqrt{K}$ is 1.80 which agrees with the lattice number.

As mentioned previously, an alternative scale from the potential is r_0. We have also compiled lattice results for r_0 in table 3. We see that it scales very well with $\sqrt{K}$, as the product $r_0\sqrt{K}$ is approximately constant at about 1.19, while the lattice spacing a changes by a factor of more than five. However, the physical value of $r_0\sqrt{K}$ is 1.06, taking r_0^{-1} as 402 MeV which follows from the same potential that gives $\sqrt{K} = 427\,\mathrm{MeV}$ [21]. It does not seem that this discrepancy will vanish as $a \to 0$. It is telling us that the lattice potential has a slightly different shape to the continuum potential. This may be an effect of quenching.

5.3.4 Mass splitting

The vector-pseudoscalar mass splitting

$$\Delta_{V-PS} = m_V^2 - m_{PS}^2 \tag{5.17}$$

is experimentally rather constant for all quark flavours. One finds

$$\begin{aligned} m_\rho^2 - m_\pi^2 &= 0.57\,\mathrm{GeV}^2, \\ m_{K^*}^2 - m_K^2 &= 0.55\,\mathrm{GeV}^2, \\ m_{D^*}^2 - m_D^2 &= 0.55\,\mathrm{GeV}^2. \end{aligned} \tag{5.18}$$

Quenched lattice calculations with Wilson fermions are unable to reproduce these numbers. Wilson fermions give a splitting which is much too small. In fig. 15 we compare the experimental values of $m_\rho^2 - m_\pi^2$ and

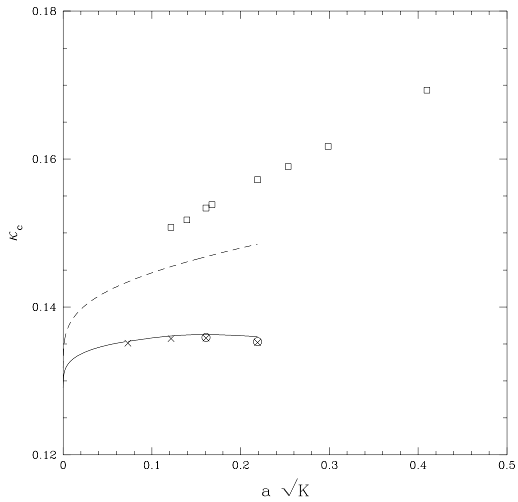

Figure 16: The critical value of κ as a function of the lattice spacing for Wilson fermions ($\square$). The dashed curve is the prediction of tadpole improved perturbation theory. This is compared with the results for improved fermions from fig. 10.

$m^2_{K^*} - m^2_K$ with the lattice data and the mass fits. As before, we have taken the string tension eq. (5.16) as the scale. In fig. 15 we also show the results for improved fermions and the corresponding mass fits as well. There is a noticeable change when going to the improved case. We find good agreement with experiment for the absolute values.

In the heavy quark effective theory [22]

$$\Delta_{V-PS} \propto \langle \overline{\Psi} \sigma_{\mu\nu} F_{\mu\nu} \Psi \rangle, \tag{5.19}$$

where Ψ is the heavy quark field. So it is natural that turning on the Sheikholeslami-Wohlert term would increase the mass splitting, and this is what we see.

5.3.5 Wilson κ_c

Let us now come back to the critical value of κ for Wilson fermions. In table 4 we have given the values of

β	κ_c
6.40	0.150759(145)
6.30	0.151774(36)
6.20	0.153374(17)
6.17	0.153838(37)
6.00	0.157211(8)
5.93	0.158985(73)
5.85	0.161716(23)
5.70	0.169313(72)

Table 4: The critical values of κ, κ_c, for the Wilson world data.

κ_c from a fit of the world data using the phenomenological ansatz (5.10). In fig. 16 we plot these results as a function of $a\sqrt{K}$ (the string tension being taken from table 3). We see that κ_c is a linear function of a over the whole range of the data which extends from $\beta = 5.7$ to 6.4. Comparing this with the improved κ_c, which is approximately constant, we conclude that the Wilson κ_c has large $O(a)$ effects. We also compare the Wilson data with the predictions of tadpole improved perturbation theory as given by eq. (5.12) with $c_{SW} = 0$. Here we have taken the one-loop perturbative formula for a beyond $\beta = 6.8$ where there are no numerical values for the string tension available any more. Not even at the smallest value of a can perturbation theory describe the Wilson data. For improved fermions, on the other hand, the agreement with tadpole improved perturbation theory is quite good, as we have already noticed.

6 Quark Masses

We shall now turn to the calculation of the quark masses. When chiral symmetry is dynamically broken, care has to be taken in defining renormalised masses. In the continuum the renormalised quark mass at scale $p^2 = \mu^2$ can be written [23]

$$\frac{1}{4}\mathrm{Tr}[S_F^{-1}(m) - S_F^{-1}(0)] = m(\mu), \tag{6.1}$$

where S_F is the renormalised quark propagator which is to be evaluated in a given gauge. This definition refers to the momentum subtraction scheme. It is usual to give the quark masses in the $\overline{MS}$ scheme. To convert from one scheme to the other, one has to go to high enough scales so that one can use perturbation theory. If the quark mass is defined in this way, then the renormalised mass is proportional to the bare mass.

On the lattice the standard assignment of the bare mass is

$$am(a) = \frac{1}{2}\left(\frac{1}{\kappa} - \frac{1}{\kappa_c}\right), \tag{6.2}$$

giving the renormalised mass as

$$m^{\overline{MS}}(\mu) = Z_m^{\overline{MS}}(a\mu, am)\, m(a), \tag{6.3}$$

where $Z_m^{\overline{MS}}(a\mu, am)$ is the mass renormalisation constant. We call this method of determining the renormalised mass the standard method.

An alternative way of defining a bare mass is by means of the $PCAC$ relation between the divergence of the axial vector current $A_\mu = \overline{\psi}\gamma_\mu\gamma_5\psi$ and the pseudoscalar density $P = \overline{\psi}\gamma_5\psi$,

$$\widetilde{m}(a) = \frac{\partial_4\langle A_4(x)\mathcal{O}\rangle}{2\langle P(x)\mathcal{O}\rangle}, \tag{6.4}$$

where $\mathcal{O}$ is a suitable operator having zero three-momentum and no physical overlap with $A_4(x)$ and $P(x)$ to avoid contact terms. (See later on for a precise definition.) All operators are bare operators. To avoid anomaly terms in eq. (6.4), flavour non-singlet operators are taken. We call this method the Ward identity method. The renormalised mass is then given by

$$m^{\overline{MS}}(\mu) = \frac{Z_A(am)}{Z_P^{\overline{MS}}(a\mu, am)}\widetilde{m}(a), \tag{6.5}$$

where $Z_A(am)$ and $Z_P^{\overline{MS}}(a\mu, am)$ are the renormalisation constants of the axial vector current and the pseudoscalar density, respectively.

The quark mass inherits its scale dependence from the renormalisation constants Z_m and Z_P which involve logarithms of μ. In the following we will compute Z_m and Z_P perturbatively to one-loop order for lack of a better, nonperturbative determination. To keep the logarithms under control it is best to take $a\mu = 1$ and do the transformation to any other scale by the renormalisation group formula

$$m^{\overline{MS}}(\mu') = \left(\frac{\alpha_s^{\overline{MS}}(\mu')}{\alpha_s^{\overline{MS}}(\mu)}\right)^{\frac{8}{22}} m^{\overline{MS}}(\mu). \tag{6.6}$$

In the continuum limit both procedures should give identical results for $m^{\overline{MS}}(\mu)$. Note, however, that the two bare masses m and $\widetilde{m}$ can be different, though they both vanish in the chiral limit. On the lattice the two procedures may give different results for $m^{\overline{MS}}(\mu)$ due to non-universal discretisation errors.

The lattice calculation of the quark masses now proceeds in two steps. In the first step one has to find the κ values corresponding to the real world by adjusting (e.g.) the pseudoscalar meson masses to their experimental numbers. In case of the Ward identity method one furthermore has to compute $\widetilde{m}$. In the second step the bare quark masses have to be converted to renormalised masses. We shall compute the masses of the u and d quarks, which we assume to be equal, and the mass of the strange (s) quark.

6.1 Improved Fermions

Let us consider the case of improved fermions first. Later on we shall compare our results with the predictions of Wilson fermions to see the effect of improvement.

We will discuss the Ward identity method first. For the operator $\mathcal{O}$ we take the pseudoscalar density

$$P(0) = \sum_{\vec{x}} P(x_4 = 0, \vec{x}) \tag{6.7}$$

and smear it as we did in the hadron mass calculations. As the $P(0)$ part is common to all two-point functions, we could have used any operator projecting onto the pseudoscalar state. Similarly, we write

$$A_4(t) = \sum_{\vec{x}} A_4(x_4 = t, \vec{x}). \tag{6.8}$$

For improved fermions the axial vector current in eq. (6.4) is to be replaced by

$$A_4 \to A_4 + c_A a \partial_4 P(x), \tag{6.9}$$

where c_A is a function of the coupling only. The time derivative ∂_4 is taken to be the average of the forward and backward derivative. The coefficient c_A has been computed in [20] giving $c_A = -0.083$ at $\beta = 6.0$ and $c_A = -0.037$ at $\beta = 6.2$. The resulting bare mass

$$\widetilde{m}(a) = \frac{\partial_4 \langle A_4(t) P(0)\rangle + c_A a \partial_4^2 \langle P(t) P(0)\rangle}{2\langle P(t) P(0)\rangle} \tag{6.10}$$

has been plotted in fig. 17 for $\beta = 6.0$ and our smallest quark mass on the $16^3 32$ lattice. In fig. 18 we show

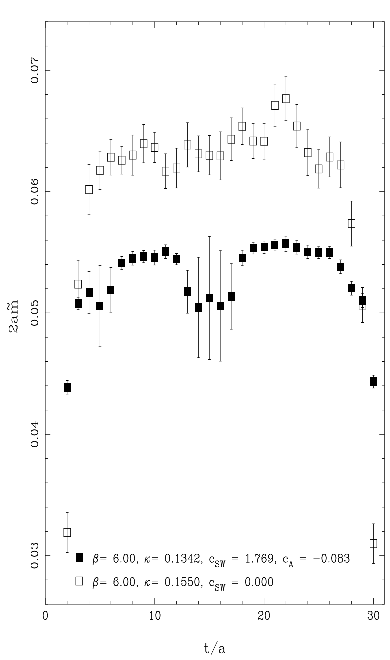

Figure 17: The bare mass $\widetilde{m}$ from the Ward identity method at $\beta = 6.0$ for Wilson (□) and improved fermions (■) on the $16^3 32$ lattice. The errors are bootstrap errors.

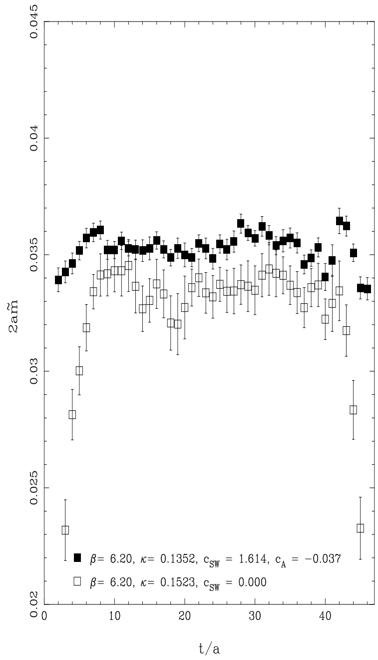

Figure 18: The same as fig. 17 but for $\beta = 6.2$ for Wilson (□) and improved fermions (■).

the same quantity for $\beta = 6.2$ and our smallest quark mass on the $24^3 48$ lattice. (Also shown in these figures are the results for Wilson fermions which we will discuss later on.) Equation (6.10) should be independent of t, except where the operators physically overlap with the source, if the cut-off effects have been successfully removed. In both cases, but in particular at $\beta = 6.2$, we see a smaller deviation from the plateau at small and large t values. To obtain the mass, we fit the ratio (6.10) to a constant. We have used the same fit ranges as for the pion mass. The results of the fit are given in tables 5, 6. At $\beta = 6.0$ in the improved case we see that at $\kappa = 0.1342$ we have small finite size effects, indicating again that our results on the $16^3 32$ lattice are not significantly volume dependent.

$\beta = 6.0$		
$c_{SW} = 0$		
V	κ	$2a\widetilde{m}$
$16^3 32$	0.1487	0.2959(5)
	0.1515	0.1866(5)
	0.1530	0.1321(5)
	0.1550	0.0642(7)
$c_{SW} = 1.769$		
V	κ	$2a\widetilde{m}$
$16^3 32$	0.1300	0.2836(3)
	0.1310	0.2279(3)
	0.1324	0.15231(10)
	0.1333	0.10380(11)
	0.1342	0.0553(2)
$24^3 32$	0.1342	0.0551(3)
	0.1346	0.0330(3)
	0.1348	0.0214(4)

Table 5: The bare quark masses $\widetilde{m}$ for Wilson fermions ($c_{SW} = 0$) and improved fermions ($c_{SW} = 1.769$) at $\beta = 6.0$. The errors are bootstrap errors.

For both the Ward identity and the standard method we choose to determine the κ values from the pseudoscalar meson masses. Sometimes the $\phi(1020)$ meson is taken for the determination of the strange quark mass. However, we do not think that this is a good idea because of potential $\omega - \phi$ mixing. We generalise eq. (5.10) to the case of two different quark masses by writing

$$\frac{1}{2}\left(\frac{1}{\kappa_1} + \frac{1}{\kappa_2}\right) - \frac{1}{\kappa_c} = b_2 m_{PS}^2 + b_3 m_{PS}^3 \tag{6.11}$$

with the same coefficients b_2, b_3 as before. This is inspired by chiral perturbation theory where it is expected that the pseudoscalar mass is a function of the sum of quark and antiquark mass, $m_q + m_{\overline{q}}$, even when quark and antiquark have different flavours. By fixing m_{PS} to the physical pion mass $m_{\pi^\pm}$, using the string tension values compiled in table 3 with eq. (5.16) as the scale, we find the value for $\kappa_{u,d} = \kappa_1 \equiv \kappa_2$. The strange quark mass is obtained by identifying m_{PS} with the kaon mass $m_{K^\pm}$, taking $\kappa_1 = \kappa_{u,d}$ as input and solving for $\kappa_2 = \kappa_s$. This gives for the light mass

$$m_{u,d}a = \frac{1}{2}\left(\frac{1}{\kappa_{u,d}} - \frac{1}{\kappa_c}\right) = \begin{cases} 0.001836(36) & \text{for } \beta = 6.0, \\ 0.001384(36) & \text{for } \beta = 6.2. \end{cases} \tag{6.12}$$

For the strange mass we get

$$m_s a = \frac{1}{2}\left(\frac{1}{\kappa_s} - \frac{1}{\kappa_c}\right) = \begin{cases} 0.0419(11) & \text{for } \beta = 6.0, \\ 0.0310(11) & \text{for } \beta = 6.2, \end{cases} \tag{6.13}$$

where $m_{u,d} = 1/2\,(m_u + m_d)$.

The bare masses $\widetilde{m}_{u,d}$, $\widetilde{m}_s$ are computed analogously. We write

$$\widetilde{m} \equiv \frac{1}{2}(\widetilde{m}_1 + \widetilde{m}_2) = \widetilde{b}_2 m_{PS}^2 + \widetilde{b}_3 m_{PS}^3. \tag{6.14}$$

Using this parameterisation we first fit the masses in tables 5, 6 to the pseudoscalar masses in tables 1, 2. This gives us $\widetilde{b}_2$, $\widetilde{b}_3$. We then determine $\widetilde{m}_{u,d}$, $\widetilde{m}_s$ by fixing m_{PS} to the physical pion and kaon masses, respectively, as before.

The mass dependence of the renormalisation constant $Z_A(am)$ can be parameterised as [24]

$$Z_A(am) = (1 + b_A am) Z_A. \tag{6.15}$$

$\beta = 6.2$		
$c_{SW} = 0$		
V	κ	$2a\widetilde{m}$
	0.1468	0.2474(3)
	0.1489	0.1616(3)
$24^3 48$	0.1509	0.0845(3)
	0.1518	0.0514(3)
	0.1523	0.0336(3)
$c_{SW} = 1.614$		
V	κ	$2a\widetilde{m}$
	0.1321	0.2161887)
	0.1333	0.14585(7)
$24^3 48$	0.1344	0.08185(7)
	0.1349	0.05283(8)
	0.1352	0.03538(9)

Table 6: The bare quark masses $\widetilde{m}$ for Wilson fermions ($c_{SW} = 0$) and improved fermions ($c_{SW} = 1.614$) at $\beta = 6.0$. The errors are bootstrap errors.

The renormalisation constant Z_A has been computed nonperturbatively in ref. [25]. The fit formula in this paper gives $Z_A = 0.7924$ at $\beta = 6.0$ and $Z_A = 0.8089$ at $\beta = 6.2$. The coefficient b_A is only known perturbatively to one-loop order [26]. The best we can do at present is to take the tadpole improved value. For the boosted coupling we use $\alpha_s^{\overline{MS}}(1/a)$, giving

$$b_A = 1 + \alpha_s^{\overline{MS}}(1/a)\, 1.912, \tag{6.16}$$

where we take $\alpha_s^{\overline{MS}}(1/a) = 0.1981$ at $\beta = 6.0$ and $\alpha_s^{\overline{MS}}(1/a) = 0.1774$ at $\beta = 6.2$ [27]. For $Z_P^{\overline{MS}}(a\mu, am)$ we write

$$Z_P^{\overline{MS}}(a\mu, am) = (1 + b_P am) Z_P^{\overline{MS}}(a\mu). \tag{6.17}$$

The renormalisation constant $Z_P^{\overline{MS}}(a\mu)$ has been computed perturbatively [28]. The result is

$$Z_P^{\overline{MS}}(a\mu) = 1 - \frac{g^2}{16\pi^2} C_F(-6\ln(a\mu) + 22.595 - 2.249 c_{SW} + 2.036 c_{SW}^2), \tag{6.18}$$

with $C_F = 4/3$. We shall take the scale $\mu = 1/a$ and use the tadpole improved value of eq. (6.18) which turns out to be

$$Z_P^{\overline{MS}}(a\mu = 1) = \left[1 - \frac{\alpha_s^{\overline{MS}}(1/a)}{4\pi}\left(16.967 - 2.999 c_{SW} u_0^3 + 2.715 (c_{SW} u_0^3)^2\right)\right] u_0. \tag{6.19}$$

(We use $u_0 = 0.8778$ at $\beta = 6.0$ and $u_0 = 0.8851$ at $\beta = 6.2$). The coefficient b_P has also been computed perturbatively to one-loop order [26]. Again we shall use the tadpole improved value

$$b_P = 1 + \alpha_s^{\overline{MS}}(1/a)\, 1.924. \tag{6.20}$$

We have also computed the renormalisation constants $Z_A(am)$, $Z_P(a\mu, am)$ non-perturbatively [29]. So far we have results for $\beta = 6.0$ only. Our numbers are in fair agreement with the nonperturbative calculation in ref. [25] and the tadpole improved value (6.19). However, for small μ the constant Z_P behaves very differently from the perturbative formula.

To compare the results at the two different β values, we rescale them both to $\mu' = 2\,\mathrm{GeV}$ using formula (6.6). As before, we use the string tension to convert the lattice spacing into physical units. The resulting quark masses $m_{u,d}^{\overline{MS}}(2\,\mathrm{GeV})$, $m_s^{\overline{MS}}(2\,\mathrm{GeV})$ are given in table 7.

β	c_{SW}	$m_{u,d}^{\overline{MS}}$ Ward	Standard	$m_s^{\overline{MS}}$ Ward	Standard
6.0	0	4.40 ± 0.17	6.47 ± 0.20	105.0 ± 4.5	141.8 ± 6.0
6.2	0	4.73 ± 0.14	6.39 ± 0.25	108.5 ± 4.2	138.8 ± 7.4
6.0	1.769	4.02 ± 0.10	4.94 ± 0.93	92.8 ± 2.9	109.4 ± 3.9
6.2	1.614	4.47 ± 0.06	5.09 ± 0.16	101.6 ± 1.7	111.7 ± 4.7
∞		5.00 ± 0.18	5.27 ± 0.36	111.9 ± 5.0	114.4 ± 11.1

Table 7: Our results of the renormalised quark masses $m^{\overline{MS}}(2\,\mathrm{GeV})$ in MeV for improved and Wilson fermions, together with the extrapolation to the continuum limit ($\beta = \infty$). The continuum numbers refer to improved fermions. We give the results for both the Ward identity and the standard method.

Let us now discuss the standard method. We already have determined $m_{u,d}(a)$, $m_s(a)$ in eqs. (6.12), (6.13). For the renormalisation constant $Z_m^{\overline{MS}}(a\mu, am)$ we write

$$Z_m^{\overline{MS}}(a\mu, am) = (1 + b_m am) Z_m^{\overline{MS}}(a\mu). \tag{6.21}$$

The constant $Z_m^{\overline{MS}}(a\mu)$ has been computed perturbatively [28]. We obtain

$$Z_m^{\overline{MS}}(a\mu) = 1 - \frac{g^2}{16\pi^2} C_F (6\ln(a\mu) - 12.952 - 7.738 c_{SW} + 1.380 c_{SW}^2). \tag{6.22}$$

The tadpole improved value, which we will be using, is

$$Z_m^{\overline{MS}}(a\mu = 1) = \left[1 - \frac{\alpha_s^{\overline{MS}}(1/a)}{4\pi}\left(-4.110 - 10.317 c_{SW} u_0^3 + 1.840 (c_{SW} u_0^3)^2\right)\right] u_0^{-1}. \tag{6.23}$$

The coefficient b_m has been computed in [26] (see also eq. (9.23)). The tadpole improved value is

$$b_m = -\frac{1}{2} - \alpha_s^{\overline{MS}}(1/a)\, 1.210. \tag{6.24}$$

Again we extrapolate the quark masses to $\mu' = 2\,\mathrm{GeV}$ using eq. (6.6). The results which follow from this approach are listed in table 7 as well.

The results of the Ward identity and the standard method may differ by $O(a^2)$ effects, and they do. We can 'fit' the a dependence by

$$m_q^{\overline{MS}} = c_0 + c_2 a^2. \tag{6.25}$$

The result of the fit is shown in figs. 19, 20.

The continuum values from this fit are given in table 7. We find that the two methods give consistent results in the continuum limit. Taking the statistical average of the two results we obtain the continuum values

$$m_{u,d}^{\overline{MS}}(2\mathrm{GeV}) = 5.1 \pm 0.2\,\mathrm{MeV}, \tag{6.26}$$

$$m_s^{\overline{MS}}(2\mathrm{GeV}) = 112 \pm 5\,\mathrm{MeV}. \tag{6.27}$$

The Ward identity method appears to have larger $O(a^2)$ effects than the standard method.

We may compare our results with the prediction of chiral perturbation theory, which cannot give absolute values but can determine the ratio of m_s to $m_{u,d}$. A recent calculation gives [30] $m_s/m_{u,d} = 24.4 \pm 1.5$. We find $m_s/m_{u,d} = 22.2 \pm 1.2$.

6.2 Wilson Fermions

Let us now consider the case of Wilson fermions. We proceed in the same way as before. The situation here is that $Z_A(am)$ is known nonperturbatively only for $\beta = 6.0$ [31], and that b_A, b_P and b_m are only known to

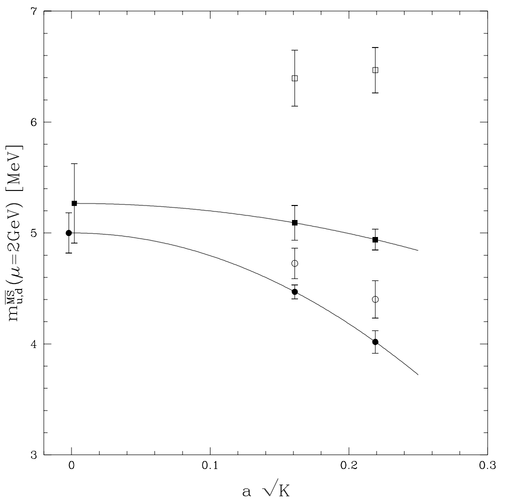

Figure 19: The light quark mass $m_{u,d}^{\overline{MS}}$ as a function of the lattice spacing for improved fermions using the Ward identity (●) and standard method (■). This is compared with the Wilson result for the Ward identity (○) and standard method (□). The curves are quadratic extrapolations to the continuum limit.

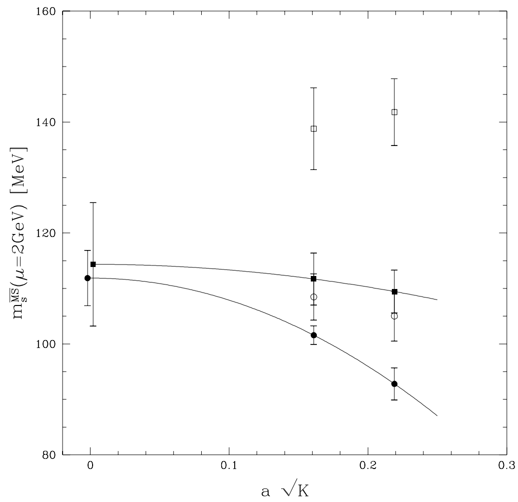

Figure 20: The same as fig. 19 but for the strange quark mass $m_s^{\overline{MS}}$.

tree-level. So for Z_A we use the tadpole improved perturbative value

$$Z_A = \left[1 - \frac{\alpha_s^{\overline{MS}}(1/a)}{4\pi}\, 7.901\right] u_0, \tag{6.28}$$

and for b_A, b_P and b_m we take the tree-level results. Comparing Z_A with the nonperturbative determination at $\beta = 6.0$ [31], as well as with a nonperturbative calculation at $\beta = 5.9$, 6.1 and 6.3 using the Ward identity [44], we find good agreement. The renormalisation constants $Z_P^{\overline{MS}}(a\mu = 1)$ and $Z_m^{\overline{MS}}(a\mu = 1)$ are obtained from eqs. (6.19), (6.23) by setting $c_{SW} = 0$. The resulting quark masses are given in table 7, and they are plotted and compared with the improved results in figs. 19, 20. In this case we expect discretisation errors of $O(a)$ instead of $O(a^2)$. So it is not surprising that the Ward identity and the standard method give results which are far apart. We find that the Ward identity method gives mass values which are closer to the continuum result.

Finally, in figs. 21, 22 we compare our improved quark masses with the world data of Wilson quark masses as compiled in ref. [32] for the standard method. These authors use the ρ mass extrapolated to the chiral limit to set the scale. At $\beta = 6.0$ the scale set by the string tension and by the Wilson action ρ mass differ by about 20% which explains the difference between our Wilson data and the world data in figs. 21, 22. We see that the improved action improves the scaling behaviour.

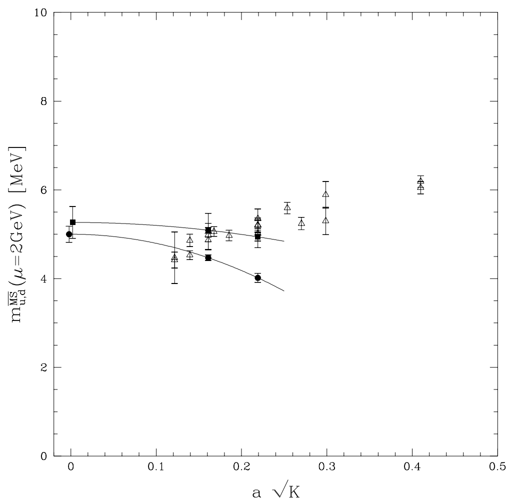

Figure 21: The light quark mass $m_{u,d}^{\overline{MS}}$ for improved fermions from fig. 19 compared with the world Wilson masses ($\triangle$) compiled in [32].

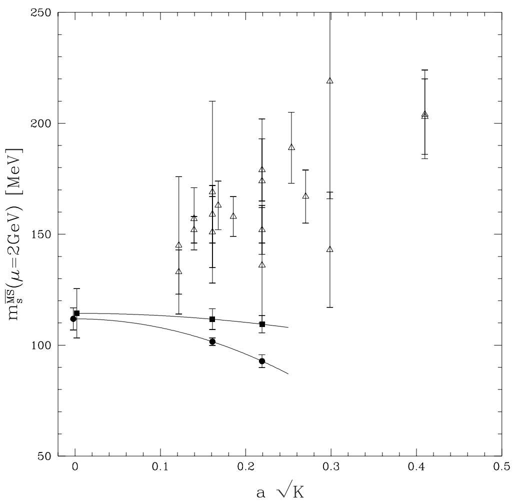

Figure 22: The strange quark mass $m_s^{\overline{MS}}$ for improved fermions from fig. 20 compared with the world Wilson masses ($\triangle$) compiled in [32]. These authors use the $\phi(1020)$ meson to determine the strange quark mass.

7 Decay constants for light fermions

7.1 Definition on the lattice

The pion decay constant f_π is well known experimentally and can be determined from the two-point correlation functions on the lattice as well, allowing for a further test of scaling of the improved theory. We shall also look at the decay constants of the K, ρ, K^* and the a_1 meson.

In Euclidean space at zero three-momentum we define

$$\begin{aligned} \langle 0|\mathcal{A}_4|\pi\rangle &= m_\pi f_\pi, \\ \langle 0|\mathcal{A}_i|a_1,\lambda\rangle &= \epsilon_i(\lambda)\, m_{a_1}^2 f_{a_1}, \\ \langle 0|\mathcal{V}_i|\rho,\lambda\rangle &= \epsilon_i(\lambda)\frac{m_\rho^2}{f_\rho}, \end{aligned} \tag{7.1}$$

where $\mathcal{A}$ and $\mathcal{V}$ are the renormalised axial vector and vector current, respectively, and $e(\lambda)$ is the polarisation vector with $\sum_\lambda e_i^*(\lambda)e_j(\lambda) = \delta_{ij}$. The pseudoscalar and vector states are normalised by

$$\langle p|p'\rangle = (2\pi)^3 2p_0\delta(\vec{p}-\vec{p}\,'). \tag{7.2}$$

Note that our f_{a_1} is defined to be dimensionless.

In the improved theory the renormalised operators are

$$\mathcal{A}_\mu = (1+b_A am)Z_A(A_\mu + c_A a\partial_\mu P), \tag{7.3}$$

$$\mathcal{V}_\mu = (1+b_V am)Z_V(V_\mu + \mathrm{i}c_V a\partial_\lambda T_{\mu\lambda}), \tag{7.4}$$

where $V_\mu = \overline{\psi}\gamma_\mu\psi$ and $T_{\mu\nu} = \overline{\psi}\sigma_{\mu\nu}\psi$ are the vector and tensor operators, respectively. We use the definition $\sigma_{\mu\nu} = \mathrm{i}[\gamma_\mu,\gamma_\nu]/2$. Both currents are (partially) conserved, and hence no scale enters into their definition. The renormalisation constant Z_A and the improvement coefficients c_A and b_A have already been given in the last section. The renormalisation constant Z_V and the coefficients b_V and c_V have been computed nonperturbatively in ref. [25, 43]. At $\beta = 6.0$ the values are $Z_V = 0.7780$, $b_V = 1.472$ and $c_V = -0.32(6)$, and at $\beta = 6.2$ the numbers are $Z_V = 0.7927$, $b_V = 1.409$ and $c_V = -0.22(7)$. While for most of these quantities the authors have given fit formulae in g^2, for c_V we have read the numbers from the graph in [43], as no such formula exists yet. We have also determined Z_V and b_V at $\beta = 6.0$ from our nucleon three-point functions and find consistent results.

On the lattice we extract the meson decay constant from two-point correlation functions. For large times we expect that

$$\begin{aligned} C_{\mathcal{O}_1\mathcal{O}_2}(t) &= \langle \mathcal{O}_1(t)\mathcal{O}_2^\dagger(0)\rangle \\ &= \frac{1}{2m_H}\left[\langle 0|\mathcal{O}_1|H\rangle\langle 0|\mathcal{O}_2|H\rangle^* e^{-m_H t} + \langle 0|\mathcal{O}_1^\dagger|H\rangle^*\langle 0|\mathcal{O}_2^\dagger|H\rangle e^{-m_H(T-t)}\right] \\ &\equiv A_{\mathcal{O}_1\mathcal{O}_2}\left[e^{-m_H t} + \eta_1\eta_2 e^{-m_H(T-t)}\right], \end{aligned} \tag{7.5}$$

where $\mathcal{O}(t)$ is of the form $V_s^{-\frac{1}{2}}\sum_{\vec{x}}\overline{\psi}(\vec{x},t)\Gamma\psi(\vec{x},t)$, V_s being the spatial volume of the lattice, and $\mathcal{O}^\dagger = \eta\mathcal{O}$ with $\eta = \pm 1$ being given by $\gamma_4\Gamma^\dagger\gamma_4 = \eta\Gamma$. The η factor tells us how $\mathcal{O}$ behaves under time reversal, i.e. whether the two-point function is symmetric or antisymmetric with respect to $t \to T-t$. Here T is the temporal extent of the lattice. In general we have computed correlation functions with local (L) and smeared (S) operators.

We shall now consider the appropriate matrix elements separately. We start with those matrix elements necessary for the π. With our conventions we set

$$\begin{aligned} \langle 0|A_4|\pi\rangle &= m_\pi f_\pi^{(0)}, \\ \langle 0|a\partial_4 P|\pi\rangle &= -\sinh am_\pi\langle 0|P|\pi\rangle = m_\pi a f_\pi^{(1)}, \end{aligned} \tag{7.6}$$

where $f^{(0)}$, $f^{(1)}$ are defined to be real and positive. By computing $C_{A_4P}^{LS}$ and C_{PP}^{SS} we find for the matrix element of A_4 from eq. (7.6)

$$m_\pi f_\pi^{(0)} = -2\kappa\frac{\sqrt{2m_\pi}A_{A_4P}^{LS}}{\sqrt{A_{PP}^{SS}}}, \tag{7.7}$$

and for the matrix element of $\partial_4 P$ we obtain from the ratio of the C_{PP}^{LS} and $C_{A_4P}^{LS}$ correlation functions

$$\frac{af_\pi^{(1)}}{f_\pi^{(0)}} = \sinh am_\pi \frac{A_{PP}^{LS}}{A_{A_4P}^{LS}}. \tag{7.8}$$

Alternatively, we can take the time derivative from the plateau in the correlation function. Numerically we found that it made very little difference to the result.

For the a_1 we set

$$\langle 0|A_i|a_1,\lambda\rangle = \epsilon_i(\lambda)\, m_{a_1}^2 f_{a_1}^{(0)}, \tag{7.9}$$

and we find

$$m_{a_1}^2 f_{a_1}^{(0)} = 2\kappa \frac{\sqrt{2m_{a_1}}\sum_k A_{A_kA_k}^{LS}}{\sqrt{3\sum_k A_{A_kA_k}^{SS}}}. \tag{7.10}$$

For the ρ we set

$$\begin{aligned} \langle 0|V_i|\rho,\lambda\rangle &= \epsilon_i(\lambda)\, m_\rho^2 f_\rho^{(0)}, \\ \langle 0|a\partial_4 T_{i4}|\rho,\lambda\rangle &= -\sinh am_\rho \langle 0|T_{i4}|\rho,\lambda\rangle = \mathrm{i}\epsilon_i(\lambda)\, m_\rho^2 a f_\rho^{(1)}, \end{aligned} \tag{7.11}$$

and we obtain

$$m_\rho^2 f_\rho^{(0)} = 2\kappa \frac{\sqrt{2m_\rho}\sum_k A_{V_kV_k}^{LS}}{\sqrt{3\sum_k A_{V_kV_k}^{SS}}} \tag{7.12}$$

and

$$\frac{af_\rho^{(1)}}{f_\rho^{(0)}} = -\mathrm{i}\sinh am_\rho \frac{\sum_k A_{T_{k4}T_{k4}}^{LS}\sqrt{\sum_k A_{V_kV_k}^{SS}}}{\sum_k A_{V_kV_k}^{LS}\sqrt{\sum_k A_{T_{k4}T_{k4}}^{SS}}}. \tag{7.13}$$

7.2 Decay constants for Wilson and improved fermions

In tables 8 and 9 we give the lattice results for the matrix elements calculated from the above formulas.

$\beta = 6.0$						
$c_{SW} = 0$						
V	κ	$af_\pi^{(0)}$	$-$	$f_\rho^{(0)}$	$-$	$f_{a_1}^{(0)}$
16^332	0.1487	0.136(2)		0.305(5)		0.161(5)
	0.1515	0.122(2)		0.364(5)		0.207(3)
	0.1530	0.113(2)		0.397(7)		0.231(3)
	0.1550	0.098(2)		0.459(9)		0.262(4)
$c_{SW} = 1.769$						
V	κ	$af_\pi^{(0)}$	$af_\pi^{(1)}/f_\pi^{(0)}$	$f_\rho^{(0)}$	$af_\rho^{(1)}/f_\rho^{(0)}$	$f_{a_1}^{(0)}$
16^332	0.1300	0.1341(15)	1.792(7)	0.209(9)	0.670(2)	0.131(7)
	0.1310	0.1295(15)	1.698(8)	0.228(3)	0.588(2)	0.153(13)
	0.1324	0.1204(8)	1.599(5)	0.261(2)	0.4823(12)	0.172(7)
	0.1333	0.1128(9)	1.541(3)	0.288(3)	0.4147(15)	0.202(16)
	0.1342	0.1037(8)	1.511(6)	0.323(3)	0.353(2)	0.208(16)
24^332	0.1342	0.105(2)	1.521(16)	0.330(7)	0.348(3)	0.212(10)
	0.1346	0.101(2)	1.58(3)	0.352(7)	0.327(6)	0.225(14)
	0.1348	0.100(3)	1.62(5)	0.352(15)	0.324(19)	0.25(2)

Table 8: The various contributions to the decay constants f_π, f_ρ and f_{a_1} at $\beta = 6.0$.

The fits to the correlation functions, as for the masses, are all made using the bootstrap method.

$\beta = 6.2$						
$c_{SW} = 0$						
V	κ	$af_\pi^{(0)}$	$-$	$f_\rho^{(0)}$	$-$	$f_{a_1}^{(0)}$
24^348	0.1468	0.1025(19)		0.268(5)		0.127(9)
	0.1489	0.0930(17)		0.315(6)		0.180(4)
	0.1509	0.0798(14)		0.376(7)		0.230(4)
	0.1518	0.0719(13)		0.412(9)		0.261(4)
	0.1523	0.0669(14)		0.438(10)		0.276(5)
$c_{SW} = 1.614$						
V	κ	$af_\pi^{(0)}$	$af_\pi^{(1)}/f_\pi^{(0)}$	$f_\rho^{(0)}$	$af_\rho^{(1)}/f_\rho^{(0)}$	$f_{a_1}^{(0)}$
24^348	0.1321	0.0985(11)	1.297(3)	0.211(3)	0.4637(8)	0.133(2)
	0.1333	0.0913(11)	1.198(4)	0.243(3)	0.3719(10)	0.167(2)
	0.1344	0.0818(10)	1.133(2)	0.283(4)	0.2900(15)	0.204(3)
	0.1349	0.0758(9)	1.118(7)	0.308(5)	0.255(2)	0.226(3)
	0.1352	0.072(3)	1.131(11)	0.327(16)	0.235(4)	0.241(11)

Table 9: The same as table 8 but for $\beta = 6.2$.

Collecting all the terms, the physical decay constants are given by

$$\begin{aligned} f_\pi &= (1 + b_A am) Z_A (f_\pi^{(0)} + c_A a f_\pi^{(1)}), \\ f_{a_1} &= (1 + b_A am) Z_A f_{a_1}^{(0)}, \\ 1/f_\rho &= (1 + b_V am) Z_V (f_\rho^{(0)} + c_V a f_\rho^{(1)}). \end{aligned} \tag{7.14}$$

When the improvement terms are weighted with the appropriate c factors, they contribute about 10-20% at $\beta = 6.0$ and up to 10% at $\beta = 6.2$. It is thus important to improve the operators as well.

To perform the chiral extrapolation, we make fits similar to those for the hadron masses, namely

$$f_\pi^2 = b_0 + b_2 m_\pi^2 + b_3 m_\pi^3, \tag{7.15}$$

$$f_{a_1}^2 = b_0 + b_2 m_\pi^2 + b_3 m_\pi^3, \tag{7.16}$$

$$1/f_\rho^2 = b_0 + b_2 m_\pi^2 + b_3 m_\pi^3. \tag{7.17}$$

We decided to fit the square of the decay constants rather than the decay constants themselves because this shows less curvature. The fits and the data are shown in fig. 23 for f_π and f_ρ. We compare this result with the meson decay constants computed with the Wilson action. These follow from eq. (7.14) with $c_A, c_V = 0$. For Z_A we use the tadpole improved value given in eq. (6.28), and for b_A we take the tree-level result ($b_A = 1$). The renormalisation constant Z_V (in the chiral limit) has been determined nonperturbatively from a two-point correlation function of the local vector current [44] at $\beta = 5.9$, 6.1 and 6.3. Unlike the case of Z_A, we find significant differences between this determination and our determination using the nucleon three-point function. The latter gives $Z_V = 0.651(15)$ at $\beta = 6.0$ which is close to the tadpole improved result. This indicates large $O(a)$ effects. Since we are applying Z_V to a two-point function, we chose to use the nonperturbative result from ref. [44]. We interpolate this result to $\beta = 6.0$ and 6.2 and find $Z_V = 0.565$ and 0.618, respectively. For b_V we again take the tree-level result. Although the individual contributions of the improvement terms are significant, the overall result for f_π in fig. 23 is not much changed when compared with the Wilson case for smaller quark masses. For larger quark masses, especially at $\beta = 6.0$, the Wilson f_π is larger. The situation is different for f_ρ. Here we find a systematic difference of 10-20% at $\beta = 6.0$ and approximately 10% at $\beta = 6.2$ for all quark masses. In both cases the difference between the two actions becomes smaller with increasing β as one would expect.

Our results extrapolated to the chiral limit are given in table 10, and we compare f_π and f_ρ with experiment in fig. 24 For f_π we find reasonable agreement of the improved results with the experimental value using, as before, the string tension as the scale. When including the data of ref. [45], one sees that the Wilson results lie lower, and it appears that the values are increasing as we approach the continuum limit. For f_ρ both our improved and Wilson results lie within 5% of the experimental value. There is, however, a

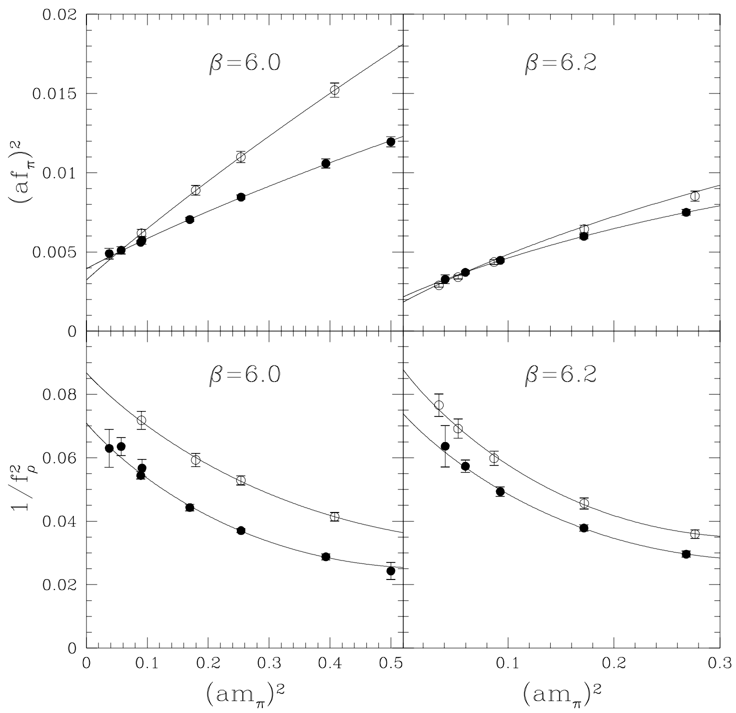

Figure 23: Fits and chiral extrapolations of the decay constants f_π and f_ρ for improved (●) and Wilson (○) fermions.

β	c_{SW}	af_π	f_{a_1}	$1/f_\rho$	af_K	$1/f_{K^*}$
6.0	0	0.0569(77)	0.2240(76)	0.295(11)	0.0732(26)	0.2385(24)
6.2	0	0.0423(36)	0.2429(48)	0.2971(71)	0.0537(11)	0.2345(28)
6.0	1.769	0.0627(20)	0.195(10)	0.2664(39)	0.0721(8)	0.2020(13)
6.2	1.614	0.0462(38)	0.2130(45)	0.2726(74)	0.0557(14)	0.2149(19)

Table 10: The decay constants f_π, f_{a_1}, f_ρ extrapolated to the chiral limit, as well as f_K, f_{K^*} taken at the physical quark mass.

definite difference as we previously remarked. The Wilson numbers lie above the experimental value, while the improved ones lie below. One must remember though that in the Wilson case there is a systematic error in the renormalisation constant Z_V which may be larger than the statistical errors in the figure. The experimental number for the decay constant of the a_1 is [46] $f_{a_1} = 0.17(2)$ (in our notation). The agreement between experimental and lattice values is encouraging.

We can avoid errors from extrapolating to the chiral limit by considering quark masses within our data range, as we have already done in figs. 14 and 15. The most physical κ values to use are those corresponding to the K mass. To obtain the decay constants we take eqs. (7.15) and (7.17) at $m_\pi = m_K$. (Remember that we are using m_π as a generic name for the pseudoscalar meson mass.) We give the results for f_K and f_{K^*} in table 10, and in fig. 25 we show the scaling behaviour together with the experimental value for f_K.

We find the errors to be substantially reduced. For f_K we see no difference between improved and Wilson results, both lying 10% below the experimental value. For f_{K^*} the error bars have become small enough to attempt an extrapolation to the continuum limit. The curves are a simultaneous fit, linear for the Wilson and quadratic for the improved data, constrained to agree in the continuum limit. In this quantity there appear to be large $O(a^2)$ effects in the improved case.

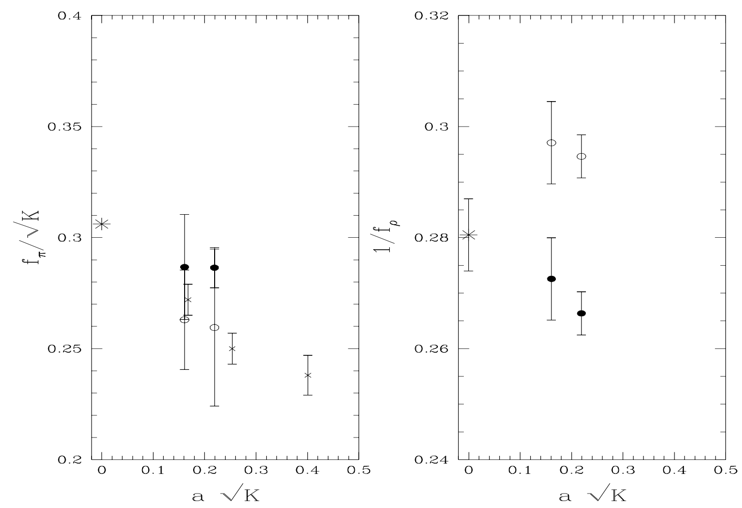

Figure 24: The decay constants f_π and f_ρ as a function of the lattice spacing for improved (●) and Wilson (○) fermions together with the experimental values (✻). The errors on f_ρ for improved fermions are statistical only. Our results for f_π are compared with the Wilson results of ref. [45] ($\times$).

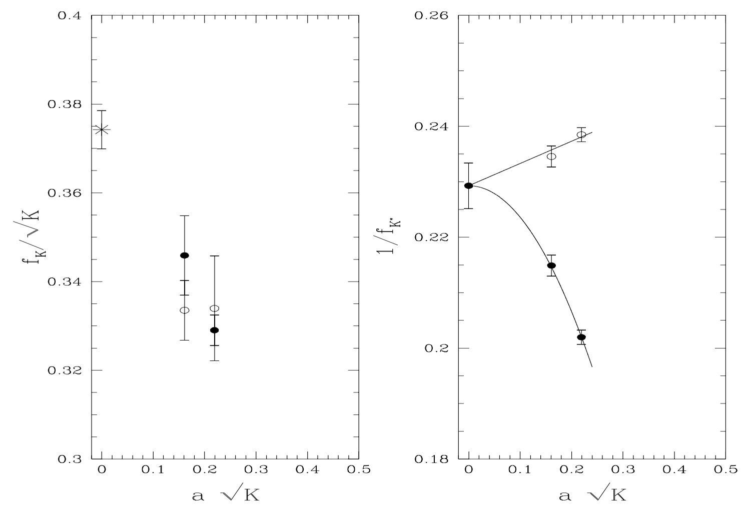

Figure 25: The decay constants f_K and f_{K^*} as a function of the lattice spacing for improved (●) and Wilson (○) fermions. The errors on f_{K^*} for improved fermions are statistical only. The solid lines in the f_{K^*} figure are from a simultaneous linear fit to the Wilson data and a quadratic fit to the improved data. Our results for f_K are compared with the experimental value (✻).

8 Some Results on Hadron Structure Functions from Lattice QCD

8.1 Fixing some notations for nucleon structure functions

The theoretical basis of the calculation is the operator product expansion. For large Q^2 the moments of the nucleon structure functions are given by

$$
\begin{aligned}
2\int_0^1 dx x^{n-1} F_1(x,Q^2) &= \sum_{f=u,d,g} c_{1,n}^{(f)}(\mu^2/Q^2, g(\mu))\, v_n^{(f)}(\mu), \\
\int_0^1 dx x^{n-2} F_2(x,Q^2) &= \sum_{f=u,d,g} c_{2,n}^{(f)}(\mu^2/Q^2, g(\mu))\, v_n^{(f)}(\mu), \\
2\int_0^1 dx x^{n} g_1(x,Q^2) &= \frac{1}{2}\sum_{f=u,d,g} e_{1,n}^{(f)}(\mu^2/Q^2, g(\mu))\, a_n^{(f)}(\mu), \\
2\int_0^1 dx x^{n} g_2(x,Q^2) &= \frac{1}{2}\frac{n}{n+1}\sum_{f=u,d,g} [e_{2,n}^{(f)}(\mu^2/Q^2, g(\mu))\, d_n^{(f)}(\mu) \\
&- e_{1,n}^{(f)}(\mu^2/Q^2, g(\mu))\, a_n^{(f)}(\mu)],
\end{aligned}
\tag{8.1}
$$

where c_1, c_2 and e_1, e_2 are the Wilson coefficients, and v_n, a_n and d_n are forward nucleon matrix elements of certain local operators $\mathcal{O}$. For details see (e.g.) ref. [11, 87].

The coefficient functions $c_{1,n}$, $c_{2,n}$, $e_{1,n}$ and $e_{2,n}$ are calculable in QCD perturbation theory, the measured scaling violations are usually described by their Q^2 evolution. Note that μ–dependence in the matrix elements $v_n^{(f)}(\mu)$, $a_n^{(f)}(\mu)$ and $d_n^{(f)}(\mu)$ arising from the μ–dependence of the renormalisation constants defined below should be cancelled by the corresponding μ–dependence in the coefficient functions since the moments of structure functions themselves are independent of scale μ.

In parton model language

$$
v_{n+1}^{(f)} = \langle x^n\rangle^{(f)} = \int_0^1 \mathrm{d}x x^n \frac{1}{2}[q_\uparrow^{(f)}(x) + q_\downarrow^{(f)}(x)],\ f=u,d, \tag{8.2}
$$

$$
v_{n+1}^{(g)} = \langle x^n\rangle^{(g)} = \int_0^1 \mathrm{d}x x^n g_1(x), \tag{8.3}
$$

and

$$
a_n^{(f)} = 2\Delta^{(n)}q^{(f)} = 2\int_0^1 \mathrm{d}x x^n \frac{1}{2}[q_\uparrow^{(f)}(x) - q_\downarrow^{(f)}(x)],\ f=u,d \tag{8.4}
$$

with $\Delta^{(0)}q^{(f)} \equiv \Delta q^{(f)}$, and $q_\uparrow(x)$, $q_\downarrow(x)$ being the quark distribution functions with spin $\uparrow$, $\downarrow$ with respect to the direction of motion. In eqs. (8.2), (8.4) we have omitted the sea quark contributions because we are working in the quenched approximation. The matrix elements d_n have twist three and so have no parton model interpretation.

In the following we shall consider only *non-singlet* structure functions and distributions. Only these distribution functions are accessible in quenched lattice QCD.

For unpolarised DIS we use as conventional basis for twist two quark and gluon operators

$$
\mathcal{O}_{\mu_1\ldots\mu_n}^{(u,d)} = \left(\frac{i}{2}\right)^{n-1} \overline{\psi}^{(f)}\gamma_{\mu_1} \overset{\leftrightarrow}{D}_{\mu_2}\ldots\overset{\leftrightarrow}{D}_{\mu_n}\psi^{(f)} - \text{traces}\,, \tag{8.5}
$$

$$
\mathcal{O}_{\mu_1\ldots\mu_n}^{(g)} = i^{n-2}\mathrm{Tr}F_{\mu_1}^{\alpha} D_{\mu_2}\ldots D_{\mu_{n-1}}F_{\alpha\mu_n} - \text{traces} \tag{8.6}
$$

where $\psi^{(f)}$ denote the quark fields, $F_{\alpha\beta}$ is the gluon field strength tensor and the covariant derivatives D_μ and $\overset{\leftrightarrow}{D}_\mu = \vec{D}_\mu - \overset{\leftarrow}{D}_\mu$.

For spin-dependent processes the structure functions g_1 and h_1 (not discussed so far) are important. Let us first consider the structure function g_1. If the sea is assumed to be flavour symmetric, the leading twist contribution can be written

$$
g_1(x,Q^2) = \frac{1}{2}\sum_f \int_x^1 \frac{\mathrm{d}y}{y} c_1^{(f)}\left(\frac{x}{y}, \frac{Q^2}{\mu^2}\right)\Delta q^{(f)}(y,\mu), \tag{8.7}
$$

where

$$\Delta q^{(f)}(x,\mu) = q_\uparrow^{(f)}(x,\mu) - q_\downarrow^{(f)}(x,\mu), \tag{8.8}$$

and $q_{\uparrow(\downarrow)}^{(f)}$ is the probability distribution of a quark of flavour f and spin parallel (anti-parallel) to the parent spin of the nucleon. The so-called splitting functions $c_1^{(f)}$ are determined by the Wilson coefficients

$$c_{1,n}^{(f)}\left(\frac{Q^2}{\mu^2}\right) = \int_0^1 \mathrm{d}x x^n c_1^{(f)}\left(x, \frac{Q^2}{\mu^2}\right) \tag{8.9}$$

through an inverse Mellin transform. Similarly, the distribution functions can be derived from their moments,

$$\Delta^{(n)} q^{(f)}(\mu) = \int_0^1 \mathrm{d}x x^n \Delta q^{(f)}(x,\mu). \tag{8.10}$$

We denote the lowest moment by

$$\Delta q^{(f)} \equiv \Delta^{(0)} q^{(f)}. \tag{8.11}$$

According to the operator product expansion the moments are given by forward nucleon matrix elements of local operators. For $\Delta^{(n)}q^{(f)}$ we have

$$\langle \vec{p}, \vec{s} | \mathcal{O}^{5(f)}_{\{\sigma\mu_1\cdots\mu_n\}} | \vec{p}, \vec{s}\rangle = \frac{2}{n+1} \Delta^{(n)} q^{(f)} [s_\sigma p_{\mu_1} \cdots p_{\mu_n} + \cdots - \text{traces}], \tag{8.12}$$

where

$$\mathcal{O}^{(f,5)}_{\{\sigma\mu_1\cdots\mu_n\}} = \left(\frac{\mathrm{i}}{2}\right)^n \overline{\psi}^{(f)} \gamma_\sigma \gamma_5 \overleftrightarrow{D}_{\mu_1} \cdots \overleftrightarrow{D}_{\mu_n} \psi^{(f)} - \text{traces}. \tag{8.13}$$

Here $\{\cdots\}$ means symmetrisation. The lowest moment $\Delta q^{(f)}$ measures the *axial vector charge* of the nucleon.

Similar expressions can be derived for the structure function h_1 [66]. One simply has to replace $\Delta q^{(f)}(x,\mu)$ in eq. (8.7) by

$$\delta q^{(f)}(x,\mu) = q_\perp^{(f)}(x,\mu) - q_\top^{(f)}(x,\mu), \tag{8.14}$$

where $q_{\perp(\top)}^{(f)}$ is the probability distribution of a quark of flavour f and spin $\not{s}_\perp\gamma_5$ parallel (anti-parallel) to the spin of the nucleon, giving

$$\delta^{(n)} q^{(f)}(\mu) = \int_0^1 \mathrm{d}x x^n \delta q^{(f)}(x,\mu). \tag{8.15}$$

We denote the lowest moment by

$$\delta q^{(f)} \equiv \delta^{(0)} q^{(f)}. \tag{8.16}$$

The moments are given by the matrix elements

$$\langle \vec{p}, \vec{s} | \mathcal{O}^{(f)}_{\sigma\{\mu_1\cdots\mu_n\}} | \vec{p}, \vec{s}\rangle = \frac{2}{m_N} \delta^{(n-1)} q^{(f)} [(s_\sigma p_{\mu_1} - s_{\mu_1} p_\sigma) p_2 \cdots p_{\mu_n} + \cdots - \text{traces}], \tag{8.17}$$

where

$$\mathcal{O}^{(f)}_{\sigma\{\mu_1\cdots\mu_n\}} = \left(\frac{\mathrm{i}}{2}\right)^{n-1} \overline{\psi}^{(f)} \sigma_{\sigma\mu_1} \gamma_5 \overleftrightarrow{D}_{\mu_2} \cdots \overleftrightarrow{D}_{\mu_n} \psi^{(f)} - \text{traces}. \tag{8.18}$$

The lowest moment $\delta q^{(f)}$ measures the *tensor charge* of the nucleon. In the non-relativistic quark model axial vector and tensor charges are equal, i.e. $\delta q^{(f)} = \Delta q^{(f)}$. The structure function h_1 has opposite chiral properties to g_1. It can be measured in polarised Drell-Yan processes, but not in deep-inelastic lepton-hadron scattering. For other ideas see [65].

For a spin-zero target like the pion one has $q_\uparrow(x) = q_\downarrow(x)$. For a spin-one target like the rho the quark-spin distribution will depend on the spin projection m of the particle. Writing $q^m(x) = 1/2\,[q_\uparrow^m(x) + q_\downarrow^m(x)]$, one finds the new structure function [3]

$$b_1(x) = q^0(x) - q^1(x). \tag{8.19}$$

On the lattice one computes bare operators $\mathcal{O}(a)$, where a is the lattice spacing. These operators are in general divergent and must be renormalised. One may define finite operators renormalised at the finite scale μ by

$$\mathcal{O}(\mu) = Z_{\mathcal{O}}(a\mu, g(a)) \mathcal{O}(a). \tag{8.20}$$

The renormalisation condition here must match the renormalisation condition used to calculate the Wilson coefficients, so that the μ-dependence drops out of the product of Wilson coefficients and $Z_{\mathcal{O}}$'s. In principle the renormalisation constants can be calculated in perturbation theory. The problem is only that lattice perturbation theory converges very slowly [27].

8.2 Nucleon Structure Functions

8.2.1 Unpolarised case, Wilson fermions

The lattice calculation of structure functions divides into two parts. Part one is the calculation of the hadron matrix elements. Part two is the determination of the renormalisation constants $Z_{\mathcal{O}}$. Altogether we have considered $O(20)$ different operators so far. On the hypercubic lattice one is limited to operators with spin ≤ 4. In the notation of eqs. (8.2)-(8.4) this means $n \leq 3$.

For nearly all of the operators the renormalisation constants have been computed perturbatively to one loop order [89, 84, 51, 52]. A nonperturbative calculation has been started recently (see Sect. 10 and [53, 54]). In the few cases where we can compare perturbative and nonperturbative results we see differences of not more than 5% if boosted perturbation theory [27] is applied.

The numerical calculations of the matrix elements have been done at the coupling $\beta \equiv 6/g^2 = 6.0$. At this coupling the lattice spacing is $a \approx 0.1\,\mathrm{fm}$. We did calculations on two volumes, $16^3 \times 32$ and $24^3 \times 32$, and for several quark masses ranging from $\approx$ 30 to 200 MeV. It is important to have data at many quark masses to do a reliable extrapolation to the chiral limit. The calculation of nucleon matrix elements, in particular of higher derivative operators, requires high statistics. Our calculations on the $16^3 \times 32$ lattice involved $O(1000)$ gauge field configurations, and $O(100)$ configurations on the $24^3 \times 32$ lattice. The calculations on the large volume were nearly as expensive in computer time as the high statistics calculations on the smaller volume as we went to smaller quark masses. For the calculation of the gluon distribution function we even used $O(5000)$ configurations. By comparing the results on the two volumes, we find that our calculations on the $16^3 \times 32$ lattice do not suffer from finite size effects.

A summary of our results for the unpolarised structure functions are listed in table 11. We compare the

Moment	Lattice (quenched, $\mu^2 \approx 5\,GeV^2$)	Experiment ($\mu^2 = 4\,GeV^2$)
$\langle x \rangle^{(u)}$	0.410(34)	0.284
$\langle x \rangle^{(d)}$	0.180(16)	0.102
$\langle x \rangle^{(u)}$-$\langle x \rangle^{(d)}$	0.230(38)	0.182
$\langle x^2 \rangle^{(u)}$	0.108(16)	0.083
$\langle x^2 \rangle^{(d)}$	0.036(8)	0.025
$\langle x^3 \rangle^{(u)}$	0.020(10)	0.032
$\langle x^3 \rangle^{(d)}$	0.000(6)	0.008
$\langle x \rangle^{(g)}$	0.53(23)	0.441

Table 11: Results for the unpolarised structure functions in the chiral limit. The lattice numbers are compared with the *CTEQ3M* [55] fit of the valence quark distribution functions. For $\langle x \rangle$, which has been calculated using different procedures, we have averaged over the results in ref. [47].

lattice results directly with experiment, where possible, and otherwise with the phenomenological valence quark distribution functions, namely *CTEQ3M* [55] for the unpolarised case.

Let us discuss the results in some detail. We see that the lattice prediction for the lowest moment, $\langle x \rangle$, is significantly larger than the lowest moment of the phenomenological valence quark distribution function, both for the u and the d quark. When one goes to the higher moments the agreement improves.

What does this mean for the structure functions themselves? The x-dependence of the structure functions carries valuable information about the dynamics of quarks and gluons which is not immediately available from the moments. Furthermore, because of limited experimental data, moments are sometimes hard to compare with experiment. This is, in particular, the case for the higher moments. Theoretically, the structure functions can be obtained from the moments by an inverse Mellin transform.

In ref. [49] the moments from table 11 have been converted to 'real' structure functions. In fig. 26 the result is shown for the u-quark distribution function. This is compared with the phenomenological curve. We see that the 'lattice' structure function is quite different in shape from the experimental one. The difference shows mainly at x values around 1/2. We do not expect that the missing internal quark loops will have an effect at such large values of x. If the effect is real, it could mean that the experimental structure functions contain substantial higher-twist contributions. One would expect higher-twist contributions to show up predominantly at large x.

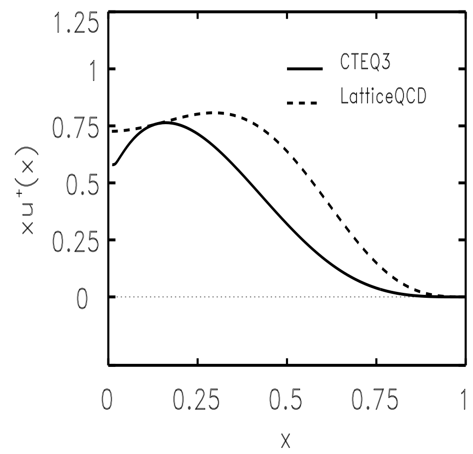

Figure 26: The u-quark distribution function extracted from the lattice data compared with the experimental valence quark distribution function taken from ref. [49].

The lowest moment of the gluon distribution function, $\langle x\rangle^{(g)}$, turns out to be consistent with experiment. The relatively large error has to do with the fact that the calculation requires a delicate subtraction between two terms similar in magnitude [48]. Quark and gluon contributions to $\langle x\rangle$ must add up to one, as a result of energy-momentum conservation. We obtain

$$\langle x\rangle^{(u)} + \langle x\rangle^{(d)} + \langle x\rangle^{(g)} = 1.12(23). \tag{8.21}$$

8.2.2 Polarised case, Wilson fermions

Let us now turn to the polarised structure functions in table 12. Again the measurements have been done

Moment	Lattice (quenched, $\mu^2 \approx 5\,GeV^2$)	Experiment ($\mu^2 = 3-5\,\mathrm{GeV}^2$)
Δu	0.841(52)	0.823 *valence*
Δd	–0.245(15)	–0.303 *valence*
g_A	1.086(67)	1.26
$\int_0^1 \mathrm{d}x(g_1^p - g_1^n)$	0.176(14)	0.163(10)(16)
$\Delta^{(1)}u$	0.198(8)	0.169(18)(12)
$\Delta^{(1)}d$	–0.048(3)	–0.055(27)(11)
$\int_0^1 \mathrm{d}x x^2 g_1^{(p)}$	0.0150(32)	0.012(1)
$\int_0^1 \mathrm{d}x x^2 g_1^{(n)}$	–0.0012(20)	–0.004(3)
$\int_0^1 \mathrm{d}x x^2 g_2^{(p)}$	–0.0261(38)	–0.006(2)
$\int_0^1 \mathrm{d}x x^2 g_2^{(n)}$	–0.0004(22)	0.005(8)

Table 12: Results for the polarised structure functions in the chiral limit. The lattice numbers are compared with experiment [56, 71] and the LO [57] fit to the valence quark distribution functions. The latter are referred to as *valence*. The data for $\Delta^{(1)}u$ and $\Delta^{(1)}d$ refer to $\mu^2 = 10\,\mathrm{GeV}^2$.

for the same parameters as mentioned before, and we compare the lattice results directly with experiment, where possible, and otherwise with the phenomenological valence quark distribution functions LO [57] for the polarised structure functions.

For the polarisation asymmetry [69] of π^+ minus π^- inclusive cross sections one finds to lowest order in α_s

$$A_p^{\pi^+-\pi^-} = \frac{4\Delta u^{\rm val}(x) - \Delta d^{\rm val}(x)}{4u^{\rm val}(x) - d^{\rm val}(x)} \tag{8.22}$$

for a proton target, and

$$A_d^{\pi^+-\pi^-} = \frac{\Delta u^{\rm val}(x) + \Delta d^{\rm val}(x)}{u^{\rm val}(x) + d^{\rm val}(x)} \tag{8.23}$$

for a deuteron target. The fragmentation functions, as well as the sea quark contributions, drop out because of isospin invariance relating the various fragmentation functions with each other.

The polarisation asymmetries have been measured by the SMC-Collaboration. For the lowest moment of the valence quark distribution they found [70] $\Delta u^{\rm val} = 1.01 \pm 0.19 \pm 0.14$ and $\Delta d^{\rm val} = -0.57 \pm 0.22 \pm 0.11$. The experimental errors are still a little too large to make a quantitative comparison with the lattice results. Recent work on Δq by two other groups [1] [58, 59] give similar numbers to ours.

Let us discuss in some detail the second moment of polarised valence quark distribution $\Delta^{(1)}q$. This moment is found from the $n = 1$ case of eqs. (8.12), (8.13). Note that the operator is odd under charge conjugation. The special feature of this moment is that it is directly accessible experimentally, which allows us to test the valence quark distribution without further phenomenological analysis.

The SMC-Collaboration has recently extended their analysis to the second moment [71]. At $\mu^2 = 10\text{GeV}^2$ they obtain the result

$$\Delta^{(1)}u^{\rm val} = 0.169 \pm 0.018 \pm 0.012, \tag{8.24}$$

$$\Delta^{(1)}d^{\rm val} = -0.055 \pm 0.027 \pm 0.011. \tag{8.25}$$

Lattice results for the second moment of the polarised valence quark distribution are shown in fig. 27. This

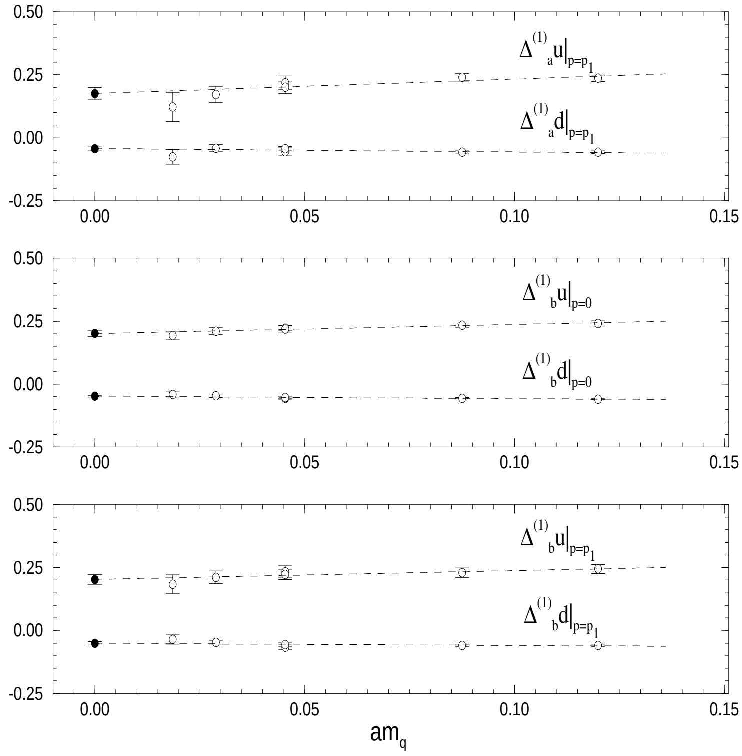

Figure 27: The chiral extrapolation for $\Delta^{(1)}q$ at $\mu^2 = 4\text{GeV}^2$ for different measurements with zero and non-zero momentum.

calculation, renormalised at the same scale μ^2, gives [72]

$$\Delta^{(1)}u = 0.189 \pm 0.08, \tag{8.26}$$

$$\Delta^{(1)}d = -0.0455 \pm 0.0032. \tag{8.27}$$

[1]These groups also compute the sea quark contribution which one might object to in a quenched calculation.

The lattice and experimental results agree within their respective errors.

For the higher moments sea quark effects should not play any significant role any more because they are restricted to the region of small x.

With two exceptions, the moments of the polarised structure functions agree surprisingly well with experiment. One exception is the axial vector coupling constant $g_A = \Delta u - \Delta d$. Experimentally, this is one of the best known quantities, and the sea quark contribution is expected to cancel out. The lattice result turns out to be quite a bit lower than the experimental value. The other exception is the twist-three matrix element d_2, contributing to the second moment of the structure function g_2. Comparing existing data on g_1 and g_2, one is lead to the result $d_2 \approx 0$, both for the u and the d quark. We find that $d_2 \approx -a_2$ in the chiral limit. In the heavy quark limit, on the other hand, d_2 vanishes as one would expect. We have no explanation for this discrepancy. We do not think that it can be explained by finite cut-off effects and the effect of quenching.

Knowing the first three moments (a calculation of a fourth moment is possible) we can try to reconstruct the polarised nucleon structure function g_1 We use a different method now as compared to ref. [49]. and restrict ourselves to the coarse lattice at $\beta = 6.0$. The moments can be well described by the formula

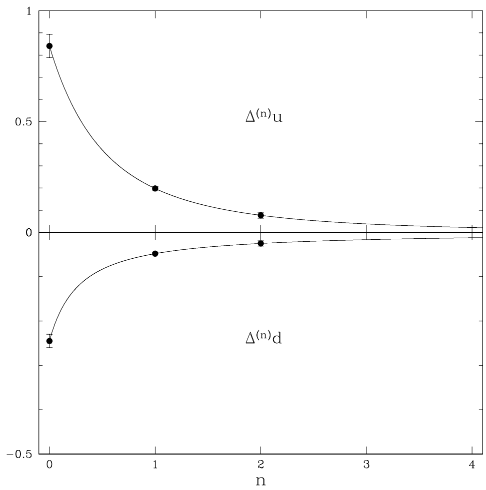

Figure 28: The lattice results for the first three moments of $\Delta u(x)$ and $\Delta d(x)$ at $\beta = 6.0$ and $\mu^2 = 4\ \mathrm{GeV}^2$. The curves are fits to the lattice data of the form (8.28) with parameters $\alpha = 0.04(6)$ and $\beta = 2.21(9)$.

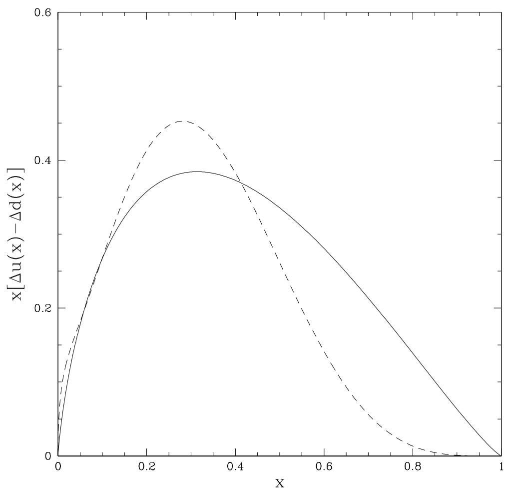

Figure 29: The distribution $x[\Delta u(x) - \Delta d(x)]$, together with the phenomenological valence quark distribution. The solid line is the result of the fit, the dashed line is taken from ref. [57].

$$\Delta^{(n)} q = c\,\Gamma(\beta)(n + 1 + \alpha)^{-\beta}. \tag{8.28}$$

This formula seems to describe the moments of the unpolarised structure functions reasonably well too. A fit is shown in fig. 28. An inverse Mellin transform of (8.28) gives

$$\Delta q(x) = c\, x^{\alpha}(-\ln x)^{\beta-1}. \tag{8.29}$$

In fig. 29 we compare the result for $\Delta u(x) - \Delta d(x)$ with the phenomenological distributions. The outcome is encouraging. We have hope that with one more moment and precise lattice data we are able to derive phenomenologically useful quark distribution functions.

It must be said that one can only combine even and odd moments to make a single structure function if u and d sea quark contributions are assumed to be equal, as is commonly done [57]. However, this may not be a good approximation [73].

8.3 Pion and Rho Structure Functions

The pion and rho structure functions have been computed from $O(500)$ gauge field configurations on the $16^3 \times 32$ lattice. As before, the coupling was taken to be $\beta = 6.0$. On these configurations we have computed the matrix elements v_n, a_n, d_n and r_n, using Wilson fermions. The calculations are done for three hopping parameters, $\kappa = 0.1515$, 0.1530 and 0.1550, corresponding roughly to quark masses of 190, 130 and 70 MeV, respectively.

A typical ratio of three- to two-point functions

$$R = \frac{\langle \eta(t)\mathcal{O}(\tau)\eta^\dagger(0)\rangle}{\langle \eta(t)\eta^\dagger(0)\rangle} \tag{8.30}$$

for $t \gg \tau \gg 0$, where $\eta = \pi, \rho$ is the source/sink. used to obtain the reduced matrix elements is shown in fig. 30.

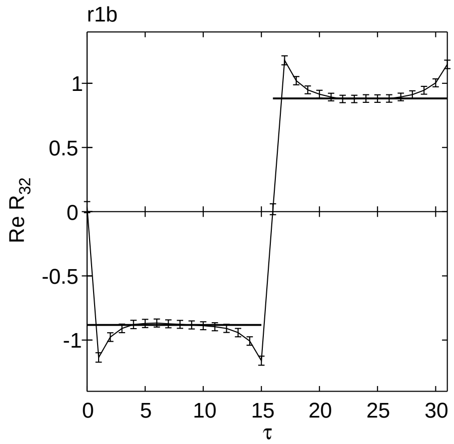

Figure 30: The ratio ReR_{32} for the polarized operator r_{1b}. The subscript b stands for a particular representation [6]. The sink is placed at $t = 16$, so that we can use both plateaus.

We work at a scale of $\mu^2 = (1/a)^2 \approx 4\text{GeV}^2$. In fig. 31 we show the moments of the π structure function F_1 (see eq. (3.52)). For each moment the heaviest quark mass is on the right. The leftmost value is the extrapolation to the chiral limit. For the pion we obtain in the chiral limit

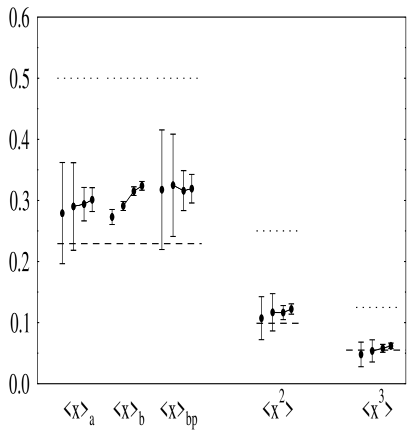

Figure 31: The moments of the unpolarised π structure function. The subscripts a, b, bp stand for different representations [6]. The heavy quark mass limit is given by the dotted lines, the experimental value [96] by the dashed lines.

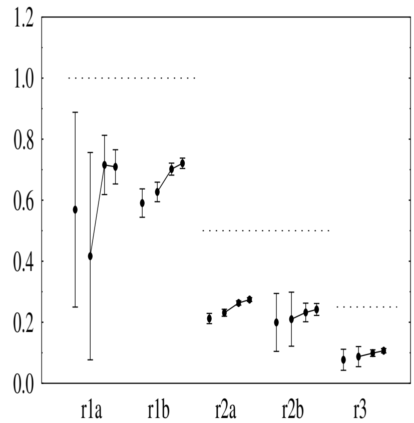

Figure 32: The moments r_n of the polarised ρ structure function g_1 for different representations. The lattice data are plotted in the same way as in fig. 31.

$$\langle x \rangle = 0.274(13)\,, \quad \langle x^2 \rangle = 0.107(35)\,, \quad \langle x^3 \rangle = 0.048(20)\,. \tag{8.31}$$

If we compare this result with indirect information from the Drell-Yan cross section [60], we find the same picture as for the nucleon: $\langle x \rangle$ comes out to be significantly larger than the phenomenological value, while $\langle x^2 \rangle$ and $\langle x^3 \rangle$ are consistent with the data. The unpolarised rho structure function looks very similar to the pion structure function.

In fig. 32 we show the moments of the polarised ρ structure function g_1 (see eq. (3.53)). The lowest moment $r_1 = 0.59(5)$ indicates that the valence quarks carry about 60% of the total spin of the ρ. A similar calculation for the nucleon gave a quark spin fraction of the same value.

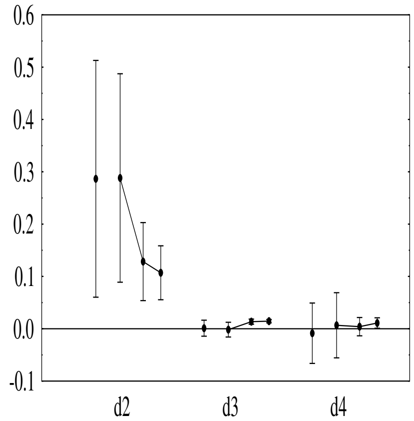

Figure 33: The moments r_n of the polarised ρ structure function g_1 for different representations. The lattice data are plotted in the same way as in fig. 31.

In fig. 33 we present the moments of the polarised ρ structure function b_1.The lowest moment of the polarised structure function b_1 turns out to be positive and unexpectedly large, albeit with large statistical errors. A possible interpretation of this is that the valence quarks have a significant orbital angular momentum.

8.4 Improvement Developments

Wilson fermions give rise to systematic errors of $O(a)$, while the standard gluonic action induces errors of $O(a^2)$ only. Therefore, as we have noticed already in Sect. 5.1 it is the fermionic action which is most in need of attention. From hadron mass calculations we know that discretisation errors can have a significant effect on the results at present values of the coupling [12].

In the following we discuss a few results obtained for moments of structure functions using the improved action of eq. (5.1). Provided that the operators have been improved as well (see a discussion on that in Sects. 9 and 10), one can reduce the cut-off errors from $O(a)$ to $O(a^2)$.

Momentum fraction $< x >$ and axial vector charge Δq

In figs. 34 and 35 we show some results of the $O(a)$ improved theory for the moments $\langle x \rangle$ and Δq as function of the quark mass to study the chiral limit. The calculations are done on the $16^3 \times 32$ lattice at $\beta = 6.0$. We compare the improved results with the unimproved numbers. To facilitate the comparison, we have only looked at one operator on one lattice. In the case of Δq we see no difference between the improved and unimproved approach at any value of the (bare) quark mass. In the case of the moment $\langle x \rangle$ we see only a small effect, which is however not statistically significant. For both moments the quark mass dependence is rather weak and unspectacular, so that a linear extrapolation to the chiral limit is justified.

To study the the continuum limit we have compared calculations at two values of the coupling, $\beta = 6.0$ and 6.2, corresponding to lattice spacings of $a \approx 0.1$ and 0.07 fm, respectively. The results for Δu and Δd are plotted in fig. 36. The values given in the figure refer to the chiral limit, i.e. zero quark mass, which are obtained from the lattice data by the linear extrapolation shown before.

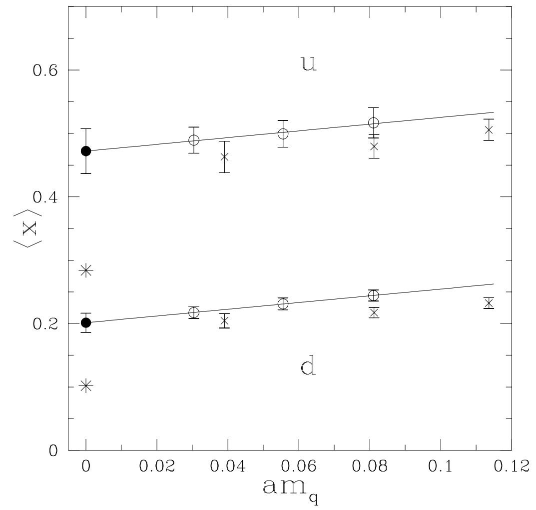

Figure 34: The moment $\langle x \rangle$ for u and d quark distributions as a function of the quark mass at $\beta = 6.0$. We compare results using the Wilson action ($\circ$) with results from the improved action ($\times$). The lines are a linear extrapolation of the Wilson action data to the chiral limit. The extrapolated values ($\bullet$) are compared with the *CTEQ* results ($\ast$).

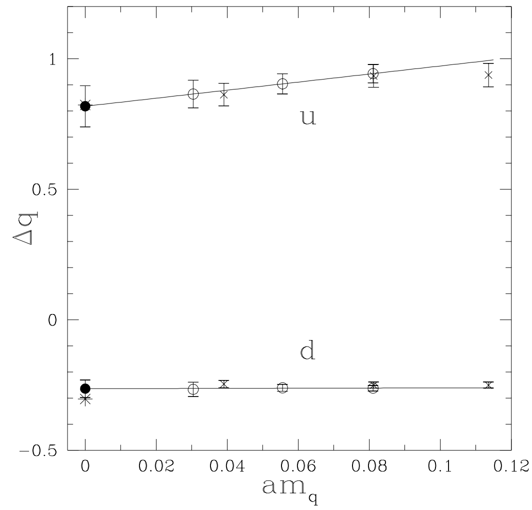

Figure 35: The same as fig. 34 but for Δq. Here the extrapolated values are compared with the phenomenological distribution *LO* of ref. [57].

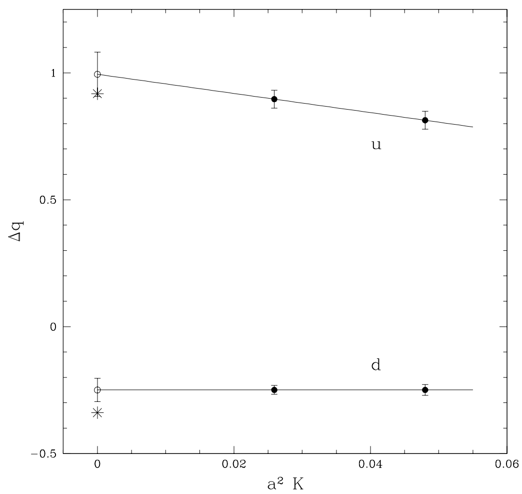

Figure 36: The quenched moments Δu and Δd plotted as a function of a^2. The lattice spacing is given in units of the string tension, K. The lattice data are denoted by $\bullet$, the extrapolated values by $\bigcirc$. The phenomenological values [57] are denoted by $\ast$.

Axial vector coupling of the nucleon g_A

A quantity, which is known very precisely experimentally, is the axial vector coupling of the nucleon,

$$g_A = \Delta u - \Delta d = 1.26. \tag{8.32}$$

In fig. 37 we show our results for g_A, together with the extrapolation of the lattice data to the continuum limit. We find the continuum result to be in good agreement with the experimental value. This figure indicates quite clearly how important it is to correct for finite cut-off effects. Even after improving the action and the operators, cut-off corrections can be quite substantial still. We see that the lattice result increases by approximately 20% going from our coarsest lattice at $\beta = 6.0$ to the continuum limit.

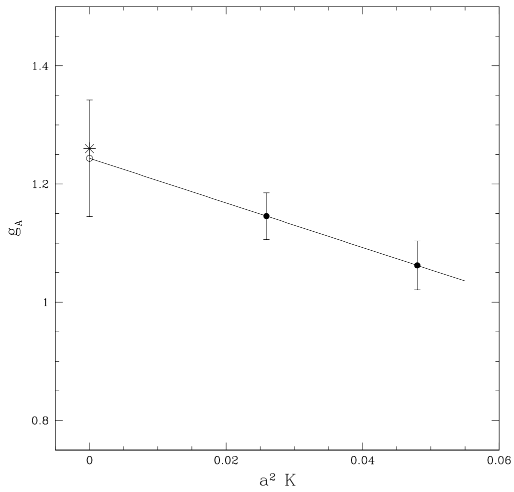

Figure 37: The axial vector coupling of the nucleon g_A as a function of a^2. The lattice spacing is given in units of the string tension, K. The lattice results are denoted by ●, the extrapolated values by ○. The experimental value is denoted by ∗.

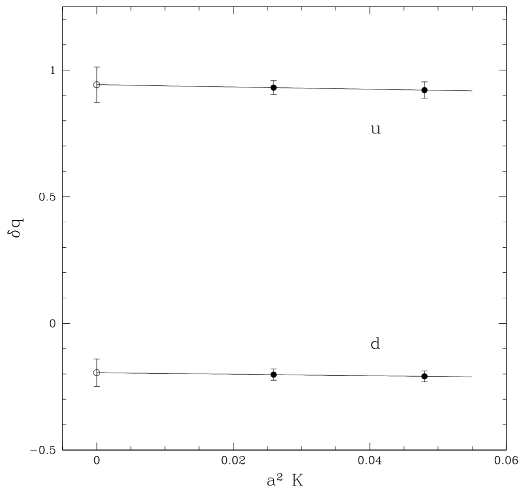

Figure 38: The quenched moments δu, δd as a function of a^2. The lattice spacing is given in units of the string tension, K. The lattice results are denoted by ●, the extrapolated values by ○. The numbers are renormalised at the scale $\mu^2 = 4$ GeV^2.

Tensor charge δq

The moments δu, δd have been computed using the improved action, but (so far) the operator has not been improved. For the renormalisation constant we have taken the tadpole improved [27] one-loop perturbative result [68]. This means that the $O(a)$ corrections have not completely been removed in this case, as opposed to the previous case. The result of the calculation is shown in fig. 38.

Before we discuss the result, let us find out what the tensor charge actually tells us about the structure of the nucleon. For a stationary nucleon the operator (8.18) differs from (8.13) by a factor of γ_0. In the non-relativistic limit fermions are in eigenstates of γ_0, and so δq and Δq are equal. By comparing δq and Δq for a real nucleon, we can gain insight into how relativistic the constituents are.

Comparing δq and Δq in figs. 36, 38 now, we see that they are equal within the error bars. This shows that a non-relativistic description of the spin structure of the nucleon is quite adequate. Does this mean that the quarks are in a relative s-wave and the missing spin is coming from the gluons and the sea quarks? Further investigations will have to show.

Because the operator (8.18) with $n = 1$ is odd under charge conjugation, sea quarks do not contribute to δq. This means that we might hope that the quenched calculation is giving an answer close to the true value.

9 Perturbative renormalisation of local bilinear lattice operators and $O(a)$ improvement

9.1 Operator improvements for O(a) improved action

To reduce systematic discretisation errors in realistic lattice calculations to $O(a^2)$, an improved action can be used (comp. Sect. 5.1). If the parameter c_{SW} in that action (eq.(5.1)), which gives the strength of the higher dimensional operator, is correctly chosen this action has no $O(a)$ errors for on-shell quantities such as hadron masses. The extra action piece adds a vertex contribution to the lattice Feynman rules. To be consistent in an improvement program, besides of an improved action, the operators in three-point functions have to be improved, too.

In Euclidean space-time the Lorentz group is replaced by the orthogonal group $O(4)$, which on the lattice reduces to the hypercubic group $H(4) \subset O(4)$. Accordingly, the lattice operators are classified by their transformation properties under the hypercubic group and charge conjugation. In ref. [5] we have identified all irreducible representations of the operators $\mathcal{O}$ and $\mathcal{O}^5$ up to rank four. In the (Wick rotated) operators the covariant derivatives are replaced by the lattice covariant derivatives (with the link matrix $U_{x,\mu}$)

$$
\begin{aligned}
\overrightarrow{D}_\mu \, \psi(x) &= \frac{1}{2a}\left(U_{x,\mu}\psi(x+\hat{\mu}) - U^\dagger_{x-\hat{\mu},\mu}\psi(x-\hat{\mu})\right) , \\
\overline{\psi}(x)\, \overleftarrow{D}_\mu &= \frac{1}{2a}\left(\overline{\psi}(x+\hat{\mu})U^\dagger_{x,\mu} - \overline{\psi}(x-\hat{\mu})U_{x-\hat{\mu},\mu}\right) .
\end{aligned}
\tag{9.1}
$$

Our improvement strategy, both for the quark propagator and the three-point functions, is to look at the tree-level results for the Green's functions, and see what $O(a)$ effects are present, and what has to be done to remove them. We then look at the one-loop perturbative results, and see whether the tree-level procedure still works. We find that at one particular value of the clover coupling the $O(a)$ effects are of the same form as in tree-level, and that then we can remove $O(a)$ effects completely, and find improved Green's functions that are free of $O(a)$ discretisation errors, both on-shell and off-shell.

There are several reasons why it would be desirable to be able to look at off-shell quantities in perturbation theory. In particular the nonperturbative renormalisation suggested in [53] needs to be matched to perturbation theory in order to relate lattice measurements to conventional renormalisation schemes such as $\overline{\text{MS}}$. This matching will only work well at large virtualities, where the running coupling constant is small, and the effects of nonperturbative phenomena such as chiral symmetry breaking has died away. Even within perturbation theory it is easier to calculate Green's functions at $p^2 \gg m^2$ than in the region where p^2 and m^2 are comparable.

However an action with a single tuneable improvement parameter (such as the Sheikholeslami-Wohlert action) only improves on-shell quantities. Off-shell quantities still have $O(a)$ errors, which arise from short-distance "contact" terms. Here we will show how the contact terms can be removed, and off-shell quantities with discretisation errors $O(a^2)$ can be extracted from Green's functions.

The point operators which we want to improve are

$$
\overline{\psi}\Gamma\psi, \quad \Gamma = 1,\ \gamma_\mu,\ \gamma_5,\ \gamma_\mu\gamma_5,\ \sigma_{\mu\nu}\gamma_5. \tag{9.2}
$$

In the later discussion we will restrict ourselves to one particular example.

The bases are constructed by adding higher dimensional operators with the same symmetry properties (parity, charge conjugation) as the original unimproved operators:

- $S = \overline{\psi}\psi$

$$
\left(\overline{\psi}\psi\right)^{\text{imp}} = (1 + a\,b\,m)\overline{\psi}\psi - \frac{1}{2}ac_1\overline{\psi}\,\overleftrightarrow{\not{D}}\psi .
$$

- $P = \overline{\psi}\gamma_5\psi$

$$
\left(\overline{\psi}\gamma_5\psi\right)^{\text{imp}} = (1 + a\,b\,m)\overline{\psi}\gamma_5\psi + \frac{1}{2}ac_2\partial_\mu\left(\overline{\psi}\gamma_\mu\gamma_5\psi\right).
$$

- $V_\mu = \overline{\psi}\gamma_\mu\psi$

$$
\left(\overline{\psi}\gamma_\mu\psi\right)^{\text{imp}} = (1 + a\,b\,m)\overline{\psi}\gamma_\mu\psi - \frac{1}{2}ac_1\overline{\psi}\,\overleftrightarrow{D}_\mu\,\psi + \tfrac{1}{2}aic_2\partial_\lambda\left(\overline{\psi}\sigma_{\mu\lambda}\psi\right),
$$

- $A_\mu = \overline{\psi}\gamma_\mu\gamma_5\psi$

$$\left(\overline{\psi}\gamma_\mu\gamma_5\psi\right)^{\rm imp} = (1 + a\, b\, m)\overline{\psi}\gamma_\mu\gamma_5\psi - \tfrac{1}{2}aic_1\overline{\psi}\sigma_{\mu\lambda}\gamma_5 \overleftrightarrow{D}_\lambda \psi + \tfrac{1}{2}ac_2\partial_\mu\left(\overline{\psi}\gamma_5\psi\right),$$

- $H_{\mu\nu} = \overline{\psi}\sigma_{\mu\nu}\gamma_5\psi$

$$\begin{aligned}\left(\overline{\psi}\sigma_{\mu\nu}\gamma_5\psi\right)^{\rm imp} &= (1 + a\, b\, m)\overline{\psi}\sigma_{\mu\nu}\gamma_5\psi + \tfrac{1}{2}aic_1\overline{\psi}\left(\gamma_\mu \overleftrightarrow{D}_\nu - \gamma_\nu \overleftrightarrow{D}_\mu\right)\gamma_5\psi + \\ &\quad \tfrac{1}{2}aic_2\epsilon_{\mu\nu\lambda\tau}\partial_\tau\left(\overline{\psi}\gamma_\lambda\psi\right),\end{aligned} \tag{9.3}$$

In all cases we are interested in the flavour non-singlet operators. The improvement terms we add have dimension 1 higher than the original operator, and do not include any operators with dimension 2 higher than the original, for example operators such as $a^2m\frac{1}{2}\overline{\psi}\overleftrightarrow{\not{D}}\psi$ in the scalar case. The reason that it is better to avoid such a^2 terms is that they lead to more complicated results in which the effects of the equations of motion are no longer simple. Again using the scalar operator as an example, there is an equation of motion that says that for on-shell measurements $\overline{\psi}\overleftrightarrow{\not{D}}\psi + \eta m\overline{\psi}\psi = 0$, where η is a g-dependent coefficient. This allows us to compensate for changes in c_1 by making changes in b, which would allow us to eliminate one of the improvement terms if we were only interested in on-shell quantities. This equation of motion means that b is linear in c_1 if we parameterise our operators as in eq.(9.3). If we use other parameterisations, for example $(1 + ab'm)(\overline{\psi}\psi - \frac{1}{2}ac_1'\overline{\psi}\overleftrightarrow{\not{D}}\psi)$ we would no longer find that b' was linear in c_1'.

It is also useful to consider the conserved vector current, because we know that this should need no improvement for forward matrix elements.

- C_μ

If these operators are inserted into forward matrix elements the surface term $\partial_\mu\left(\overline{\psi}\mathcal{O}\psi\right)$ (where $\mathcal{O}$ is any operator) vanishes due to momentum conservation. Using the equation of motion it is possible for each improved operator to eliminate one base operator if we are only interested in on-shell measurements.

9.2 Improving the quark lattice propagator

9.2.1 Method

Even when the fermion action has been improved for on-shell quantities there are still $O(a)$ effects present in off-shell quantities such as the fermion propagator at Euclidean momentum p. In this section we will discuss how to find an improved fermion propagator off-shell. First we will look at the tree-level Wilson propagator and show how to remove its off-shell discretisation errors, then we will generalise this improvement method for the interacting case.

We are used to writing down expressions for S^{-1}, the inverse quark propagator. In S^{-1} the main $O(a)$ effect is the addition of the momentum-dependent Wilson mass term. However it is also instructive to look at the quark propagator S, rather than the inverse propagator.

Let us start by looking at the tree-level propagator.

$$\begin{aligned}(S^{\rm tree})^{-1}(p,m) &= \frac{i}{a}\sum_\mu \gamma_\mu\sin(ap_\mu) + m + \frac{1}{a}\sum_\mu(1-\cos(ap_\mu)) \\ &= i\not{p} + m + \tfrac{1}{2}ap^2 + O(a^2) \\ &= (i\not{p} + m - \tfrac{1}{2}am^2)(1+am)(1 - \tfrac{1}{2}a(i\not{p}+m)) + O(a^2) \\ \Rightarrow S^{\rm tree}(p,m) &= \frac{1-am}{i\not{p} + m - \frac{1}{2}am^2} + \frac{a}{2} + O(a^2) \\ &\equiv (1-am)S_\star^{\rm tree}(p,m_\star) + \frac{a}{2} + O(a^2).\end{aligned} \tag{9.4}$$

The lattice propagator consists of two parts, one part proportional to a normal continuum propagator with a mass $m_\star \equiv m - \frac{1}{2}am^2$, and a momentum independent term. The nature of these two parts becomes even more clear when we write them in position space.

$$S_{\rm latt}^{\rm tree}(x,y,m) = (1-am)S_\star^{\rm tree}(x,y,m_\star) + \frac{1}{2a^3}\delta_{xy} + O(a^2). \tag{9.5}$$

We see that (except at short distances, where an additional contact term appears) the lattice Wilson-fermion propagator is proportional to $S_\star$, which has the form of a continuum propagator with an "improved" mass $m_\star$, This is the behaviour we should expect, the fermion propagator at $|x| \gg a$ is an on-shell quantity, so we should expect that it is automatically improved when the action is improved. It is only at distances $\sim a$ that the lattice propagator has a different form from the continuum propagator. The necessity of subtracting a δ function from the lattice propagator to obtain an improved propagator has been discussed in [53].

What should we expect beyond tree level? Let us write the inverse fermion propagator (at $r = 1$) as a series in the lattice spacing a.

$$S^{-1}(p,m) = \sigma_0(p,m) + a\sigma_1(p,m) + O(a^2) \tag{9.6}$$

where $ma \equiv 1/(2\kappa) - 1/(2\kappa_c)$. σ_0 and σ_1 will be power series in g^2. On-shell improvement tells us that the lattice fermion propagator should be proportional to a continuum fermion propagator except at short distances, so we expect equations of the same form as eq.(9.4,9.5) to hold, though only at the value of c_{SW} corresponding to on-shell improvement. Thus the propagator should satisfy

$$\begin{aligned} S(p,m) &= \frac{1+ab_\psi m}{\sigma_0(p,m_\star)} + \frac{a}{2}\lambda_\psi + O(a^2) \\ &\equiv (1+ab_\psi m)S_\star(p,m_\star) + \frac{a}{2}\lambda_\psi + O(a^2) \end{aligned} \tag{9.7}$$

where the improved bare mass $m_\star$ is related to m through

$$m_\star = m(1 + ab_m m). \tag{9.8}$$

The improvement coefficients b_ψ, b_m and λ_ψ are independent of p and m, and should only depend on the coupling constant g^2. By comparing with eq.(9.4) we see that the tree-level values of b_ψ, b_m and λ_ψ are $-1, -1/2$ and $+1$ respectively. The propagator $S_\star$ is free of $O(a)$ effects so we call it the improved fermion propagator. Later, when we come to define renormalisation constants, we will always define them in terms of the improved propagator $S_\star$ and improved bare mass $m_\star$.

What does eq.(9.7) tell us about the inverse propagator?

$$S(p,m) = \frac{1+ab_\psi m}{\sigma_0(p,m_\star)} + \frac{a}{2}\lambda_\psi + O(a^2) \tag{9.9}$$

Taking the inverse gives

$$\begin{aligned} \Rightarrow S^{-1}(p,m) &= \sigma_0(p,m_\star)\,(1-ab_\psi m)\left(1-\tfrac{1}{2}a\lambda_\psi\sigma_0(p,m_\star)\right) + O(a^2) \qquad (9.10) \\ &= \left(\sigma_0(p,m) + ab_m m^2\frac{\partial}{\partial m}\sigma_0(p,m)\right)(1-ab_\psi m)\left(1-\tfrac{1}{2}a\lambda_\psi\sigma_0(p,m)\right) + O(a^2). \end{aligned}$$

Dropping terms of order a^2 we arrive at

$$S^{-1}(p,m) = \sigma_0(p,m) + a\left[-\tfrac{1}{2}\lambda_\psi\left(\sigma_0(p,m)\right)^2 - b_\psi m\sigma_0(p,m) + b_m m^2\frac{\partial}{\partial m}\sigma_0(p,m)\right] + O(a^2). \tag{9.11}$$

Comparing with eq.(9.6) we see that the improvement prescription eq.(9.7) can only work if

$$\sigma_1(p,m) = -\tfrac{1}{2}\lambda_\psi\left(\sigma_0(p,m)\right)^2 - b_\psi m\sigma_0(p,m) + b_m m^2\frac{\partial}{\partial m}\sigma_0(p,m). \tag{9.12}$$

We can see from eq.(9.10) that the improvement coefficient λ_ψ only has an effect when the fermion is off-shell. The pole-mass of the fermion is the p value where $\sigma_0(p,m_\star)$ vanishes, so for an on-shell fermion the factor $(1-\frac{1}{2}a\lambda_\psi\sigma_0(p,m_\star))$ simply reduces to 1. So we only need to know λ_ψ if we are interested in extracting numbers from off-shell lattice measurements.

The significance of $S_\star$ is that it is a quantity free of $O(a)$ effects which can be found from the quark propagator, which is something we can measure on the lattice. From eq.(9.7) we have

$$S_\star(p,m_\star) = \frac{1}{1+amb_\psi}\left(S(p,m) - \frac{a}{2}\lambda_\psi\right) = \frac{1}{\sigma_0(p,m_\star)} \tag{9.13}$$

and

$$S_\star^{-1}(p,m_\star) = (1+amb_\psi)\left(S^{-1}(p,m) + S^{-1}(p,m)\frac{a}{2}\lambda_\psi S^{-1}(p,m)\right) = \sigma_0(p,m_\star). \tag{9.14}$$

We will find that eq.(9.12) is satisfied at one particular value of the clover coefficient c_{SW}. At this c_{SW} value one can use eq.(9.13) or eq.(9.14) to extract σ_0 from lattice measurements. The clover action does not have enough tuneable parameters to make the off-shell fermion propagator free of $O(a)$ effects, but this does not really matter, because equations such as eq.(9.14) never-the-less allow us to recover the improved off-shell propagator from quantities which we can measure.

9.2.2 One–loop results for the quark propagator

We have calculated $S^{-1}(p,m)$ in 1-loop perturbation theory. We now want to use these results to see if the propagator improvement scheme suggested in eq.(9.7) holds, and to calculate the improvement coefficients and renormalisation factors to $O(g^2)$.

We can write

$$S^{-1}(p,m) = m + i\not p + \frac{a}{2}p^2 - \frac{g^2 C_F}{16\pi^2}\left(\rho_0(p,m) + a\rho_1(p,m)\right) + O(a^2, g^4) \tag{9.15}$$

where $C_F = (N_c^2-1)/(2N_c)$ for $SU(N_c)$ and

$$ma \equiv \frac{1}{2\kappa} - \frac{1}{2\kappa_c}. \tag{9.16}$$

To one loop [12]

$$\kappa_c = \frac{1}{8}\left(1 + \frac{g^2C_F}{16\pi^2}\left(12.8587 - 3.4333c_{SW} - 1.4288c_{SW}^2\right)\right) + O(g^4). \tag{9.17}$$

Comparing with eq.(9.6) we see that

$$\begin{aligned} \sigma_0(p,m) &= i\not p + m - \frac{g^2C_F}{16\pi^2}\rho_0(p,m) + O(g^4) \\ \sigma_1(p,m) &= \tfrac{1}{2}p^2 - \frac{g^2C_F}{16\pi^2}\rho_1(p,m) + O(g^4). \end{aligned} \tag{9.18}$$

We also expand the improvement coefficients to lowest order in g^2

$$\begin{aligned} \lambda_\psi &= 1 + \frac{g^2C_F}{16\pi^2}d_{\lambda_\psi} + \cdots \\ b_\psi &= -\left(1 + \frac{g^2C_F}{16\pi^2}d_{b_\psi} + \cdots\right) \\ b_m &= -\tfrac{1}{2}\left(1 + \frac{g^2C_F}{16\pi^2}d_{b_m} + \cdots\right). \end{aligned} \tag{9.19}$$

If we substitute (9.18) and (9.19) into the quadratic equation (9.12) we find that the ρs must obey the following linear condition if the improvement procedure eq.(9.7) works.

$$\begin{aligned} \rho_1(p,m) + i\not p\rho_0(p,m) \quad + \quad & \frac{m^2}{2}\frac{\partial}{\partial m}\rho_0(p,m) = \\ & -d_{\lambda_\psi}p^2/2 + \left(d_{\lambda_\psi} - d_{b_\psi}\right) i\not p m + \left(d_{\lambda_\psi} - 2d_{b_\psi} + d_{b_m}\right) m^2/2 . \end{aligned} \tag{9.20}$$

The expressions for ρ_0 and ρ_1 (evaluated at $r=1$) are:

$$\begin{aligned} \rho_0(p,m) = \quad & i\not p \quad \Big[16.64441 - \alpha - 2.24887c_{SW} - 1.39727c_{SW}^2 + \alpha L(ap,am) \\ & \quad + \alpha\frac{m^2}{p^2}\left(1 - T\left(p^2/m^2\right)\right)\Big] \\ & + m \quad \Big[11.06803 - 2\alpha - 9.98679c_{SW} - 0.01689\,c_{SW}^2 + (3+\alpha)L(ap,am) \\ & \quad + (3+\alpha)T\left(p^2/m^2\right)\Big] \end{aligned} \tag{9.21}$$

and

$$
\begin{aligned}
\rho_1(p,m) = \quad & p^2 & & \Big[7.13891 - 0.07187\,\alpha + 0.48567 c_{SW} - 0.08173 c_{SW}^2 \\
& & & - \left(\frac{3}{2} - \alpha - \frac{3}{2} c_{SW}\right) L(ap,am)\Big] \\
& +i\,m\,\not p & & \Big[-6.34664 + 0.14375\,\alpha - 1.48503 c_{SW} + 1.28605 c_{SW}^2 \\
& & & - \left(\frac{3}{2} + \alpha + \frac{3}{2} c_{SW}\right) L(ap,am) - (\alpha + 3c_{SW})\, T\left(p^2/m^2\right) \\
& & & - \left(\frac{3}{2} + 2\alpha - \frac{3}{2} c_{SW}\right) \frac{m^2}{p^2}\,\left(1 - T\left(p^2/m^2\right)\right)\Big] \\
& +m^2 & & \Big[-14.03413 + 1.07187\,\alpha + 15.48574 c_{SW} - 1.52344 c_{SW}^2 \\
& & & - \left(\frac{9}{2} + \frac{\alpha}{2} - 3c_{SW}\right) L(ap,am) - \left(6 + \frac{5}{2}\alpha - \frac{3}{2} c_{SW}\right)\, T\left(p^2/m^2\right)\Big]
\end{aligned}
\tag{9.22}
$$

where $T(x) \equiv \ln(1+x)/x$ and $L(x,y) = \gamma_E - F_0 + \ln(x^2+y^2)$, with $F_0 = 4.369225\cdots$, $\gamma_E = 0.577216\cdots$. The gauge parameter α is 0 for the Landau gauge, 1 for the Feynman. Previously we calculated the fermion propagator in the limit $m^2 \ll p^2$, but now eqs.(9.21,9.23) are valid for any ratio m^2/p^2, (but a^2m^2 and a^2p^2 must both be small). Despite the complicated form of eq. (9.21) and (9.23) it can easily be checked (with the help of Mathematica) that, at $c_{SW} = 1$, eq.(9.21) is satisfied by ρ_0 and ρ_1. The resulting improvement coefficients are, for $r = 1$ and in a general gauge:

$$
\begin{aligned}
c_{SW} &= 1 + \cdots \\
\lambda_\psi &= 1 + \frac{g^2 C_F}{16\pi^2}(10.91085 - 1.85625\alpha) + \cdots \\
b_\psi &= -\left(1 + \frac{g^2 C_F}{16\pi^2} 16.39210 + \cdots\right) \\
b_m &= -\tfrac{1}{2}\left(1 + \frac{g^2 C_F}{16\pi^2} 22.79406 + \cdots\right).
\end{aligned}
\tag{9.23}
$$

Both b coefficients are gauge invariant.

We can use eqs.(9.21 , 9.23) to find an equation for the quark's pole mass, the place where the quark propagator has a pole (in perturbation theory).

$$
\begin{aligned}
m_{\rm pole}\Big(1 \;&+\; \frac{g^2 C_F}{16\pi^2}(1 + am(c_{SW}-1)) 6\ln(am_{\rm pole})\Big) = \\
& m \quad \left(1 + \frac{g^2 C_F}{16\pi^2}\left(16.95241 + 7.73792 c_{SW} - 1.38038 c_{SW}^2\right)\right) \\
& \times \left(1 - \frac{am}{2}\left(1 + \frac{g^2 C_F}{16\pi^2}\left(12.32005 + 18.70718 c_{SW} - 8.23318 c_{SW}^2\right)\right)\right).
\end{aligned}
\tag{9.24}
$$

Note that $m_{\rm pole}$ is gauge invariant, as it should be. At $c_{SW} = 1$ the pole mass is given by

$$
m_{\rm pole}\left(1 + \frac{g^2 C_F}{16\pi^2} 6\ln(am_{\rm pole})\right) = m\,\left(1 + \frac{g^2 C_F}{16\pi^2} 23.30995\right)\left(1 - \frac{am}{2}\left(1 + \frac{g^2 C_F}{16\pi^2} 22.79406\right)\right).
\tag{9.25}
$$

The pole mass becomes a function of $m_\star$, with the same value of b_m as in eq.(9.23). The unwanted $am\ln(am)$ term vanishes, and the mass has the same anomalous dimension as in the continuum. We will see that this is always the case, that when $c_{SW} \neq 1$ anomalous dimensions are changed by an amount proportional to am, but at $c_{SW} = 1$ all anomalous dimensions have their correct values.

We define our renormalisation constants Z in two different renormalisation schemes, $\overline{\rm MS}$, and a lattice momentum subtraction scheme, which we will call MOM. In both cases we define the Zs in terms of the improved fermion propagator $S_\star$. $Z^{\overline{\rm MS}}$ is the renormalisation constant needed to change the lattice result into a propagator renormalised according to the $\overline{\rm MS}$ scheme. The $\overline{\rm MS}$ renormalisation constants are defined from

$$
S_\star(p, m_\star) = Z_2^{\overline{\rm MS}}(\mu^2; a^2) S_{\overline{\rm MS}}\left(p, m^{\overline{\rm MS}}\right) = Z_2^{\overline{\rm MS}}(\mu^2; a^2) S_{\overline{\rm MS}}\left(p, Z_m^{\overline{\rm MS}}(\mu^2; a^2) m_\star\right)
\tag{9.26}
$$

where $S_{\overline{\rm MS}}$ is the continuum fermion propagator calculated perturbatively in $\overline{\rm MS}$ at the scale μ.

$$
\begin{aligned}
& S^{-1}_{\overline{\rm MS}}(p, m_{\overline{\rm MS}}) = i\not{p} + m_{\overline{\rm MS}} \\
& -i\not{p}\frac{g^2 C_F}{16\pi^2}\left[-\alpha + \alpha\ln\left(\frac{p^2+m^2_{\overline{\rm MS}}}{\mu^2}\right) + \alpha\frac{m^2_{\overline{\rm MS}}}{p^2}\left(1 - T\left(p^2/m^2_{\overline{\rm MS}}\right)\right)\right] \\
& -m_{\overline{\rm MS}}\frac{g^2 C_F}{16\pi^2}\left[-4 - 2\,\alpha + (3+\alpha)\ln\left(\frac{p^2+m^2_{\overline{\rm MS}}}{\mu^2}\right) + (3+\alpha)T\left(p^2/m^2_{\overline{\rm MS}}\right)\right].
\end{aligned}
\tag{9.27}
$$

In MOM we define the Zs at the subtraction scale p through

$$
S_\star(p, m_\star) = Z_2^{\rm MOM}(p^2;a^2)/\left(i\not{p} + Z_m^{\rm MOM}(p^2;a^2)m_\star\right). \tag{9.28}
$$

The advantage of the MOM scheme is that it only involves lattice quantities, so in principle it can be used nonperturbatively too. This is different from the $\overline{\rm MS}$ scheme, where we need to compare with a continuum quantity which we can only find perturbatively.

In $\overline{\rm MS}$ at the scale μ^2 we find for the renormalisation coefficients $Z_\psi^{\overline{\rm MS}}$ and $Z_m^{\overline{\rm MS}}$ (at $r=1$)

$$
\begin{aligned}
Z_2^{\overline{\rm MS}}(\mu^2;a^2) &= 1 + \frac{g^2}{16\pi^2}C_F\left(16.64441 - 2.24887c_{SW} - 1.39727c_{SW}^2 + \alpha L(a\mu)\right), && (9.29)\\
Z_m^{\overline{\rm MS}}(\mu^2;a^2) &= 1 + \frac{g^2}{16\pi^2}\,C_F\,\left(1.57638 + 7.73792c_{SW} - 1.38038c_{SW}^2 - 3L(a\mu)\right) && (9.30)
\end{aligned}
$$

where $L(x) = \gamma_E - F_0 + \ln(x^2)$.

The MOM scheme Zs are not so simple, they still have mass and gauge dependences which cancel in the $\overline{\rm MS}$ case.

$$
\begin{aligned}
Z_2^{\rm MOM}(p^2;a^2) &= 1 + \frac{g^2}{16\pi^2}C_F\Big(16.64441 - \alpha - 2.24887c_{SW} - 1.39727c_{SW}^2 + \alpha\,L(ap, am_\star) \\
&\qquad + \alpha\,\frac{m_\star^2}{p^2}\left(1 - T\left(p^2/m_\star^2\right)\right)\Big) && (9.31)\\
Z_m^{\rm MOM}(p^2;a^2) &= 1 + \frac{g^2}{16\pi^2}\,C_F\,\Big(5.57638 + \alpha + 7.73792c_{SW} - 1.38038c_{SW}^2 - 3L(ap, am_\star) \\
&\qquad - (3+\alpha)\,T\left(p^2/m_\star^2\right) + \alpha\,\frac{m_\star^2}{p^2}\left(1 - T\left(p^2/m_\star^2\right)\right)\Big) && (9.32)
\end{aligned}
$$

Note that the dependence on the lattice spacing a and clover coefficient c_{SW} is the same in the $\overline{\rm MS}$ and MOM schemes, so that the ratio $Z^{\overline{\rm MS}}/Z^{\rm MOM}$ is independent of c_{SW}. This is as it should be, the ratio $Z^{\overline{\rm MS}}/Z^{\rm MOM}$ is simply the conversion factor between the two schemes, which can be calculated in the continuum, and so should not refer to the lattice in any way.

$Z_m^{\rm MOM}$ is gauge-dependent, but it becomes gauge independent when the fermion is on-shell (at the point $p^2 = -m^2_{\rm pole}$).

9.2.3 Discussion

We illustrate the improvement procedure for the fermion propagator by taking the example of a free propagator with momentum in the direction $(1,1,1,1)$ and with bare mass $am = 0.2$. The pole mass of this propagator is at

$$
m_{\rm pole} = 2\ln[(4 + am + \sqrt{4 + 8am + a^2m^2})/6] = 0.18299\cdots
$$

(the dotted line in fig. 39).

We have used the improvement condition of eq.(9.14)

$$
S_\star^{-1}(p, m_\star) = (1 + amb_\psi)\left(S^{-1}(p,m) + S^{-1}(p,m)\frac{a}{2}\lambda_\psi S^{-1}(p,m)\right) \tag{9.33}
$$

to remove $O(a)$ effects from the measured fermion propagator S^{-1}. We plot this as curve (a) in fig. 39. We see that it does indeed remove $O(a)$ effects at small momenta, unfortunately the $O(a^2)$ errors are rather

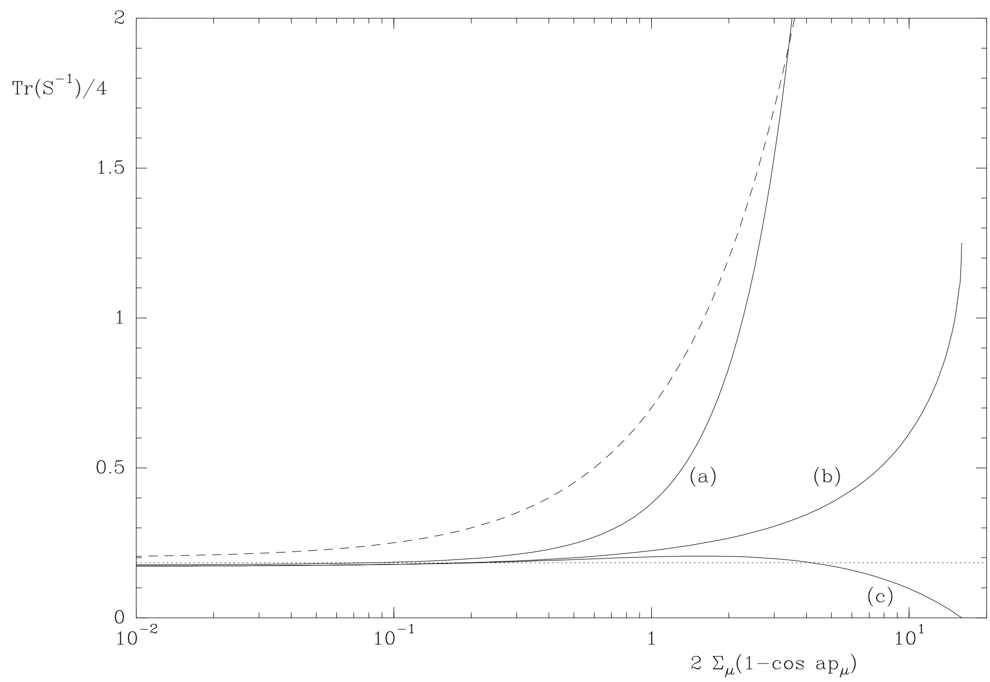

Figure 39: The trace of the unimproved inverse tree-level propagator (dashed line) and of three different $O(a)$ improved inverse propagators, improved according to eqs. (9.33), (9.34) and (9.35). The dotted line shows the pole mass of the propagator (i.e. the "correct" value of $Tr(S^{-1}(p))$). All three improvement methods are clearly better than the unimproved propagator, but we see that the non-linear methods (b) and (c) work for a larger range of a^2p^2 than the simple method (a).

large, and soon become important. Fortunately there are many other equations differing from eq. (9.33) by terms of $O(a^2)$. One possibility is the non-linear improvement condition suggested in [82],

$$S_\star^{-1}(p,m_\star) = (1 + amb_\psi)\left(S^{-1}(p,m) + S_\star^{-1}(p,m_\star)\frac{a}{2}\lambda_\psi S_\star^{-1}(p,m_\star)\right). \tag{9.34}$$

This is plotted as curve (b), and we see that it remains valid to much larger values of a^2p^2. This equation still has its faults. If we solve it for the $m = 0$ free Wilson lattice propagator, $S_\star^{-1}$ has a trace proportional to a^3p^4. Although this is better than the unimproved propagator, which has a trace proportional to ap^2, it would be better to have an improved propagator which is completely traceless when the mass is 0. A variant of eq. (9.34) which achieves this is

$$S_\star^{-1}(p,m_\star) = (1 + amb_\psi)\left(S^{-1}(p,m) + S_\star^{-1}(p,m_\star)\frac{a}{2}\lambda_\psi\frac{2\sum(1-\cos ap_\mu)}{\sum \sin^2 p_\mu}S_\star^{-1}(p,m_\star)\right). \tag{9.35}$$

The extra factor in the improvement term is $1 + O(a^2p^2)$, so eq. (9.35) differs from eq. (9.34) at $O(a^3)$. The factor is chosen so that if S^{-1} is the massless free Wilson propagator, the solution is $S_\star^{-1} = i/a\sum\gamma_\mu \sin ap_\mu$. The solution of eq. (9.35) is shown as curve (c) in fig. 39. It seems to be an improvement over curve (b).

The difference between these versions of the improvement condition is irrelevant when doing perturbation theory, they all lead to the same values for λ_ψ and b_ψ, but if we want to apply the methods of this paper to find nonperturbative values for renormalisation constants and improvement coefficients, it is important to choose a form of the equation that works well up to large values of a^2p^2.

9.3 Renormalisation of point operators including $O(a)$ effects

In order to compare the matrix elements computed on the lattice to continuum matrix elements the so called Z factors have to be calculated. A consistent way would be to do this also nonperturbatively, e.g. on the lattice[53]. For the improved operators given in the preceding subsection this will be presented in Sect. 10. In this paper we discuss the results of one loop perturbative calculation using totally anticommuting γ_5.

The renormalisation of improved point operators obtained by the general covariant transformation has been discussed by several groups[81],[79],[80]. They use the values for the constants c_i as given by lowest order perturbation theory. Furthermore, the constant c_{SW} in the Sheikholeslami Wohlert action has been set to its lowest order value, too. The same settings have been used to calculate the renormalisation factors for the one link ([89]) and two link ([84]) quark operators in the chiral limit without discussing a base representation. We discuss the Z factors with coefficients c_i and c_{SW} kept arbitrary. This allows us to determine the perturbative contributions of the various terms and their relative magnitudes. Moreover, this will allow to implement tadpole improved perturbation theory.

9.3.1 Method for a general point operator

We are principally interested in calculating the Z factors for quark bilinear operators. Let us set out our notation for a general point operator. We consider forward matrix elements only, so c_2 is unnecessary (because it is the coefficient of an absolute derivative.)

Let Γ be a 4×4 matrix. All the point operators in eq.(9.3) have the form

$$\mathcal{O}_\Gamma^{\rm imp} = \overline{\psi}\Gamma\psi - \frac{a}{4} c_1^\Gamma \overline{\psi} \left\{ \overleftrightarrow{\not{D}}, \Gamma \right\} \psi + a b_\Gamma m \overline{\psi}\Gamma\psi \tag{9.36}$$

where $\{A, B\} \equiv A \cdot B + B \cdot A$ is the anti-commutator of two Dirac matrices. We denote the unamputated three-point function corresponding to the operator part

$$\overline{\psi}\Gamma\psi - \frac{a}{4} c_1^\Gamma \; \overline{\psi} \; \{\overleftrightarrow{\not{D}}, \Gamma\}\psi \tag{9.37}$$

by $G^\Gamma(p, m, c_1^\Gamma)$. The corresponding amputated three-point function will be written as $\Lambda^\Gamma(p, m, c_1^\Gamma)$. The two are related by

$$G^\Gamma(p, m, c_1^\Gamma) = S(p, m)\Lambda^\Gamma(p, m, c_1^\Gamma)S(p, m). \tag{9.38}$$

Because the operator definition eq. (9.36) is linear in c_1^Γ, both $G^\Gamma(p, m, c_1^\Gamma)$ and $\Lambda^\Gamma(p, m, c_1^\Gamma)$ will be linear functions of c_1^Γ. The Green's function from the improved operator eq.(9.36) is

$$G^{\mathcal{O}_\Gamma^{\rm imp}}(p, m, c_1^\Gamma, b_\Gamma) = G^\Gamma(p, m, c_1^\Gamma) + a m b_\Gamma G^\Gamma(p, m, 0). \tag{9.39}$$

If we want to improve our Green's function off-shell as well as on-shell, we have to use the improved operator $\mathcal{O}_\Gamma^{\rm imp}$, and we also have to subtract a contact term of the form $\Gamma S(p, m) + S(p, m)\Gamma$. The resulting expression then has to be renormalised. Our final formula for the renormalised and improved Green's function is

$$\begin{aligned} G_R^\Gamma(p, m_R) \quad &= \quad \frac{1}{Z_2(1 + amb_\psi)} \frac{Z_\Gamma}{1 + \zeta^\Gamma c_1^\Gamma} \Big(G^\Gamma(p, m, c_1^\Gamma) \\ &\qquad + amb_\Gamma G^\Gamma(p, m, 0) - \frac{a}{2}\lambda_\Gamma \left\{\Gamma, S(p, m)\right\}\Big) \; . \end{aligned} \tag{9.40}$$

The first factor $1/(Z_2(1 + amb_\psi))$ accounts for the wave-function renormalisation. Z_Γ is defined to be independent of c_1, the c_1 dependence of the renormalisation constant is all placed in the factor $1/(1 + \zeta^\Gamma c_1^\Gamma)$. Z_Γ contains no am effects.

The improvement coefficients b, λ and ζ are independent of the renormalisation scheme, while the renormalisation constants Z are of course scheme dependent. Therefore it can be useful to split the renormalisation and improvement into two stages, and to define "improved bare" Green's functions by

$$\begin{aligned} G_\star^\Gamma(p, m_\star) \quad &= \quad \frac{1}{1 + amb_\psi} \frac{1}{1 + \zeta^\Gamma c_1^\Gamma} \Big[G^\Gamma(p, m, c_1^\Gamma) \\ &\qquad + amb_\Gamma G^\Gamma(p, m, 0) - \frac{a}{2}\lambda_\Gamma \left\{\Gamma, S(p, m)\right\}\Big]. \end{aligned} \tag{9.41}$$

where $m_\star = m(1 + amb_m)$, using the same value for b_m as found from the fermion propagator (eq.(9.23)). The second step is to renormalise this improved Green's function in the usual way,

$$G_R^\Gamma(p, m_R) = \frac{Z_\Gamma}{Z_2} G_\star^\Gamma(p, m_\star). \tag{9.42}$$

We define an amputated improved Green's function by

$$\Lambda^\Gamma_\star(p,m_\star) = S^{-1}_\star(p,m_\star) G^\Gamma_\star(p,m_\star) S^{-1}_\star(p,m_\star). \tag{9.43}$$

Substituting eq. (9.14) and eq.(9.41) and using eq.(9.38) we find

$$\begin{aligned}\Lambda^\Gamma_\star(p,m_\star) &= (1+amb_\psi)\frac{1}{1+\zeta^\Gamma c_1^\Gamma}\Big[\Lambda^\Gamma(p,m,c_1^\Gamma) + amb_\Gamma \Lambda^\Gamma(p,m,0) \\ &\quad -\frac{a}{2}\lambda_\Gamma\left\{S^{-1}(p,m),\Gamma\right\} + \frac{a}{2}\lambda_\psi\left\{S^{-1}(p,m),\Lambda^\Gamma(p,m,c_1^\Gamma)\right\}\Big].\end{aligned} \tag{9.44}$$

What conditions must Λ fulfil for this improvement to work? Let us expand both Λ and S^{-1} as series in a.

$$\begin{aligned}S^{-1}(p,m) &= \sigma_0(p,m) + a\sigma_1(p,m) + O(a^2) \\ \Lambda^\Gamma(p,m,c_1^\Gamma) &= \Lambda_0^\Gamma(p,m,c_1^\Gamma) + a\Lambda_1^\Gamma(p,m,c_1^\Gamma) + O(a^2).\end{aligned} \tag{9.45}$$

We say that all $O(a)$ effects have been removed from $\Lambda^\Gamma_\star$ if

$$\begin{aligned}\Lambda^\Gamma_\star(p,m_\star) &= \Lambda_0^\Gamma(p,m(1+ab_m m),0) + O(a^2) \\ &= \Lambda_0^\Gamma(p,m,0) + ab_m m^2 \frac{\partial}{\partial m}\Lambda_0^\Gamma(p,m,0) + O(a^2)\end{aligned} \tag{9.46}$$

This is only satisfied if there are improvement coefficients such that

$$\Lambda_0^\Gamma(p,m,c_1^\Gamma) = \left(1+\zeta^\Gamma c_1^\Gamma\right)\Lambda_0^\Gamma(p,m,0) \tag{9.47}$$

and

$$\begin{aligned}\Lambda_1^\Gamma(p,m,c_1^\Gamma) &= -\frac{1}{2}\lambda_\psi\left\{\sigma_0(p,m),\Lambda_0^\Gamma(p,m,c_1^\Gamma)\right\} + \frac{1}{2}\lambda_\Gamma\left\{\sigma_0(p,m),\Gamma\right\} \\ &\quad -b_\Gamma m\Lambda_0^\Gamma(p,m,0) - b_\psi m\Lambda_0^\Gamma(p,m,c_1^\Gamma) + b_m m^2\frac{\partial}{\partial m}\Lambda_0^\Gamma(p,m,c_1^\Gamma).\end{aligned} \tag{9.48}$$

The parameter ζ^Γ depends only on g^2. We can explain the significance of ζ^Γ as follows. Just as the continuum operator $\overline{\psi}\Gamma\psi$ acquires an improvement term on the lattice, the irrelevant operator $(a/4)\overline{\psi}\{\overleftrightarrow{\not{D}},\Gamma\}\psi$ is also "rotated" on the lattice. The "purely irrelevant" operator, the operator which has an expectation value $O(a)$ in any state, is not
$(a/4)\overline{\psi}\{\overleftrightarrow{\not{D}},\Gamma\}\psi$ as one might naively expect. Instead it is $(a/4)\overline{\psi}\{\overleftrightarrow{\not{D}},\Gamma\}\psi + \zeta^\Gamma\overline{\psi}\Gamma\psi$.

From eq.(9.44) we can see that the two improvement coefficients λ_ψ and λ_Γ associated with the contact terms are only needed for off-shell improvement, because the inverse propagator $S^{-1}(p,m)$ vanishes on-shell.

9.3.2 Example: Perturbative results of point scalar quark operator

If one calculates the renormalised forward matrix elements of improved operators as derived in the preceding section the problem of the $a \ln a$ terms has to be considered. The Sheikholeslami Wohlert action is constructed to cancel all $g^2 a \ln a \propto a$ terms in the final result if the calculation is performed on shell. For the point operators this has been demonstrated explicitly by Heatlie et al.[81].

For off–shell calculations these arguments do not apply straightforwardly. Therefore, we have calculated the matrix elements of all point operators up to order $O(g^2 a)$ including the finite terms.

We give the general structure of the matrix elements of the point quark operator of order $O(g^2)$ in lattice perturbation theory up to order $O(a)$ in the lattice spacing. The calculations are carried out for arbitrary m^2/p^2, not just for $m^2 \ll p^2$ as in our previous papers. We give the results for the amputated Green's functions, i.e. the leg corrections removed.

In this section we show how the improvement coefficients and renormalisation constants are calculated in one particular case, the scalar operator.

The amputated scalar Green's function is

$$\begin{aligned}\Lambda^s(p,m,c_1^s) &= 1 - a\, i\, \not{p}\, c_1^s \\ &\quad + \frac{g^2 C_F}{16\pi^2}\Big[-11.06803 + 2\,\alpha + 9.98679 c_{SW} + 0.01689\, c_{SW}^2 + c_1^s(-19.17181\end{aligned}$$

$$+13.80068c_{SW} - 3.53833\,c_{SW}^2) - (3+\alpha)\,L(ap,am) - 3\,(3+\alpha)\;T\left(p^2/m^2\right)\Big]$$
$$+i\,\not{p}\,\frac{g^2C_F}{16\pi^2}\,4\,\alpha\,\frac{m}{p^2}\,\Big[-1+T\left(p^2/m^2\right)\Big]$$
$$+a\,i\,\not{p}\,\frac{g^2C_F}{16\pi^2}\Big[6.34664 - 0.14375\,\alpha + 1.48503c_{SW} - 1.28605\,c_{SW}^2 + c_1^s(11.65102$$
$$-\alpha - 1.41422c_{SW} + 0.78465\,c_{SW}^2) + (\frac{3}{2}+\alpha+\alpha\,c_1^s+\frac{3}{2}c_{SW})\,L(ap,am)$$
$$+3\,(\alpha+3c_{SW})\;T\left(p^2/m^2\right) - 4\,\alpha\,\frac{m^2}{m^2+p^2}$$
$$+\left(\frac{15}{2}+10\,\alpha-3\,\alpha\,c_1^s-\frac{15}{2}c_{SW}\right)\,\frac{m^2}{p^2}\left(1-T\left(p^2/m^2\right)\right)\Big]$$
$$+a\,m\,\frac{g^2C_F}{16\pi^2}\Big[31.06826 - 4.14375\,\alpha - 33.97148c_{SW} + 3.04688\,c_{SW}^2$$
$$+c_1^s(-6.08204 + 2.20074c_{SW} + 1.44647\,c_{SW}^2) + (9+\alpha-6c_{SW})\,L(ap,am)$$
$$+2\,(12+5\,\alpha-3\,c_1^s-\alpha\,c_1^s-3c_{SW})\;T\left(p^2/m^2\right) - 2\,(3+\alpha)\,\frac{m^2}{m^2+p^2}\Big].$$

We find that this expression satisfies eq.(9.48) at $c_{SW}=1$. Therefore we can find perturbative expressions for the improvement coefficients. The improvement coefficients are

$$\begin{aligned} b_s &= 1 - c_1^s - \frac{g^2C_F}{16\pi^2}(-22.79406 + 8.45146c_1^s) \\ \lambda_s &= 1 - c_1^s + \frac{g^2C_F}{16\pi^2}(16.39210 - 10.88629c_1^s) \\ \zeta_s &= \frac{g^2C_F}{16\pi^2}8.90946. \end{aligned} \tag{9.49}$$

There is a particularly interesting value of c_1 where λ_s vanishes, which means that the scalar three-point function contains no contact terms, and so even off-shell it is simply renormalised by a multiplicative factor. This value of c_1 is

$$c_1^s = 1 + \frac{g^2C_F}{16\pi^2}5.50582 + O(g^4). \tag{9.50}$$

The improvement coefficients b_s and λ_s are only defined at $c_{SW}=1$. ζ can also be defined for general c_{SW} values, the result is

$$\zeta_s = \frac{g^2C_F}{16\pi^2}(-19.17181 + 13.80068c_{SW} - 3.53833c_{SW}^2) \tag{9.51}$$

All these results are gauge invariant.

9.4 Summary of improvement and renormalisation condition

For the improved action renormalisation constants and improvement coefficients are defined by

$$m_R = Z_m m(1 + amb_m) \tag{9.52}$$

$$S_R(p,m_R) = \frac{1}{Z_2(1+amb_\psi)}\left(S_(p,m) - \frac{a}{2}\lambda_\psi\right) \tag{9.53}$$

Here we consider only Green's functions without momentum transfer, so we do not need to consider the absolute derivative improvement terms in eq.(9.3). The operators in eq.(9.3) therefore all have the form

$$\mathcal{O}_\Gamma^{\rm imp} = \overline{\psi}\Gamma\psi - \frac{a}{4}c_1^\Gamma\overline{\psi}\left\{\overleftrightarrow{\not{D}},\Gamma\right\}\psi + ab_\Gamma m\overline{\psi}\Gamma\psi. \tag{9.54}$$

We have defined $G^\Gamma(p,m,c_1^\Gamma)$ as the unamputated Green's function of the operator $\overline{\psi}\Gamma\psi - \frac{a}{4}c_1^\Gamma\overline{\psi}\left\{\overleftrightarrow{\not{D}},\Gamma\right\}\psi$, so the Green's function of the operator $\mathcal{O}_\Gamma^{\rm imp}$ is $G^\Gamma(p,m,c_1^\Gamma)$

$+ amb_\Gamma G^\Gamma(p,m,0)$. If we want to improve our Green's function off-shell as well as on-shell, we have to use the improved operator $\mathcal{O}_\Gamma^{\rm imp}$, and we also have to subtract a contact term of the form $\Gamma S(p,m) + S(p,m)\Gamma$. The resulting expression then has to be renormalised. Our final formula for the renormalised and improved Green's function is

$$\begin{aligned} G_R^\Gamma(p,m_R) &= \frac{1}{Z_2(1+amb_\psi)} \frac{Z_\Gamma}{1+\zeta^\Gamma c_1^\Gamma} \Big(G^\Gamma(p,m,c_1^\Gamma) + amb_\Gamma G^\Gamma(p,m,0) \\ &\quad - \frac{a}{2}\lambda_\Gamma \left\{\Gamma, S(p,m)\right\}\Big) . \end{aligned} \tag{9.55}$$

Z_Γ is defined to be independent of c_1, the c_1 dependence of the renormalisation constant is all placed in the factor $1/(1+\zeta^\Gamma c_1^\Gamma)$.

We usually work with the inverse quark propagator and the amputated three-point functions Λ^Γ, so it is useful to rewrite eqs.(9.53, 9.55) for these quantities. A little manipulation leads to

$$S_R^{-1}(p,m_R) = Z_2(1+amb_\psi)\Big(S^{-1}(p,m) + S^{-1}(p,m)\frac{a}{2}\lambda_\psi S^{-1}(p,m)\Big) \tag{9.56}$$

and

$$\begin{aligned} \Lambda_R^\Gamma(p,m_R) &= Z_2(1+amb_\psi)\frac{Z_\Gamma}{1+\zeta^\Gamma c_1^\Gamma}\Big[\Lambda^\Gamma(p,m,c_1^\Gamma) + amb_\Gamma \Lambda^\Gamma(p,m,0) \\ &\quad - \frac{a}{2}\lambda_\Gamma\left\{S^{-1}(p,m),\Gamma\right\} + \frac{a}{2}\lambda_\psi\left\{S^{-1}(p,m),\Lambda^\Gamma(p,m,c_1^\Gamma)\right\}\Big] \end{aligned} \tag{9.57}$$

where terms $O(a^2)$ have been dropped. (Eq.(9.57) follows from $\Lambda_R \equiv S_R^{-1} G_R S_R^{-1}$.)

If c_{SW} and the improvement coefficients are chosen correctly, these renormalised quantities have discretisation errors of $O(a^2)$.

The improvement coefficients b, λ and ζ are independent of the renormalisation scheme, while the renormalisation constants Z are of course scheme dependent. Therefore it can be useful to split the renormalisation and improvement into two stages, and to define "improved bare" Green's functions by

$$m_\star = m(1+amb_m) \tag{9.58}$$

$$S_\star(p,m_\star) = \frac{1}{1+amb_\psi}\Big(S(p,m) - \frac{a}{2}\lambda_\psi\Big) \tag{9.59}$$

$$S_\star^{-1}(p,m_\star) = (1+amb_\psi)\Big(S^{-1}(p,m) + S^{-1}(p,m)\frac{a}{2}\lambda_\psi S^{-1}(p,m)\Big) \tag{9.60}$$

$$\begin{aligned} G_\star^\Gamma(p,m_\star) &= \frac{1}{1+amb_\psi}\frac{1}{1+\zeta^\Gamma c_1^\Gamma}\Big[G^\Gamma(p,m,c_1^\Gamma) + amb_\Gamma G^\Gamma(p,m,0) \\ &\quad - \frac{a}{2}\lambda_\Gamma\left\{\Gamma, S(p,m)\right\}\Big]. \end{aligned} \tag{9.61}$$

$$\begin{aligned} \Lambda_\star^\Gamma(p,m_\star) &= (1+amb_\psi)\frac{1}{1+\zeta^\Gamma c_1^\Gamma}\Big[\Lambda^\Gamma(p,m,c_1^\Gamma) + amb_\Gamma\Lambda^\Gamma(p,m,0) \\ &\quad - \frac{a}{2}\lambda_\Gamma\left\{S^{-1}(p,m),\Gamma\right\} + \frac{a}{2}\lambda_\psi\left\{S^{-1}(p,m),\Lambda^\Gamma(p,m,c_1^\Gamma)\right\}\Big] \end{aligned} \tag{9.62}$$

These $\star$ quantities have all $O(a)$ effects removed, but are not yet renormalised. They are renormalised in the conventional way

$$m_R = Z_m m_\star \tag{9.63}$$

$$S_R(p,m_R) = \frac{1}{Z_2}S_\star(p,m_\star) \tag{9.64}$$

$$G_R^\Gamma(p,m_R) = \frac{Z_\Gamma}{Z_2}G_\star^\Gamma(p,m_\star) \tag{9.65}$$

$$\Lambda_R^\Gamma(p,m_R) = Z_2 Z_\Gamma \Lambda_\star^\Gamma(p,m_\star). \tag{9.66}$$

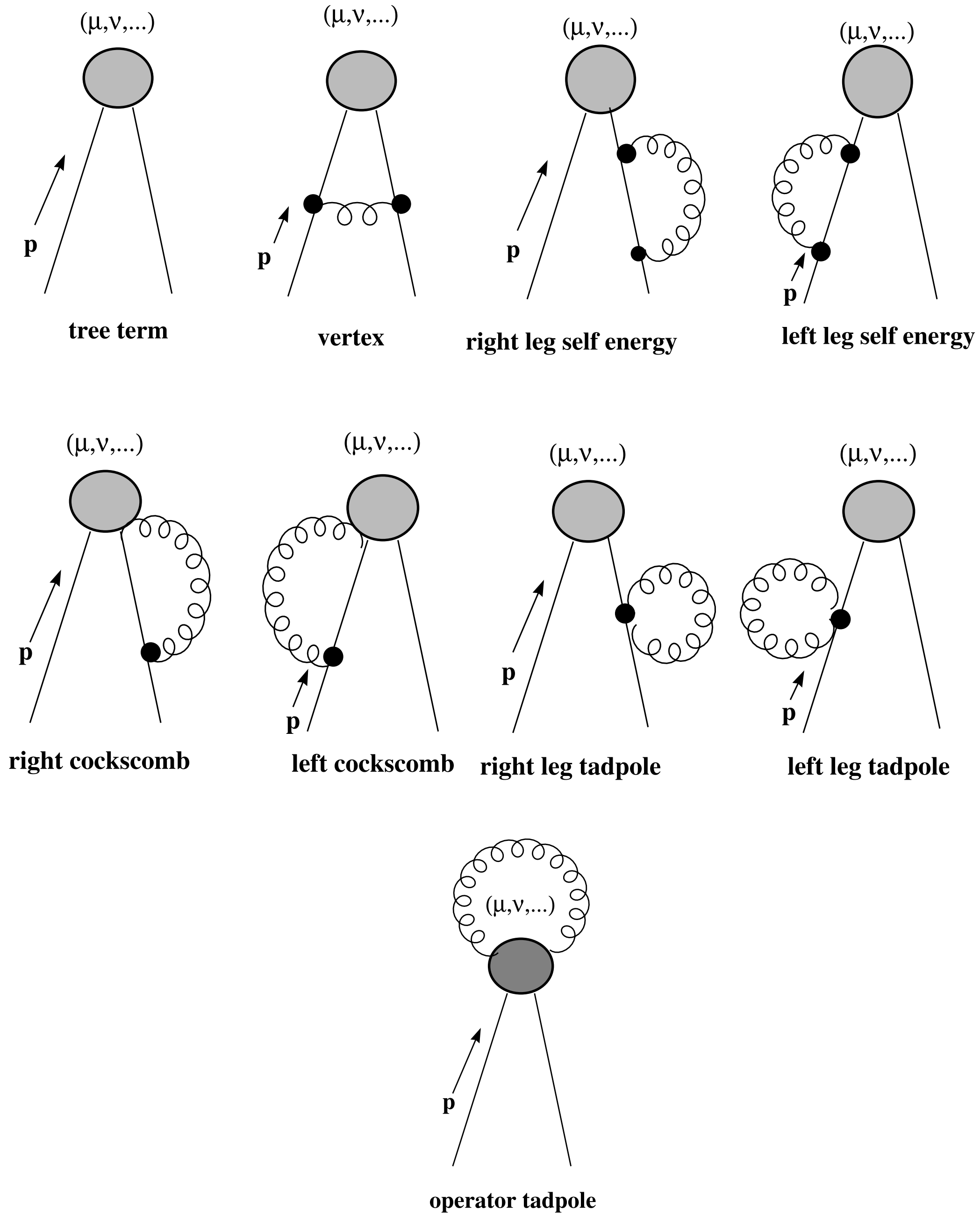

Figure 40: Lattice Feynman diagrams

9.5 About the calculation and program code

The typical diagrams to be calculated are shown in fig. 40 The calculation basically amounts to the computation of integrals of the form

$$\mathcal{I}_{\mu_1\cdots\mu_n}(a,p) = \int \frac{\mathrm{d}^4 k}{(2\pi)^4} \mathcal{K}_{\mu_1\cdots\mu_n}(a,p,k)\,, \tag{9.67}$$

where $\mathcal{K}$ contains lattice quark and gluon propagators and sin, cos of lattice momenta p_μ and k_μ, the integration is over the first Brillouin zone $-\pi/a \le k_\mu < \pi/a$. The calculation of the loop integrals $\mathcal{I}$ is performed in two parts. We decompose (9.67) [78, 51]

$$\mathcal{I} = \widetilde{\mathcal{I}} + (\mathcal{I} - \widetilde{\mathcal{I}})\,, \tag{9.68}$$

where

$$\widetilde{\mathcal{I}}(a,p) = \sum_{n=0}^{N} \frac{p_{\alpha_1}\dots p_{\alpha_n}}{n!} \frac{\partial^n}{\partial p_{\alpha_1}\dots\partial p_{\alpha_n}} \mathcal{I}(a,p)\Big|_{p=0} \tag{9.69}$$

and the order of the expansion N is determined by the degree of ultraviolet (UV) divergences of $\mathcal{I}(a,P)$ in the limit $a \to 0$. Therefore, $\mathcal{I} - \widetilde{\mathcal{I}}$ is rendered UV finite and is computed in the continuum. The Taylor expansion of the lattice integral (the first term) will in general create an infrared (IR) divergence. To regularise the integrals dimensional regularisation is used. The IR poles of $\widetilde{\mathcal{I}}$ cancel those of $\mathcal{I} - \widetilde{\mathcal{I}}$. UV divergent contributions ($\propto 1/a^n$) of the lattice integrals will cancel in the operator representations which we are interested in.

Let us summarise some of the basic features of the developed program code.

- The program package written in *Mathematica*.
- Symbolic Feynman rules used as input, the program computes one–loop forward matrix elements of bilinear quark and gluon operators on a hyper-cubic lattice including $O(a)$ contributions and in the continuum in symbolic form.
- Special features of the program:
  - Dimensional regularisation
  - Symmetrisation tables are used to accelerate the momentum integration over the Brillouin zone
  - General index handling in the complicated case of hyper-cubic H(4) symmetry (non-Lorentz covariant structures)
  - Algebraic isolation of the infrared poles which leads to an exact cancellation of the divergences
  - Results given with general index structure what allows an easy generation of all group representations
  - All *finite* lattice integrals represented by symbols which are accurately calculated numerically

A part of the results has been checked in a completely independent calculation based on a code in *Form*.

9.6 Tadpole improved Z factors

It is known that many results from (naive) lattice perturbation theory are in poor agreement with their numerically determined counterparts. One of the reasons is that tadpoles (lattice artifacts) spoil the expansion. From the one-loop perturbative analysis one can see that for operators with n_D covariant derivatives one receives n_D contributions (in a given unit) from the operator tadpole with only one compensating leg tadpole contribution.

Lepage and Mackenzie[27] proposed a rearrangement in the perturbative series in order to get rid of these numerically large tadpole contributions. These contributions are included in an essentially nonperturbative way using e.g. the measured value of the plaquette.

In lattice theory tadpole corrections renormalise the link operator so that the vev is considerably smaller than one. As a recipe ones scales the link variables with $u_0(g^2)$ measured in Monte Carlo

$$u_0 = \langle \frac{1}{3} \,\mathrm{Tr}\, U_\Box \rangle^{\frac{1}{4}} \,. \tag{9.70}$$

This leads to the consequences ($g^{\star 2}$ renormalised at some physical scale) of rescaling the variables

$$g^2 \to g^{\star 2} = u_0^{-4}\, g^2\,, \quad c_{SW} \to c^\star_{SW} = u_0^3\, c_{SW}\,, \quad c_i \to c_i^\star = u_0^{n_i - n_D}\, c_i\,. \tag{9.71}$$

Here n_i denotes the number of covariant derivatives in the higher dimensional operator part (proportional to c_i) and n_D the number of covariant derivatives (links) of the original operator.

In that case one obtains a tadpole improved perturbative expansion of Z

$$Z_{\mathcal{O}} \equiv \left(\frac{u_0}{u_0}\right)^{n_D-1} Z_{\mathcal{O}} = u_0^{1-n_D}\left(1 - \frac{g^{\star 2}}{16\pi^2} C_F \left(\gamma_{\mathcal{O}} \ln(a\mu) + B^\star_{\mathcal{O}}\right)\right) + O(g^{\star 4}) = Z^\star_{\mathcal{O}} + O(g^{\star 4}) \tag{9.72}$$

with the improved perturbative expansion

$$u_0 \approx 1 - \frac{g^{\star 2}}{16\pi^2} C_F \pi^2 \tag{9.73}$$

which implies

$$B^{\star}_{\mathcal{O}} = B_{\mathcal{O}}(c^{\star}_{SW}, c^{\star}_i) + (n_D - 1)\pi^2 \ . \tag{9.74}$$

To demonstrate the influence of tadpole improvement and addition of higher dimensional operators we show in fig. 41 [82] the dependence of the critical hopping parameter κ_c on c_{SW} and the gauge coupling.

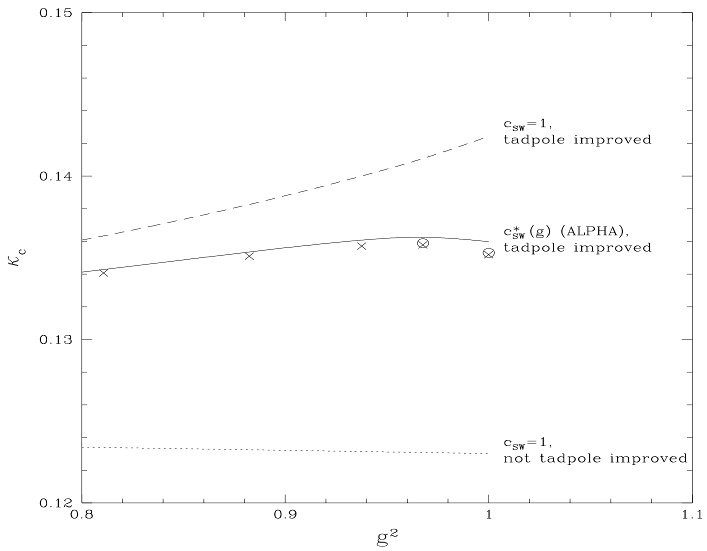

Figure 41: Dependence of critical hopping parameter κ_c on c_{SW}

The nonperturbative determination of c_{SW} is taken from the ALPHA–collaboration [61]. The tadpole improved perturbation theory describes the Monte Carlo data (crosses, circles) significantly better, however a nonperturbatively determined improvement coefficient c_{SW} is favoured.

10 Nonperturbative Renormalisation of Composite Operators

10.1 Motivation

In order to compute the moments of hadronic structure functions, for example, one needs the matrix elements of composite operators appearing in the operator product expansion of the appropriate currents [53, 89, 84, 11]. In general, one has to renormalise these operators in order to obtain finite answers in the continuum limit. Furthermore, comparison with the results of phenomenological analyses usually requires the matrix elements to be given in one of the popular continuum renormalisation schemes, e.g. the $\overline{\mathrm{MS}}$ scheme. So one has to think about the conversion of the bare lattice operators to renormalised continuum operators.

Consider the special case of the operators determining the moments of hadronic structure functions. Here the renormalised continuum matrix element has to be multiplied by the corresponding Wilson coefficient to yield the desired moment, which can be measured in deep inelastic scattering (DIS) experiments. Being an observable quantity it must be independent of any choices made in the renormalisation procedure. This is of course only possible, if the renormalised matrix element and the Wilson coefficient are calculated in the same scheme. In particular, the dependence on the renormalisation scale μ has to cancel between the renormalisation constant and the Wilson coefficient. Since the Wilson coefficients are mostly computed in the $\overline{\mathrm{MS}}$ scheme, we have to convert our lattice operators to continuum $\overline{\mathrm{MS}}$ operators if we want to make contact with phenomenology.

One obvious possibility to calculate the necessary renormalisation factors is lattice perturbation theory. However, quite often lattice perturbation theory seems to converge rather slowly. Identifying one source of these poor convergence properties, Lepage and Mackenzie proposed as a remedy the so-called tadpole improved perturbation theory [27]. Still, lattice perturbation series rarely extend beyond the one-loop level, and hence considerable uncertainty remains. It is therefore only natural to try a nonperturbative renormalisation by means of Monte Carlo simulations.

10.2 The operators

In the Euclidean continuum we should study the operators

$$\mathcal{O}^{(q)}_{\mu_1\cdots\mu_n} = \bar{q}\gamma_{\mu_1} \overleftrightarrow{D}_{\mu_2} \cdots \overleftrightarrow{D}_{\mu_n} q \,, \tag{10.1}$$

$$\mathcal{O}^{5(q)}_{\sigma\mu_1\cdots\mu_n} = \bar{q}\gamma_\sigma\gamma_5 \overleftrightarrow{D}_{\mu_1} \cdots \overleftrightarrow{D}_{\mu_n} q \tag{10.2}$$

or rather O(4) irreducible multiplets with definite C-parity. In particular, we obtain twist-2 operators by symmetrising the indices and subtracting the traces. In the flavour-nonsinglet case they do not mix and are hence multiplicatively renormalisable.

Working with Wilson fermions it is straightforward to write down lattice versions of the above operators. One simply replaces the continuum covariant derivative by its lattice analogue. However, O(4) being restricted to its finite subgroup H(4) (the hypercubic group) on the lattice, the constraints imposed by space-time symmetry are less stringent than in the continuum and the possibilities for mixing increase [89, 84, 5, 51]. Guided by the H(4) classification given in ref.[5] we have chosen the operators

$$\mathcal{O}_{v_{2,a}} = \mathcal{O}^{(q)}_{\{14\}} \,, \tag{10.3}$$

$$\mathcal{O}_{v_{2,b}} = \mathcal{O}^{(q)}_{\{44\}} - \tfrac{1}{3}(\mathcal{O}^{(q)}_{\{11\}} + \mathcal{O}^{(q)}_{\{22\}} + \mathcal{O}^{(q)}_{\{33\}}) \,, \tag{10.4}$$

$$\mathcal{O}_{v_3} = \mathcal{O}^{(q)}_{\{114\}} - \tfrac{1}{2}(\mathcal{O}^{(q)}_{\{224\}} + \mathcal{O}^{(q)}_{\{334\}}) \,, \tag{10.5}$$

$$\mathcal{O}_{v_4} = \mathcal{O}^{(q)}_{\{1144\}} + \mathcal{O}^{(q)}_{\{2233\}} - \mathcal{O}^{(q)}_{\{1133\}} - \mathcal{O}^{(q)}_{\{2244\}} \,, \tag{10.6}$$

$$\mathcal{O}_{a_1} = \mathcal{O}^{5(q)}_{\{24\}} \,, \tag{10.7}$$

$$\mathcal{O}_{a_2} = \mathcal{O}^{5(q)}_{\{214\}} \,, \tag{10.8}$$

$$\mathcal{O}_{r_{2,a}} = \mathcal{O}^{5(q)}_{\{14\}} \,, \tag{10.9}$$

$$\mathcal{O}_{r_{2,b}} = \mathcal{O}^{5(q)}_{\{44\}} - \tfrac{1}{3}(\mathcal{O}^{5(q)}_{\{11\}} + \mathcal{O}^{5(q)}_{\{22\}} + \mathcal{O}^{5(q)}_{\{33\}}) \,, \tag{10.10}$$

$$\mathcal{O}_{r_3} = \mathcal{O}^{5(q)}_{\{114\}} - \tfrac{1}{2}(\mathcal{O}^{5(q)}_{\{224\}} + \mathcal{O}^{5(q)}_{\{334\}}) \,. \tag{10.11}$$

In addition, we have studied the following operators without derivatives ("currents"):

$$\begin{aligned}
\mathcal{O}_I &= \overline{q}q\,, && (10.12)\\
\mathcal{O}_5 &= \overline{q}\gamma_5 q\,, && (10.13)\\
\mathcal{O}_\mu^V &= \overline{q}\gamma_\mu q\,, && (10.14)\\
\mathcal{O}_\mu^A &= \overline{q}\gamma_\mu\gamma_5 q = \mathcal{O}_\mu^{5(q)}\,, && (10.15)
\end{aligned}$$

where all quark fields are taken at the same lattice point, as well as the conserved vector current

$$J_\mu(x) = \tfrac{1}{2}\left(\overline{q}(x+\hat{\mu})(1+\gamma_\mu)U^+(x,\mu)q(x) - \overline{q}(x)(1-\gamma_\mu)U(x,\mu)q(x+\hat{\mu})\right) \tag{10.16}$$

with the link matrix $U(x,\mu) \in \mathrm{SU}(3)$ representing the gauge field.

Note that the operators $\mathcal{O}_{v_{2,a}}$ and $\mathcal{O}_{v_{2,b}}$ although belonging to the same irreducible O(4) multiplet transform according to inequivalent representations of H(4). Hence their renormalisation factors calculated on the lattice have no reason to coincide. The same remark applies to $\mathcal{O}_{r_{2,a}}$ and $\mathcal{O}_{r_{2,b}}$. The operators $\mathcal{O}_{a_1}$ and $\mathcal{O}_{r_{2,a}}$, on the other hand, are members of the same irreducible H(4) multiplet, whence their renormalisation factors should agree also on the lattice.

Concerning the mixing properties a few remarks are in order. Mixing with operators of equal or lower dimension is excluded for the operators $\mathcal{O}_{v_{2,a}}$, $\mathcal{O}_{v_{2,b}}$, $\mathcal{O}_{a_1}$, $\mathcal{O}_{a_2}$, $\mathcal{O}_{r_{2,a}}$, $\mathcal{O}_{r_{2,b}}$, as well as for the currents. The case of the operator $\mathcal{O}_{v_3}$, for which there are two further operators with the same dimension and the same transformation behaviour, is discussed in ref.[5]. The operators $\mathcal{O}_{v_4}$, $\mathcal{O}_{r_3}$, on the other hand, could in principle mix not only with operators of the same dimension but also with an operator of one dimension less and different chiral properties. It is of the type

$$\overline{q}\sigma_{\mu\nu}\gamma_5 \overleftrightarrow{D}_{\mu_1} \overleftrightarrow{D}_{\mu_2} \cdots \overleftrightarrow{D}_{\mu_n} q\,, \tag{10.17}$$

where $n = 2$ in the case of $\mathcal{O}_{v_4}$ and $n = 1$ for $\mathcal{O}_{r_3}$.

Our analysis ignores mixing completely. This seems to be justified for $\mathcal{O}_{v_3}$. Here a perturbative calculation gives a rather small mixing coefficient for one of the mixing operators [84, 51], whereas the other candidate for mixing does not appear at all in a one-loop calculation of quark matrix elements at momentum transfer zero, because its Born term vanishes in forward direction. The same is true for all operators of dimension less or equal to 6 which transform identically to $\mathcal{O}_{v_4}$: Their Born term vanishes in forward matrix elements, hence they do not show up in a one-loop calculation at vanishing momentum transfer. In the case of $\mathcal{O}_{r_3}$, however, the mixing with an operator of lower dimension is already visible at the one-loop level even in forward direction.

10.3 The method to derive the Z factors

Our calculation of renormalisation constants follows closely the procedure proposed by Martinelli et al. [53]. It mimics the definitions used in (continuum) perturbation theory. We work on a lattice of spacing a and volume V in Euclidean space (without improvement) For a fixed gauge let

$$G_{\alpha\beta}(p) = \frac{a^{12}}{V} \sum_{x,y,z} \mathrm{e}^{-\mathrm{i}p\cdot(x-y)} \langle q_\alpha(x)\mathcal{O}(z)\overline{q}_\beta(y)\rangle \tag{10.18}$$

denote the non-amputated quark-quark Green function with one insertion of the operator $\mathcal{O}$ at momentum zero. It is to be considered as a matrix in colour and Dirac space. With the quark propagator

$$S_{\alpha\beta}(p) = \frac{a^8}{V} \sum_{x,y} \mathrm{e}^{-\mathrm{i}p\cdot(x-y)} \langle q_\alpha(x)\overline{q}_\beta(y)\rangle \tag{10.19}$$

the corresponding vertex function (or amputated Green function) is given by (in previous Sect. Λ)

$$\Gamma(p) = S^{-1}(p)G(p)S^{-1}(p)\,. \tag{10.20}$$

Defining the renormalised vertex function by

$$\Gamma_{\mathrm{R}}(p) = Z_q^{-1} Z_{\mathcal{O}} \Gamma(p) \tag{10.21}$$

we fix the renormalisation constant $Z_{\mathcal{O}}$ by imposing the renormalisation condition

$$\tfrac{1}{4}\,\mathrm{Tr}\left(\Gamma_{\mathrm{R}}(p)\Gamma_{\mathrm{Born}}(p)^{-1}\right) = 1\,, \tag{10.22}$$

i.e. we calculate $Z_{\mathcal{O}}$ from

$$Z_q^{-1} Z_{\mathcal{O}} \tfrac{1}{4}\,\mathrm{Tr}\left(\Gamma(p)\Gamma_{\mathrm{Born}}(p)^{-1}\right) = 1\,. \tag{10.23}$$

Here $\Gamma_{\mathrm{Born}}(p)$ is the Born term in the vertex function of $\mathcal{O}$ computed on the lattice, and Z_q denotes the quark field renormalisation constant. The trace is taken over spin and colour indices. The latter can be taken as ($Z_q = Z_2^{-1}$ in Sect. 9)

$$Z_q(p) = \frac{\mathrm{Tr}\left(-\mathrm{i}\sum_\lambda \gamma_\lambda \sin(ap_\lambda) a S^{-1}(p)\right)}{12\sum_\lambda \sin^2(ap_\lambda)}\,, \tag{10.24}$$

so it is projected onto the energy-momentum part $\sin(ap_\lambda)/a$ (continuum form $\not{p}$) of the inverse propagator (The normalisation is chosen to give $Z_q = 1$ in the free case).

If the operator under study belongs to an O(4) multiplet of dimension greater than 1, i.e. if it carries at least one space-time index, the renormalisation condition (10.22) violates O(4) covariance even in the continuum limit. In the continuum, this disease is easily cured by a suitable summation over the members of the O(4) multiplet. On the lattice, this makes sense only in the few special cases where the O(4) multiplet is irreducible also under the hypercubic group H(4), because the renormalisation constants for the different H(4) multiplets within a given O(4) multiplet will in general be different. So we have to live with this noncovariance, which, of course, should finally be compensated when we convert our results to a covariant renormalisation scheme.

The scale μ at which our renormalisation constants are defined is identified with the momentum, i.e. we set $\mu^2 = p^2$. Ideally, one would like to satisfy the conditions

$$1/(aL)^2 \ll \Lambda_{\mathrm{QCD}}^2 \ll p^2 \ll 1/a^2 \tag{10.25}$$

on a lattice with linear extent aL. Whether in a concrete calculation these conditions may be considered as fulfilled remains to be seen.

10.4 A special case: vector and axial vector currents

It turns out that in the special case of the vector and axial vector currents a variant of the above method suppresses lattice artifacts. We denote the vertex function of the relevant currents generically by $J_\mu(p)$ and the corresponding Born term (evaluated on the lattice) by $J_\mu^{\mathrm{Born}}(p)$. Then we impose a renormalisation condition of the form

$$Z_q^{-1} Z_J\, \mathrm{Tr}\left(\sum_\mu Q_\mu^\perp J_\mu(p)\right) = \mathrm{Tr}\left(\sum_\mu Q_\mu^\perp J_\mu^{\mathrm{Born}}(p)\right)\,, \tag{10.26}$$

where $Q_\mu^\perp$ is a suitable Dirac matrix. In the case of the conserved vector current we know that $Z_J = 1$, hence we can calculate Z_q from (10.26). This value is then used to determine Z_J for the local vector and axial vector currents.

How is $Q_\mu^\perp$ constructed? For the conserved vector current we find

$$J_\mu^{\mathrm{Born}}(p) = \gamma_\mu \cos(ap_\mu) + \mathrm{i}\sin(ap_\mu) \tag{10.27}$$

and we choose

$$Q_\mu^\perp = Q_\mu - \frac{1}{N}\sin(ap_\mu)\sum_\lambda Q_\lambda \sin(ap_\lambda) \tag{10.28}$$

with

$$Q_\mu = \left(J_\mu^{\mathrm{Born}}\right)^{-1} = \gamma_\mu \cos(ap_\mu) - \mathrm{i}\sin(ap_\mu) \tag{10.29}$$

and

$$N = \left(\sum_\mu \sin^2(ap_\mu)\right)^2 + \sum_\mu \sin^2(ap_\mu) - \sum_\mu \sin^4(ap_\mu)\,. \tag{10.30}$$

Note that for $a \to 0$ we have $N/a^2 \to p^2$ and only the components of J_μ transverse to the momentum contribute in the above renormalisation condition. On the other hand, for all values of a

$$\sum_\mu Q_\mu^\perp J_\mu^{\mathrm{Born}} = 3\,, \tag{10.31}$$

which means that the Born term contributes with maximal weight.

For the local vector and axial vector current we have

$$J_\mu^{\mathrm{Born}} = \gamma_\mu \tag{10.32}$$

and

$$J_\mu^{\mathrm{Born}} = \gamma_\mu \gamma_5\,, \tag{10.33}$$

respectively. In both cases we choose

$$Q_\mu^\perp = Q_\mu - \frac{1}{N}\sin(ap_\mu)\sum_\lambda Q_\lambda \sin(ap_\lambda) \tag{10.34}$$

with

$$Q_\mu = \left(J_\mu^{\mathrm{Born}}\right)^{-1} \tag{10.35}$$

and

$$N = \sum_\mu \sin^2(ap_\mu)\,. \tag{10.36}$$

Then (10.31) holds in these cases as well. Working with the longitudinal (with respect to momentum) component or applying (10.36) also in the case of the conserved vector current leads to a less smooth momentum dependence, i.e. to stronger lattice effects. In the continuum limit, the renormalisation condition (10.26) is O(4) covariant.

10.5 Input from perturbative calculations

Eq.(10.22) defines an unconventional renormalisation scheme of the momentum subtraction (MOM) type, and it is desirable to convert our results into a more popular scheme like the $\overline{\mathrm{MS}}$ scheme. Moreover, we want to use our renormalisation factors in connection with the Wilson coefficients, which appear in the operator product expansion, and these are generally given in the $\overline{\mathrm{MS}}$ scheme. Hence we have to perform a finite renormalisation leading us from the renormalisation scheme defined by eq.(10.22) to the $\overline{\mathrm{MS}}$ scheme. The corresponding renormalisation constant $Z_{\mathrm{MOM}}^{\overline{\mathrm{MS}}}$ is computed in continuum perturbation theory using dimensional regularisation.

We want to compare our nonperturbative results with the corresponding values obtained in (tadpole improved) perturbation theory on the lattice. For the renormalisation factor which brings us from the bare lattice operator to the renormalised operator in the $\overline{\mathrm{MS}}$ scheme, lattice perturbation theory yields results of the form

$$Z_{\mathcal{O}}^{\mathrm{pert}} = 1 - \frac{g^2}{16\pi^2}(\gamma_0 \ln(a\mu) + C_F \Delta_{\mathcal{O}}) \tag{10.37}$$

where $\Delta_{\mathcal{O}}$ is a finite constant and γ_0 is the one-loop coefficient of the anomalous dimension. Working with an anticommuting γ_5 also in the continuum part of the calculation we arrive at the values given for some operators shown below in table 13 (see ref. [51] for more details and other operators).

In order to obtain the corresponding results in tadpole improved perturbation theory (compare Sect. 9.6) we write (with $\mu = 1/a$) for an operator with n_D covariant derivatives

$$1 - \frac{g^2}{16\pi^2} C_F \Delta_{\mathcal{O}} = \frac{u_0}{u_0^{n_D}} u_0^{n_D - 1}\left(1 - \frac{g^2}{16\pi^2} C_F \Delta_{\mathcal{O}}\right) = \frac{u_0}{u_0^{n_D}}\left(1 - \frac{g^{*2}}{16\pi^2} C_F \overline{\Delta}_{\mathcal{O}}\right) + O(g^{*4})\,, \tag{10.38}$$

where u_0 is given in eq. (9.73) and

$$\overline{\Delta}_{\mathcal{O}} = \Delta_{\mathcal{O}} + (n_D - 1)\pi^2\,. \tag{10.39}$$

This reflects the fact that one has n_D operator tadpole contributions and one leg tadpole contribution, which are of the same magnitude but contribute with opposite sign. One factor of u_0 is absorbed into the normalisation of the quark fields replacing κ_c by $\widetilde{\kappa}_c = \kappa_c u_0$. Furthermore, one chooses as the expansion

$\mathcal{O}$	$\Delta_{\mathcal{O}}$
$\mathcal{O}_{v_{2,a}}$	1.2796
$\mathcal{O}_{v_4}$	-27.2296
$\mathcal{O}_{a_1}$	0.3451
$\mathcal{O}^A_\mu$	15.7963

Table 13: Finite contributions to the renormalisation factors in lattice perturbation theory.

parameter g^* the coupling constant renormalised at some physical scale. We have taken g^* from the values given for $\alpha_{\overline{\rm MS}}(1/a)$ in Table I of Ref.[27].

At this point we have two options. Either we stay with the expression (10.37) and its tadpole improved analogue

$$Z^{\rm ti}_{\mathcal{O}} = u_0^{1-n_D}\left[1 - \frac{g^{*2}}{16\pi^2}(\gamma_0 \ln(a\mu) + C_F \overline{\Delta}_{\mathcal{O}})\right] \tag{10.40}$$

or we apply these formulae only at a fixed scale $\mu = \mu_0$ (e.g. $\mu_0 = 1/a$) using the renormalisation group to change μ.

For this scale dependence, the renormalisation group predicts (at fixed bare parameters)

$$R_{\mathcal{O}}(\mu,\mu_0) \equiv \frac{Z_{\mathcal{O}}(\mu)}{Z_{\mathcal{O}}(\mu_0)} = \exp\left\{-\int_{\overline{g}(\mu_0^2)}^{\overline{g}(\mu^2)} {\rm d}g \frac{\gamma(g)}{\beta(g)}\right\} . \tag{10.41}$$

Here the β-function is given by

$$\beta(g) = -\beta_0 \frac{g^3}{16\pi^2} - \beta_1 \frac{g^5}{(16\pi^2)^2} + \cdots \tag{10.42}$$

with

$$\beta_0 = 11 - \frac{2}{3} n_f \, , \, \beta_1 = 102 - \frac{38}{3} n_f \, . \tag{10.43}$$

In terms of the Λ parameter the running coupling reads

$$\frac{\overline{g}^2(\mu^2)}{16\pi^2} = \frac{1}{\beta_0 \ln(\mu^2/\Lambda^2)} - \frac{\beta_1}{\beta_0^3} \frac{\ln\ln(\mu^2/\Lambda^2)}{\ln^2(\mu^2/\Lambda^2)} + \cdots \tag{10.44}$$

and the anomalous dimension is expanded as

$$\gamma(g) = \gamma_0 \frac{g^2}{16\pi^2} + \gamma_1 \left(\frac{g^2}{16\pi^2}\right)^2 + \cdots \tag{10.45}$$

For our operators the one- and two-loop coefficients γ_0 and γ_1 of the anomalous dimension are known in the $\overline{\rm MS}$ scheme [92, 93]. Within the two-loop approximation we obtain

$$\frac{Z_{\mathcal{O}}(\mu)}{Z_{\mathcal{O}}(\mu_0)} = \left(\frac{\overline{g}^2(\mu^2)}{\overline{g}^2(\mu_0^2)}\right)^{\frac{\gamma_0}{2\beta_0}} \left(\frac{1 + \frac{\beta_1}{\beta_0}\frac{\overline{g}^2(\mu^2)}{16\pi^2}}{1 + \frac{\beta_1}{\beta_0}\frac{\overline{g}^2(\mu_0^2)}{16\pi^2}}\right)^{\frac{1}{2}((\gamma_1/\beta_1)-(\gamma_0/\beta_0))} . \tag{10.46}$$

Having data at two different values of the bare coupling we can also compare the dependence on the bare coupling with the behaviour expected from the renormalisation group. Keeping the renormalisation scale μ and the renormalised quantities fixed we find for the ratio of the renormalisation factors $Z_{\mathcal{O}}$ and $Z'_{\mathcal{O}}$ at the bare couplings g and g', respectively,

$$\frac{Z_{\mathcal{O}}}{Z'_{\mathcal{O}}} = \exp\left\{\int_{g'}^{g} {\rm d}g_0 \frac{\hat{\gamma}(g_0)}{\hat{\beta}(g_0)}\right\} . \tag{10.47}$$

Here $\hat{\gamma}(g)$ and $\hat{\beta}(g)$ denote the anomalous dimension and the β-function obtained by differentiation with respect to the cut-off at fixed renormalised quantities. They are considered as functions of the bare coupling. Within the two-loop approximation we get

$$\frac{Z_{\mathcal{O}}}{Z'_{\mathcal{O}}} = \left(\frac{g^2}{g'^2}\right)^{-\frac{\gamma_0}{2\beta_0}} \left(\frac{1+\frac{\beta_1}{\beta_0}\frac{g^2}{16\pi^2}}{1+\frac{\beta_1}{\beta_0}\frac{g'^2}{16\pi^2}}\right)^{\frac{1}{2}((\hat{\gamma}_1/\beta_1)-(\gamma_0/\beta_0))} , \tag{10.48}$$

where we have used the fact that β_0, β_1, and γ_0 are universal so that $\hat{\beta}_0 = \beta_0$, $\hat{\beta}_1 = \beta_1$, $\hat{\gamma}_0 = \gamma_0$. The coefficient $\hat{\gamma}_1$ reads

$$\hat{\gamma}_1 = \gamma_1 + 2\beta_0 C_F \Delta_{\mathcal{O}} - 32\pi^2\gamma_0 \left(\frac{1}{16N} - N\cdot 0.084978 + \tfrac{1}{2}n_f \cdot 0.006887\right) \tag{10.49}$$

for gauge group SU(N). The quantities $\Delta_{\mathcal{O}}$ are given in Table 13, and the funny numbers in the parentheses multiplying γ_0 stem from the ratio of the Λ-parameters on the lattice and in the $\overline{\mathrm{MS}}$ scheme (see, e.g., [4]).

10.6 Numerical implementation

Let us sketch the main ingredients of our calculational procedure. To simplify the notation we set the lattice spacing $a = 1$ in this section. In a first step gauge field configurations are generated and numerically fixed to some convenient gauge (the Landau gauge in our case). The non-amputated Green function (10.18) is calculated as the gauge field average of $\hat{G}(p)$, which is constructed from the quark propagator $\hat{S}(p)$ on the same gauge field configuration according to

$$\hat{G}(p) = \frac{1}{V} \sum_{x,y,z,z'} \mathrm{e}^{-\mathrm{i}p\cdot(x-y)} \hat{S}(x,z) J(z,z') \hat{S}(z',y) \,. \tag{10.50}$$

We omit the quark-line disconnected contribution (which would contribute only to flavour-singlet operators) and suppress Dirac as well as colour indices. The operator under study is represented by $J(z,z')$:

$$\sum_z \mathcal{O}(z) = \sum_{z,z'} \overline{q}(z) J(z,z') q(z') \,. \tag{10.51}$$

Using the relation

$$\hat{S}(x,y) = \gamma_5 \hat{S}(y,x)^+ \gamma_5 \tag{10.52}$$

we rewrite $\hat{G}(p)$ as

$$\hat{G}(p) = \sum_{z,z'} \gamma_5 \left(\sum_x \hat{S}(z,x)\mathrm{e}^{\mathrm{i}p\cdot x}\right)^+ \gamma_5 J(z,z') \left(\sum_y \hat{S}(z',y)\mathrm{e}^{\mathrm{i}p\cdot y}\right) \tag{10.53}$$

in terms of the quantities

$$\sum_x \hat{S}(z,x)\mathrm{e}^{\mathrm{i}p\cdot x} \,. \tag{10.54}$$

These can be calculated by solving the lattice Dirac equation with a momentum source:

$$\sum_z M(y,z) \left(\sum_x \hat{S}(z,x)\mathrm{e}^{\mathrm{i}p\cdot x}\right) = \mathrm{e}^{\mathrm{i}p\cdot y} \,. \tag{10.55}$$

Here $M(x,y)$ represents the fermion matrix. So the number of matrix inversions to be performed is proportional to the number of momenta considered. But the quark propagators, which we need for the amputation and the computation of the quark wave function renormalisation, are immediately obtained from the quantities already calculated.

Another computational strategy would be to choose a particular location for the operator, i.e. instead of summing over z' (and z) in (10.50) one could set $z' = 0$. Translational invariance tells us that this will give the same expectation value after averaging over all gauge field configurations. For this method we need to solve the Dirac equation with a point source at the location of the operator and (in the case of extended operators) for a small number of point sources in the immediate neighbourhood. For operators with a small number of derivatives the point source method would require fewer inversions, but it turns out that relying on translational invariance leads to much larger statistical errors [94].

10.7 Some results for nonperturbative renormalisation factors

We work with standard Wilson fermions ($r = 1$) in the quenched approximation. At $\beta = 6.0$ we have data on a $16^3 \times 32$ lattice for three values of the hopping parameter, $\kappa = 0.155$, 0.153, and 0.1515. Further configurations at $\beta = 6.2$ on a $24^3 \times 48$ lattice were studied with $\kappa = 0.152$, 0.1507, and 0.1489. Before we calculate quark correlation functions on our configurations we fix the gauge to the Landau gauge [90].

For the presentation of our results we convert lattice units to physical units using $a^{-2} = 3.8$ GeV^{-2} ($\beta = 6.0$) and $a^{-2} = 7.0$ GeV^{-2} ($\beta = 6.2$) as determined from the string tension. The Λ parameter is taken to be $\Lambda_{\overline{\text{MS}}} = 230$ MeV. This value follows from the result given in Ref.[95] by using the string tension instead of the force parameter r_0 to set the scale. As we work in the quenched approximation we have to put $n_f = 0$ in the perturbative formulae. The plotted errors are purely statistical and have been calculated by a jackknife procedure.

We first extrapolate our results to the chiral limit. This is done linearly in $1/\kappa$. In most cases the mass dependence is quite weak so that the extrapolation looks reliable, see fig. 42 for an example (operator $\mathcal{O}_{v_{2,a}}$

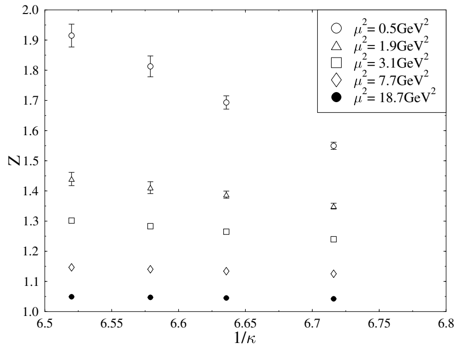

Figure 42: Chiral extrapolation of Z for $\mathcal{O}_{v_{2,a}}$ at $\beta = 6.2$. Some representative values of μ^2 have been selected.

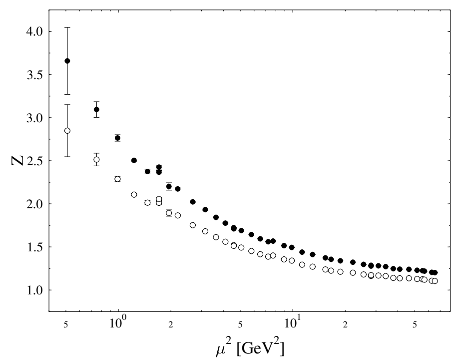

Figure 43: Z for the operator $\mathcal{O}_{a_2}$ at $\beta = 6.2$. The filled circles represent the data corresponding to the renormalisation condition (10.22), the open circles represent the values in the $\overline{\text{MS}}$ scheme.

at $\beta = 6.2$). This is not too surprising since the mass scale in the calculations is not set by the quark mass, but by the (off-shell) momentum, which is typically much larger.

Then we multiply by $Z_{\text{MOM}}^{\overline{\text{MS}}}$ in order to obtain the Z factors in the $\overline{\text{MS}}$ scheme. When evaluating the perturbative expression for $Z_{\text{MOM}}^{\overline{\text{MS}}}$ we insert for the coupling constant the running coupling in the $\overline{\text{MS}}$ scheme taken at the renormalisation scale μ^2 (cf. eq.(10.44)). Fig. 43 illustrates the effect of the conversion to the $\overline{\text{MS}}$ scheme for the operator $\mathcal{O}_{a_2}$ at $\beta = 6.2$.

Ultimately we are interested in physical observables, e.g. in the moments of the structure functions. They are obtained from the bare matrix elements calculated on the lattice after multiplication by the appropriate Z factor and the Wilson coefficient (both computed in the $\overline{\text{MS}}$ scheme). So the bridge from the lattice to continuum physics consists of the product of these two quantities. Having calculated Z nonperturbatively we can multiply with the corresponding Wilson coefficient in order to see if the expected cancellation of the μ dependence really occurs. If it does, the μ independent value of the product is the factor we need in order to calculate the moments of the structure functions from the lattice results. Since this cancellation means that the scale dependence of our Z's should be given by the renormalisation group factor (10.46) (in two-loop approximation) we shall divide our numerical results by this expression and hope to obtain a μ independent answer, at least in a reasonable window of μ values. We shall choose $\mu_0^2 = 4$ GeV^2 in (10.46).

10.7.1 Example of axial vector current

Let us begin with the axial vector current. Since in this case the anomalous dimensions vanish, the renormalisation group factor (10.46) is equal to one and we expect to find immediately scale independent results in a suitable window. As already mentioned, the standard procedure from section 10.3 suffers more strongly from lattice artifacts than the alternative method described in section 10.4. This is exemplified in figs. 44 and 45.

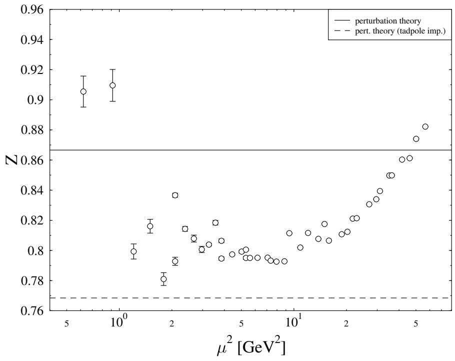

Figure 44: Z for the axial vector current $\overline{q}\gamma_4\gamma_5 q$ at $\beta = 6.0$. The lines represent the predictions of one-loop lattice perturbation theory with and without tadpole improvement.

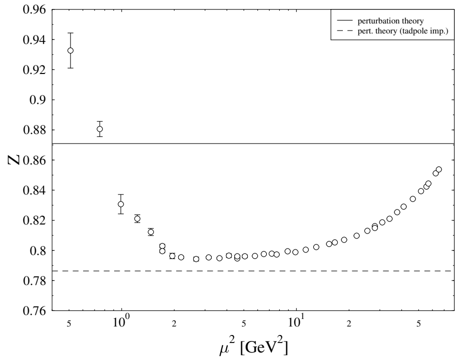

Figure 45: Z for the axial vector current at $\beta = 6.2$ determined by the method of Sect. 10.4. The lines represent the predictions of one-loop lattice perturbation theory with and without tadpole improvement.

In fig. 44 we show the results obtained by applying the standard procedure to $\overline{q}\gamma_4\gamma_5 q$ whereas the alternative method leads to fig. 45 for the axial vector current. In the remainder of this subsection we shall restrict ourselves to the values delivered by the latter procedure.

Fig. 45 nicely fulfils our expectations. We see a flat region around $\mu^2 \approx 4$ GeV^2 where Z becomes scale independent as it should. Moreover, tadpole improvement has really improved the agreement between our nonperturbative result and one-loop lattice perturbation theory.

10.7.2 Examples for DIS operators

In this subsection we want to discuss some selected operators with derivatives, which determine moments of hadronic structure functions. Again, we would like to find a "window" at moderate values of μ^2 where $Z_{\mathcal{O}}/R_{\mathcal{O}}$ is constant. There μ^2 would be large enough to allow for perturbative scaling behaviour and the multiplication with perturbative Wilson coefficients would make sense. On the other hand, μ^2 should be small enough to avoid strong cut-off effects.

In order to facilitate the comparison of the different operators we have chosen the same vertical scale for all operators with the same number of derivatives although in some cases this has the consequence that the results for a few low values of μ^2 do not appear on the plot.

In figs. 46,47 we plot as an example the ratio $Z_{\mathcal{O}}/R_{\mathcal{O}}$ versus the renormalisation scale μ^2 for two operators containing one derivative.

In most cases, a "flat" region starts only at $\mu^2 \approx 10$ GeV^2, where it is hard to believe that cut-off effects are negligible. Therefore an unambiguous determination of Z is difficult. It should also be noted that for larger values of μ^2 the scale dependence of Z itself (and of R) is already rather weak so that approximate independence of μ^2 is relatively easy to get.

In fig. 48 an operator with three derivatives is shown. Here it is simply impossible to identify a scaling window. This could be due to the neglected mixing problems. Furthermore, cut-off effects might be relatively strong in this case because of the large extent of the lattice operator.

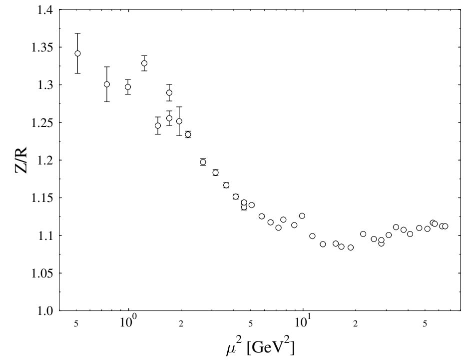

Figure 46: Z/R for $\mathcal{O}_{v_{2,a}}$ at $\beta = 6.2$.

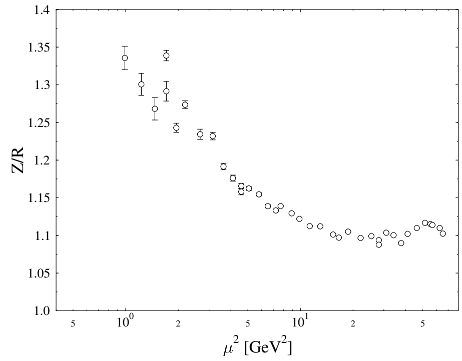

Figure 47: Z/R for $\mathcal{O}_{a_1}$ at $\beta = 6.2$.

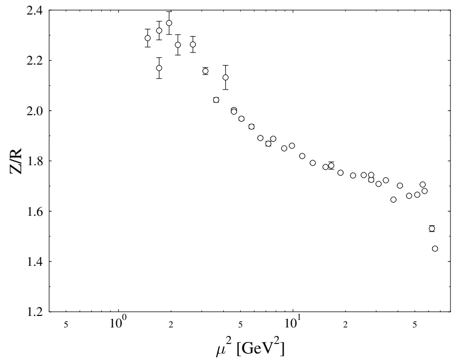

Figure 48: Z/R for $\mathcal{O}_{v_4}$ at $\beta = 6.2$.

A Conventions

The Minkowski space metric has the signature $(1,-1,-1,-1)$. Minkowski and Euclidean components are related by

$$x_4 = \mathrm{i}x^{(M)0} = \mathrm{i}x_0^{(M)} \quad , \qquad x_j = x^{(M)j} = -x_j^{(M)} \quad , \tag{A.1}$$

where j refers to spatial indices. Unless explicitly mentioned, we label Minkowski-space variables by an (M).

Covariant derivatives are defined in Minkowski space as

$$D^{(M)\mu} = \partial^{(M)\mu} - \mathrm{i}gA^{(M)\mu} \tag{A.2}$$

and are related to their Euclidean counterparts as follows:

$$\mathrm{i}D^{(M)0} = -D_4 \quad , \qquad \mathrm{i}D^{(M)j} = -\mathrm{i}D_j \quad , \tag{A.3}$$

similarly for the gamma matrices:

$$\gamma^{(M)0} = \gamma_4 \quad , \qquad \gamma^{(M)j} = \mathrm{i}\gamma_j \quad . \tag{A.4}$$

The γ_5 matrix is defined as

$$\begin{aligned} \gamma_5^{(M)} &= \mathrm{i}\gamma^{(M)0}\gamma^{(M)1}\gamma^{(M)2}\gamma^{(M)3} \\ \gamma_5 &= \gamma_1\gamma_2\gamma_3\gamma_4 = -\gamma_5^{(M)} \quad . \end{aligned} \tag{A.5}$$

The momentum of the particles is chosen in the 1-direction, $\vec{p} = (p, 0, 0)$. Polarisation vectors for vector particles satisfy

$$p^{(M)\mu}\epsilon_\mu^{(M)}(\vec{p},\lambda) = 0 \quad , \qquad \epsilon^{(M)\mu}(\vec{p},\lambda)\epsilon_\mu^{(M)}(\vec{p},\lambda') = -M^2\,\delta_{\lambda\lambda'} \tag{A.6}$$

$(\lambda = \pm, 0)$ and have the explicit form

$$\epsilon^{(M)\mu}(\vec{p},\lambda) = \left(\frac{\vec{p}\cdot\vec{e}_\lambda}{M}, \vec{e}_\lambda + \frac{\vec{p}\cdot\vec{e}_\lambda}{M(M+E)}\vec{p}\right) \tag{A.7}$$

with the basis vectors

$$\vec{e}_\pm = \mp\frac{m}{\sqrt{2}}\,(0, 1, \pm\mathrm{i}) \tag{A.8}$$

$$\vec{e}_0 = m\,(1, 0, 0) \quad . \tag{A.9}$$

They satisfy the completeness relation

$$\sum_\lambda \epsilon_i^{(M)*}(\vec{p},\lambda)\epsilon_j^{(M)}(\vec{p},\lambda) = m^2\left(\delta_{ij} + \frac{1}{m^2}p_i p_j\right) \quad . \tag{A.10}$$

Note that in Euclidean space $\epsilon_j(\vec{p},\lambda) = \epsilon^{(M)j}(\vec{p},\lambda)$.

References

[1] A.V. Manohar, Lectures presented at Lake Louise Winter Institute 1992, `hep-ph/9204208` (1992).

[2] R.L. Jaffe, Lectures presented at Erice 1995, `hep-ph/9602236` (1996).

[3] P. Hoodbhoy, R. L. Jaffe, and A. Manohar, Nucl. Phys. B312, 571 (1989).

[4] I. Montvay and G. Münster, Quantum Fields on a Lattice (Cambridge University Press, Cambridge (UK), 1994)

[5] M. Göckeler et al., Phys. Rev. D54, 5705 (1996).

[6] C. Best et al., Phys. Rev. D56, 2743 (1997).

[7] K. Symanzik, Nucl. Phys. B226 (1983) 187, 205.

[8] M. Lüscher and P. Weisz, Commun. Math. Phys. 97 (1985) 59; erratum: *ibid.* 98 (1985) 433.

[9] B. Sheikholeslami and R. Wohlert, Nucl. Phys. B259 (1985) 572.

[10] M. Göckeler, R. Horsley, E.-M. Ilgenfritz, H. Perlt, P. Rakow, G. Schierholz and A. Schiller, Nucl. Phys. B (Proc. Suppl.) 42 (1995) 337.

[11] M. Göckeler, R. Horsley, E.-M. Ilgenfritz, H. Perlt, P. Rakow, G. Schierholz and A. Schiller, Phys. Rev. D53 (1996) 2317.

[12] M. Göckeler, R. Horsley, H. Perlt, P. Rakow, G. Schierholz, A. Schiller and P. Stephenson, Phys. Lett. B391 (1997) 388.

[13] M. Göckeler, R. Horsley, H. Perlt, P. Rakow, G. Schierholz, A. Schiller, and P. Stephenson, Phys. Rev. D57 (1998) 5562.

[14] H. van der Vorst, SIAM J. Sc. Stat. Comp. 12 (1992) 631.

[15] A. Frommer, V. Hannemann, B. Nockel, T. Lippert and K. Schilling, Int. J. Mod. Phys. C5 (1994) 1073.

[16] S. R. Sharpe, Nucl. Phys. B (Proc. Suppl.) 30 (1993) 213.

[17] D. Weingarten, Nucl. Phys. B (Proc. Suppl.) 34 (1994) 29.

[18] C. Alexandrou, S. Güsken, F. Jegerlehner, K. Schilling, and R. Sommer, Nucl. Phys. B414, 815 (1994).

[19] C. R. Allton et al., UKQCD Collaboration, Phys. Rev. D47, 5128 (1993).

[20] M. Lüscher, S. Sint, R. Sommer, P. Weisz and U. Wolff, Nucl. Phys. B491 (1997) 323.

[21] E. Eichten, K. Gottfried, T. Kinoshita, K. D. Lane and T. M. Yan, Phys. Rev. D21 (1980) 203.

[22] For a review see for example: M. Neubert, CERN preprint CERN-TH/96-292 (1996) (`hep-ph/9610266`).

[23] H. Pagels, Phys. Rev. D19 (1979) 3080.

[24] M. Lüscher, S. Sint, R. Sommer and P. Weisz, Nucl. Phys. B478 (1996) 365.

[25] M. Lüscher, S. Sint, R. Sommer and H. Wittig, Nucl. Phys. B491 (1997) 344.

[26] S. Sint and P. Weisz, MPI preprint MPI-PhT/97-21 (1997) (`hep-lat/9704001`).

[27] G. P. Lepage and P. B. Mackenzie, Phys. Rev. D48 (1993) 2250.

[28] S. Capitani, M. Göckeler, R. Horsley, H. Perlt, P. Rakow, G. Schierholz and A. Schiller, in preparation.

[29] M. Göckeler, R. Horsley, H. Oelrich, H. Perlt, P. Rakow, G. Schierholz and A. Schiller, in preparation.

[30] H. Leutwyler, Phys. Lett. B378 (1996) 313.

[31] M. Göckeler, R. Horsley, H. Oelrich, H. Perlt, P. Rakow, G. Schierholz and A. Schiller, Nucl. Phys. B (Proc. Suppl.) 47 (1996)

[32] R. Gupta and T. Bhattacharya, Phys. Rev. D55 (1997) 7203.

[33] R. Sommer, Nucl. Phys. B411 (1994) 839.

[34] R. Sommer, Phys. Rep. 275 (1996) 1.

[35] G. S. Bali and K. Schilling, Phys. Rev. D47 (1993) 661.

[36] G. S. Bali, Wuppertal preprint WUB 93-37 (1993) (`hep-lat/9311009`).

[37] S. P. Booth, D. S. Henty, A. Hulsebos, A. C. Irving, C. Michael and P. W. Stephenson, Phys. Lett. B294 (1992) 385.

[38] H. Wittig, Nucl. Phys. B (Proc. Suppl.) 42 (1995) 288.

[39] H. Hoeber (1997): ref. [35] reanalyzed with link integration.

[40] C. R. Allton, C. T. Sachrajda, R. M. Baxter, S. P. Booth, K. C. Bowler, S. Collins, D. S. Henty, R. D. Kenway, C. McNeile, B. J. Pendleton, D. G. Richards, J. N. Simone, A. D. Simpson, A. McKerrell, C. Michael and M. Prisznyak, Nucl. Phys. B407 (1993) 331.

[41] S. Perantonis and C. Michael, Nucl. Phys. B347 (1990) 854.

[42] K. D. Born, R. Altmeyer, W. Ibes, E. Laermann, R. Sommer, T. F. Walsh and P. M. Zerwas, Nucl. Phys. B (Proc. Suppl.) 20 (1991) 394.

[43] R. Sommer, CERN preprint CERN-TH/97-107 (1997) (`hep-lat/9705026`).

[44] S. Aoki, M. Fukugita, S. Hashimoto, N. Ishizuka, Y. Iwasaki, K. Kanaya, Y. Kuramashi, H. Mino, M. Okawa, A. Ukawa and T. Yoshiè, Nucl. Phys. B (Proc. Suppl.) 53 (1997) 209.

[45] F. Butler, H. Chen, J. Sexton, A. Vaccarino and D. Weingarten, Nucl. Phys. B421 (1994) 217.

[46] M. Wingate, T. DeGrand, S. Collins and U. M. Heller, Phys. Rev. Lett. 74 (1995) 4596.

[47] M. Göckeler, R. Horsley, E.-M. Ilgenfritz, H. Perlt, P. Rakow, G. Schierholz and A. Schiller, Nucl. Phys. **B** (Proc. Suppl.) **53**, 81 (1997).

[48] M. Göckeler, R. Horsley, E.-M. Ilgenfritz, H. Oelrich, H. Perlt, P. Rakow, G. Schierholz, A. Schiller and P. Stephenson, Nucl. Phys. **B** (Proc. Suppl.) **53**, 324 (1997).

[49] L. Mankiewicz and T. Weigl, Phys. Lett. **B389**, 334 (1996).

[50] C. Best, M. Göckeler, R. Horsley, E.-M. Ilgenfritz, H. Perlt, P. Rakow, A. Schäfer, G. Schierholz, A. Schiller and S. Schramm, DESY preprint DESY 97-41 (1997) (`hep-lat/9703014`), to appear in Phys. Rev. **D**.

[51] M. Göckeler, R. Horsley, E.-M. Ilgenfritz, H. Perlt, P. Rakow, G. Schierholz and A. Schiller, Nucl. Phys. **B472**, 309 (1996).

[52] M. Göckeler, R. Horsley, E.-M. Ilgenfritz, H. Oelrich, H. Perlt, P. Rakow, G. Schierholz, A. Schiller and P. Stephenson, Nucl. Phys. **B** (Proc. Suppl.) **53**, 896 (1997).

[53] G. Martinelli, C. Pittori, C. T. Sachrajda, M. Testa and A. Vladikas, Nucl. Phys. **B445**, 81 (1995).

[54] M. Göckeler, R. Horsley, E.-M. Ilgenfritz, H. Oelrich, H. Perlt, P. Rakow, G. Schierholz and A. Schiller, Nucl. Phys. **B** (Proc. Suppl.) **47**, 493 (1996).

[55] H. L. Lai, J. Botts, J. Huston, J. G. Morfin, J. F. Owens, J. W. Qiu, W. K. Tung and H. Weerts, Phys. Rev. **D51**, 4763 (1995).

[56] K. Abe et al., Phys. Rev. Lett. **75**, 25 (1995), *ibid* **76**, 587 (1996).

[57] T. Gehrmann and W. J. Stirling, Phys. Rev. **D53**, 6100 (1996).

[58] M. Fukugita, Y. Kuramashi, M. Okawa and A. Ukawa, Phys. Rev. Lett. **75**, 2092 (1995).

[59] S. J. Dong, J.-F. Lagaë and K.-F. Liu, Phys. Rev. Lett. **75**, 2096 (1995), and references therein to earlier work.

[60] P. J. Sutton, A. D. Martin, R. G. Roberts and W. J. Stirling, Phys. Rev. **D45**, 2349 (1992).

[61] M. Lüscher, S. Sint, R. Sommer, P. Weisz and U. Wolff, Nucl. Phys. **B491**, 323 (1997).

[62] M. Göckeler, R. Horsley, H. Oelrich, H. Perlt, P. Rakow, G. Schierholz, A. Schiller and P. Stephenson, to be published.

[63] M. Lüscher, S. Sint and H. Wittig, Nucl. Phys. **B491**, 344 (1997).

[64] S. Capitani, M. Göckeler, R. Horsley, H. Perlt, P. Rakow, G. Schierholz and A. Schiller, to be published.

[65] R. L. Jaffe, Proc. Zeuthen 1997, DESY 97-200, p. 167

[66] R. L. Jaffe and X. Ji, Nucl. Phys. B375 (1992) 527.

[67] S. Capitani and G. Rossi, Nucl. Phys. B433 (1995) 351;
G. Beccarini, M. Bianchi, S. Capitani and G. Rossi, Nucl. Phys. B456 (1995) 271;
M. Göckeler, R. Horsley, E.-M. Ilgenfritz, H. Perlt, P. Rakow, G. Schierholz and A. Schiller, Nucl. Phys. B472 (1996) 309.

[68] M. Göckeler, R. Horsley, E.-M. Ilgenfritz, H. Oelrich, H. Perlt, P. Rakow, G. Schierholz, A. Schiller and P. Stephenson, Nucl. Phys. B (Proc.Suppl.) 53 (1997) 896.

[69] L. L. Frankfurt, M. I. Strikman, L. Mankiewicz, A. Schäfer, E. Rondio, A. Sandacz and V. Papavassiliou, Phys. Lett. B230 (1989) 141.

[70] B. Adeva et al., Phys. Lett. B369 (1996) 93.

[71] J. Pretz, Dissertation, Mainz (1997), and Proc. Zeuthen 1997, DESY 97-200, p. 41

[72] M. Göckeler, R. Horsley, L. Mankiewicz, H. Perlt, P. Rakow, G. Schierholz and A. Schiller, Phys. Lett. B414 (1997) 340.

[73] D. A. Ross and C. T. Sachrajda, Nucl. Phys. B149 (1979) 497.

[74] S. Capitani, M. Göckeler, R. Horsley, H. Oelrich, H. Perlt, D. Pleiter, P. Rakow, G. Schierholz, A. Schiller and P. Stephenson, Nucl. Phys. Proc.Suppl.**63** (1998) 315.

[75] M. Okawa, Nucl. Phys. B (Proc. Suppl.) 47 (1996) 160.

[76] R. Wohlert, `DESY 87-069` (1987).

[77] M. Lüscher, P. Weisz, *Nucl. Phys.* **B479** (1996) 429.

[78] H. Kawai, R. Nakayama, K. Seo, *Nucl. Phys.* **B189** (1981) 40.

[79] E. Gabrielli et al., *Nucl. Phys.* **B362** (1991) 475;

[80] A. Borelli et al., *Nucl. Phys.* **B409** (1993) 382.

[81] G. Heatlie et al., *Nucl. Phys.* **B352** (1991) 266.

[82] S. Capitani et al., Nucl. Phys. Proc. Suppl. **63** (1998) 874

[83] R.C. Brower et al., *Nucl. Phys.* **B** (Proc. Suppl.) **53** (1997) 318.

[84] G. Beccarini et al., *Nucl. Phys.* **B456** (1995) 271.

[85] S. Caracciolo, P. Menotti, A. Pelisetto, *Nucl. Phys.* **B375** (1992) 195.

[86] M. Göckeler et al., *Nucl. Phys.* **B** (Proc. Suppl.) **42** (1995) 337.

[87] M. Göckeler et al., Nucl. Phys. B (Proc. Suppl.) **53** (1997) 81

[88] G. Martinelli and C.T. Sachrajda, Nucl. Phys. B306 (1988) 865; Nucl. Phys. B316 (1989) 355

[89] S. Capitani and G. Rossi, Nucl. Phys. B433 (1995) 351

[90] J.E. Mandula and M. Ogilvie, Phys. Lett. B185 (1987) 127

[91] M.L. Paciello, S. Petrarca, B. Taglienti and A. Vladikas, Phys. Lett. B341 (1994) 187

[92] E.G. Floratos, D.A. Ross and C.T. Sachrajda, Nucl. Phys. B129 (1977) 66; *ibid.* 139 (1978) 545 (E)

[93] D.V. Nanopoulos and D.A. Ross, Nucl. Phys. B157 (1979) 273; R. Tarrach, Nucl. Phys. B183 (1981) 384

[94] M. Göckeler, R. Horsley, H. Oelrich, H. Perlt, P. Rakow, G. Schierholz and A. Schiller, Nucl. Phys. B (Proc. Suppl.) 63 (1998) 868

[95] S. Capitani, M. Guagnelli, M. Lüscher, S. Sint, R. Sommer, P. Weisz and H. Wittig, Nucl. Phys. B (Proc. Suppl.) 63 (1998) 153

[96] P. J. Sutton et al., Phys. Rev. D45, 2349 (1992).